IDENTIFICATION AND CHARACTERIZATION OF NOVEL ADP-RIBOSYL CYCLASE FAMILY MEMBERS

A DISSERTATION
SUBMITTED TO THE FACULTY OF THE GRADUATE SCHOOL
OF THE UNIVERSITY OF MINNESOTA
BY

Renee Marie Hirte

IN PARTIAL FULFILLMENT OF THE REQUIREMENTS
FOR THE DEGREE OF
DOCTOR OF PHILOSOPHY

Advisor
Timothy F. Walseth Ph.D.

July 2011

Abstract

CD38 and CD157 have been identified as mammalian forms of ADP-ribosyl cyclase (ADPRC). Recently novel membrane bound and cytosolic ADPRCs that are distinct from CD38 and CD157 have been identified in various tissues by our laboratory as well as others. Recently, evidence has indicated the presence of ADPRC in tissues lacking CD38. From this it is clear that there are multiple forms of mammalian ADPRC, many of which have not yet been identified or characterized. The overall goal of the research presented in this thesis was to identify and characterize the novel cytosolic cyclase(s) present in the heart cytosol and determine the mechanism(s) by which cytosolic cyclase(s) are regulated. Previously it has been shown that *Aplysia* ADPRC, CD38 and CD157 share approximately 30% sequence identity. There are two main features shared by each of these members of the ADPRC family including a conserved region near the center and ten conserved cysteine residues that can be perfectly aligned. We used a molecular approach to identify potential candidates for the cytosolic protein (or other yet unidentified ADPRCs) based on a conserved protein motif search of the mouse genome to identify proteins that shared the feature of the conserved cysteine residues. The existence of novel cyclases has implications for a broad range of cellular processes that are influenced by calcium signaling. Characterization and identification of novel ADPRCs may provide key insight into the function of the novel cyclase(s) as well as interaction and relationships to other members of the ADPRC family, which will further elucidate the complexities of calcium signaling.

Table of Contents

List of Tables

List of Figures

Chapter 1

Literature Review

Introduction to ADPRCs

The ADP-ribosyl cyclase (ADPRC) superfamily of enzymes is composed of several well-characterized members including *Aplysia* cyclase [1], CD38 [2-7], CD157 [8, 9], and three sea urchin ADPRCs [10-12]. These enzymes are multifunctional in nature and can produce at least three products, cyclic ADP-ribose (cADPR) [13], nicotinic and adenine dinucleotide 2'-phosphate (NAADP) [14], and ADP-ribose (ADPR) [15] known to be involved in calcium homeostasis [10, 14, 16-20]. In addition to ADPRC activity, which produces cADPR from NAD [1], these enzymes also can catalyze a base-exchange reaction (trans-glycosylation) [19] that produces NAADP, as well as NADase [21, 22] and cADPR hydrolase [2, 5, 6, 23] activities that can produce ADPR (Figure 1).

The hallmark member of this family is the *Aplysia* ADPRC, a soluble protein of about 30 kDa [1, 22]. Two membrane bound forms of ADPRC, CD38 [2-7] and CD157 [8, 9] have also been identified. Overall, the members of the ADPRC superfamily have approximately 30% sequence identity [9, 21, 24-26]. They share a highly conserved sequence "TLEDTL" thought to be important for catalysis [27-31] as well as ten common cysteine residues that can be aligned perfectly [24].

CD38, the best characterized mammalian cyclase, is a 45 kDa type II transmembrane glycoprotein with a hydrophobic trans-membrane domain composed of 20 amino acids with a short cytosolic tail and a large extracellular domain [32] with a catalytic pocket near a central cleft [27-31]. CD38 has been shown to be a cell surface receptor for CD31 [33] and CD38 agonistic antibodies [34]. The crystal structure of CD38 shows that it

contains both alpha helices and beta sheets, with disulphide bonds between the cysteine residues [31]. It has been shown that the cysteine residues are not key for enzyme activity, but they are critical in maintaining the catalytically active structure of CD38 and *Aplysia* cyclase [35]. Along with expression of CD38 on lymphoid tissue [36, 37], it has also been reported in brain [38, 39], eye [40], prostate [41], gut [42, 43], pancreas [44], muscle [42, 45], kidney [42] and bone tissues [46]. Although CD38 is primarily located on the cell surface [6], it is also located in certain intracellular organelles [47-49].

In terms of enzyme activity, CD38, which produces a small amount of cADPR [2], differs from *Aplysia* cyclase, which catalyzes the formation of the primary product cADPR [1]. Site directed mutagenesis revealed key structural features imperative for ADPRC and the NADase, which were all found in a pocket of the central cleft of CD38 [27-31]. Residues Phe-174 of *Aplysia* cyclase and it's equivalent Thr-221 in CD38 is a critical residue in orchestrating proper folding of the NAD substrate deciding the ratio of ADPRC to NADase activity (hydrolysis vs. cyclase) [50, 51]. Along with these residues, it has been shown that Glu(226) is important as its required for hydrogen bonding interactions necessary for positioning cADPR at the active site and upon binding of cADPR/cGDPR to the active site, which results in the rearrangement of dipeptide Glu(146)-Asp(147) [50]. Further, it was shown that the extracellular domain including the carboxyl-terminus plays a key role in enzyme activity [52], whereas the cytoplasmic tail and transmembrane domains were not required for functional enzyme activity [53]. Interestingly, it has also been shown that calcium induces an inhibited structural conformation of CD38 [54].

CD157 also referred to as bone marrow stromal cell antigen-1 (BST-1), is a membrane bound ADPRC that is a glycosylphosphatidyl inositol (GPI)-anchored protein [8, 9, 55]. CD157 expression has been reported in lymphoid tissues [26, 56-66], liver [60], vessels [67], lung [57], uterus [57], skin [68], gut [69], kidney [69], pancreas [70], and gingival fibroblasts [71].

In addition to the membrane bound CD38 and CD157 mammalian cyclases, several reports suggest existence of either cytosolic or membrane-bound enzymes not related to CD38 or CD157 [11, 12, 72-79]. In these studies we have developed a sensitive assay for ADPRC detection, which has been useful in identifying and characterizing novel ADPRCs. Further, a molecular based protein motif search was developed and utilized to identify potential novel ADPRC candidates. The most interesting candidate with conserved cysteine residues and portions of the "TLEDTL" conserved region was confirmed as a novel ADPRC.

ADPRCs in calcium ion dynamics

Metabolites of ADPRCs including ADPR, cADPR, and NAADP, are signaling molecules involved in calcium signaling [16, 80, 81]. ADPR stimulates calcium influx via plasma membrane TRPM2 channels [82]. cADPR has been shown to mobilize calcium from the sarcoplasmic reticulum (SR) via an IP_3 independent mechanism [1, 23, 83-86] and most likely involves modulation of ryanodine receptors (RyRs) [87-89]. Further, cADPR has

been shown to potentiate ADPR mediated calcium release via TRPM2 channels [90, 91]. NAADP mobilizes intracellular calcium from lysosomal and/or acidic stores and has been shown to be active in a variety of mammalian cell types [92]. Recent studies suggest that two-pore channels (TPCs) serve as receptors for NAADP and facilitate the release of calcium from acidic stores and that the calcium released upon TPC receptor signaling leads to further mobilization of calcium from sarcoplasmic and endoplasmic calcium stores via calcium-induced calcium release (CICR) [93, 94]. Accumulating evidence suggests that a wide variety of cellular functions are influenced by these messengers including: gamete fertilization [95, 96], activation of T-cells [97], neutrophil chemotaxis [98], cellular proliferation [99], insulin secretion in pancreatic β-cells [100], and long-term synaptic depression [101]. Thus, ADPRC, which catalyzes the production of these molecules, plays a significant role in cellular calcium homeostasis.

The system involving CD38 and cADPR presents what has been previously described as a topological paradox [102]. CD38 is an ectoenzyme that displays discrete activities at the cell surface [6, 103]. This activity is functionally switched off in the absence of NAD outside the cell. Since NAD is generally low outside the cell this serves as a mode of regulation. In this system, the intracellular dinucleotide NAD [104] needs to reach the extracellular space in order to be available for the catalytic site of CD38 [103], and the calcium mobilizing metabolites generated in the extracellular space by CD38 [2, 5, 6] need to reach intracellular targets to release calcium [13, 14, 105, 106]. Previous studies have pointed to a potential solution for this problem. It has been shown that NAD can be exported from the cell via connexin 43 hemichannels (Cx43) [107]. Once NAD is

outside the cell, it is accessible to CD38 as a substrate and can be converted to cADPR via CD38 enzymatic activity [1, 2, 5-7, 108]. Finally, cADPR is capable of reaching its intracellular calcium targets by two separate mechanisms. First, the dimeric form of CD38 has been shown to be responsible for the two step process of catalysis and transport of cADPR [109] and second, the presence of nucleoside transporters acting as cADPR-transporting proteins [107, 110]. Altogether this scheme presents a solution for the topological paradox (Figure 2).

Mechanistically, cADPR is known to stimulate CICR by the RyR by lowering the concentration of cytoplasmic calcium necessary to trigger CICR [84, 86, 111, 112]. It has been shown that this calcium mobilization is mediated by FK506 binding protein 12.6 (FKBP12.6) regulatory proteins from RyRs [113, 114]. Studies have shown that a calcium binding protein calmodulin (CaM) is required for the cADPR mediated calcium mobilization [111, 115-117]**.** Further, it has also been shown that cADPR can mediate calcium sequestration by increasing sarcoplasmic/endoplasmic reticulum calcium ATPase (SERCA) pump activity [118-120]. The mechanisms by which NAADP increase cytoplasmic calcium involves CICR mediated by both activation of RyRs and receptors formed by two-pore channels (TPCs) expressed on endosomal and lysosomal membranes of acidic compartments [16, 93, 121, 122]. In contrast, ADPR activates TRPM2 (transient receptor potential cation channel, subfamily melastatin, member 2) calcium-permeable cation channels, and this activation is mediated via calmodulin [91, 123].

In summary, cADPR, NAADP and ADPR are all signaling molecules produced by

ADPRCs that play an important and intricate role in calcium homeostasis that has yet to be fully elucidated.

Novel ADPRC Family Members

Aplysia ADPRC, the hallmark member of the ADPRC family [1], is a soluble mono-functional enzyme with cyclase activity with a K_m for NAD of 0.7 mM [22]. Differences in cyclase characteristics have been observed and these variances have been a useful tool for identifying novel cyclases and they suggest that alternative cyclases can play a distinct role in different environments [124]. While CD38 and CD157 are mammalian homologues of the *Aplysia* ADPRC, they are characteristically different in a variety of ways [55]. CD38 is the best-characterized mammalian ADPRC with a K_m for NAD of 21 μM [3]. CD157 is a paralogue of CD38 and is similar in terms of characterization [8, 9]. There are few differences between the two cyclases, but these differences include that CD157 is a GPI anchored protein [9] rather than an integral transmembrane protein. Further, CD157 and CD38 are activated by zinc ions, and while copper inhibits CD157, it stimulates CD38 [9, 55].

Along with the mammalian homologues of the *Aplysia* cyclase [2, 8, 9], novel members of the ADPRC family have been emerging in recent years including cell surface ADPRCs in sea urchin (spARC 1-3) [11, 12] and *Schistosoma* mansoni NAD(P)+ catabolizing enzyme (SmNACE) [75, 125]. Interestingly, despite that the members, which have been

molecularly characterized, are membrane bound and located at the outer cell surface away from the molecular targets of their enzymatic products, both membrane bound and cytosolic forms of novel ADPRCs have been identified [73]. Tissues including brain, heart and kidney from $CD38^{-/-}$ mice were found to have levels of cADPR similar to $CD38^{+/+}$ mice [98], indicating that some other ADPRC is present in these tissues. The novel membrane bound cyclase identified in murine $CD38^{-/-}$ brain [79] has been shown to be different from CD38 in that it is inactivated by zinc, an activator of CD38 cyclase activity [126] and has higher enzyme activity in developing tissues as opposed to CD38, which has higher enzyme activity in adult tissues [72]. It is also different from CD38 in that cADPR formation is favored in the murine $CD38^{-/-}$ brains resulting in 10% cADPR product formation [127] as opposed to the 1% of cADPR product formation by CD38 [6], with the remainder being ADPR. Additionally, nicotinamide guanine dinucleotide (NGD), a NAD analog, is a substrate for CD38 and CD157, but is an inhibitor of the brain enzyme [79]. Recently, novel membrane bound ADPRCs have also been reported in $CD38^{+/+}$ mouse tissues including the SR membrane associated ADPRC that has been identified in rat cardiac myocytes [128]. This ADPRC is also distinct from CD38, which is inhibited by dithiothreitol (DTT) and lectin [81], in that it is DTT and lectin insensitive. Inhibitors of CD38 cyclase activity include thiol reducing agents and lectins. Further, activation of the novel SR membrane ADPRC is regulated via a protein kinase C-dependent phosphorylation mechanism [129].

ADPRCs that are distinct from CD38 and CD157 have also been reported in the cytosol of a variety of tissues including brain [130], coronary arterial smooth muscle cells [131],

pancreatic acinar cells [74] and Jurkat T-lymphocytes [99, 132]. The novel ADPRC identified in bovine brain cytosol (30 kDa) exhibits Michaelis-Menten kinetics for NAD with an apparent K_m of 70 μM [130]. Interestingly, the novel cytosolic ADPRC identified in pancreatic acinar cells was shown to be immunologically distinct from CD38 as the ADPRC activity of the pancreatic acinar cytosol was activated by cholecystokinin (CCK), acetylcholine (ACh) and cyclic GMP (cGMP), whereas the ADPRC activity in the membrane fractions of the pancreatic acinar cells (presumably CD38/CD157) was not affected by CCK, ACh or cGMP; evidence suggesting the cytosolic cyclase was distinct from the known mammalian ADPRCs [74]. Further, the cytosolic ADPRC of Jurkat T-lymphocytes was shown to be unique as the activity of this enzyme was significantly increased in T-cells stimulated by OKT3, an effect that was potentiated by the presence of the tyrosine phosphatase inhibitor, dephosphatin [132]. Recent studies have also shown, SPN, a glycohydrolase injected into the cytosol by *Streptococcus* pyogenes, is the first glycohydrolase reported to catalyze not only hydrolysis of NAD^+, but also ADPRC and transferase activities [133].

Previous evidence has shown novel intracellular ADPRCs located within the lumen of acidic exocytotic vesicles of sea urchin egg homogenates [11]. Intraorganelle ADPRCs are shielded from cytosolic substrate and targets by the organelle membrane, but this barrier is circumvented by nucleotide transport [11, 12, 134]. Recently, CD38 was identified in bovine lung microsomal membranes and has been described as a novel NADase [135]. Several reports also indicate that nuclear CD38 is expressed in cells including those known to be CD38 surface deficient [136, 137]. Collectively, these

investigations demonstrate potential compartmentalization of ADPRC metabolite production.

Several ADPRCs have been described that are apparently distinct [11, 12, 72-79] from the known mammalian ADPRCs, CD38 and CD157 [2-9]. An in-depth characterization of these enzymes is necessary in order to delineate the role these ADPRCs play in calcium homeostasis. The basal activity of the novel ADPRCs has been shown to be very low [79], which has presented a significant challenge in the attempt to identify and characterize the novel ADPRCs. The current methods for detection of ADPRC activity are insufficient for such an in-depth characterization of these novel ADPRCs. Thus, the development of a more sensitive assay for detection of ADPRC activity is a critical factor in the advancement of our knowledge of this unique multi-functional enzyme family. Further, conventional protein purification strategies have been inadequate for isolation of the novel ADPRCs as a result of the low basal activity. To circumvent this problem, a molecular approach based on protein motif has been proposed in these studies based on the idea that enzyme function is related to protein structure.

Regulation of ADPRC Activity

Previous research has shown that ADPRC activity is highly regulated. Numerous pathways have been shown to activate the cADPR-pathway including metabolic factors [138], G-protein coupled receptors (GPCRs) [20, 139], and agonists that target

intracellular receptors [140]. Studies have also shown that stimulation of cell surface receptors can lead to activation of the cADPR-pathway such as the T-cell receptor mediated increase of cADPR production by activation of the TCR/CD3 receptor complex in T-lymphocytes [132].

It has been shown that GPCR systems, including cholecystokinin octapeptide (CCK8) and CCK in smooth muscle and pancreatic acinar cells, are involved in the cADPR-signaling pathway. Studies conducted in intestinal longitudinal smooth muscle were the first to reveal the mechanism involving a GPCR system to elicit the cADPR signaling pathway [140]. It was found that CCK-8 was capable of both increasing intracellular cADPR levels in a concentration dependent fashion as well as mobilizing calcium from ryanodine gated stores [20]. In this mechanism, CCK first activates a small and highly localized calcium release from NAADP-sensitive stores, which by itself is not sufficient to trigger calcium spiking, but requires the amplification by the cADPR sensitive stores via CICR. The calcium signal amplified by the cADPR mechanism further activates calcium mobilization from IP_3 sensitive calcium stores, which is ultimately responsible for initiating calcium spiking [141]. This signaling scheme proposes NAADP as a trigger, the cADPR stores as an intermediate amplifier, and the IP_3 stores as the ultimate activator of hormone induced calcium spiking [142]. Further, ACh was shown to provoke cADPR induced calcium mobilization in duodenal smooth muscles of rat via the M2 muscarinic cholinergic receptor subtype [139] and in airway smooth muscle cells [143, 144]. Muscarinic cholinergic receptor subtypes M2 and M3 are also present in intestinal smooth muscles. Studies utilizing methoctramine, an inhibitor of the M2

receptor subtype, showed that the ADPRC/cADPR signaling pathway in duodenal smooth muscle cells is mediated by the receptor M2 subtype [139]**.** A similar finding was observed in airway smooth muscle cells [144]. Collectively, these studies revealed regulation of cADPR/ADPRC activity by contractile agonists.

Further, it has been shown that CD38 expression is increased by inflammatory cytokines including TNF- α, resulting in an enhanced intracellular calcium response to contractile agonists [145]. The increase of CD38 expression has been shown to be mediated via MAPK signaling via NF-κB and AP-1, and can be attenuated by anti-inflammatory glucocorticoids via inhibition of MAPK signaling [146-148]. Also, it has been shown in porcine airway myocytes that the calcium release induced by ACh and bradykinin to be attenuated by 8-Bromo-cADPR, a cADPR antagonist [144]. These results suggest that activation of GPCRs in airway smooth muscle cells is responsible for cADPR induced calcium mobilization. This mechanism of activation has also been investigated in testes, where endothelin has been shown to activate cADPR induced calcium release in peritubular smooth muscles [149]. In these studies it was not shown how GPCR activation leads to activation of ADPRC and/or elevation of cADPR levels.

Furthermore, the CD38/cADPR signaling pathway has also been implicated in VSMCs, coronary arteries [73] and cardiac myocytes [120, 150, 151]. Evidence suggests activation of sympathetic ß-adrenergic GPCRs in VSMCs results in increased cADPR synthesis and cardiac function [152]. Additionally, It has been shown that contractile agonists are capable of initiating the CD38/cADPR signaling pathway via the M1

receptor subtype, which leads to calcium mobilization that results in VSMC vasoconstriction [153, 154]. Investigations have also shown that NAADP plays a role in endothelin-1 (ET-1) mediated vasoconstriction in coronary arteries [131] and renal afferent arterioles [155]. Further, it has been shown NAD(P)H oxidase (NOX) superoxide production in coronary arterial myocytes is mediated by the cADPR-RyR/Ca^{2+} signaling pathway [156]. ADPRC has also been implicated in the Renin/Ang signaling pathway [157]. Studies have shown that Ang II and NE, vasoconstrictor peptides, signal through the GPCR receptors to serve as a mediators of blood pressure increase in both renal afferent arterioles and cardiac myocytes from rats [158, 159]. In addition, a signaling pathway involving Ang II receptors in ventricular muscle cells shown to mediate increases in cADPR synthesis, has been implicated in cardiac function and development [160]. It has been shown that this Ang II-mediated hypertrophic response is attenuated by 2,2'-dihydroxyazobenzene (DAB) [161]. cADPR induced calcium release also been shown to play a key role in mediating hypoxic pulmonary vasoconstriction [162]. Previous studies indicated that cADPR-dependent vasoconstriction in this condition is caused by an elevated NADH/NAD ratio resulting in inhibition of cADPR hydrolase activity which leads to an increase in cADPR production [163].

Further, recent investigations suggest that cyclic nucleotide systems including cGMP/Nitric Oxide (NO) in sea urchin eggs, PC12 cells, and VSMCs as well as cAMP in adrenal chromaffin cells activate cADPR production [164-166]. It has been shown in sea urchin that there is a relationship between the cADPR- and NO-signaling pathways [164],

which has implications in neuronal processes including memory consolidation [167, 168] as well as in processes such as kidney filtration rate regulation [169, 170]. Furthermore, it has been shown that stimulation of ADPRC via this mechanism is mediated by cGMP-dependent kinase phosphorylation [166].

Metabolic factors such as glucose have also been shown to participate in the cADPR/ADPRC-signaling pathway [100, 138]. Pancreatic ß-cells respond to high concentrations of glucose by secreting insulin. Previous investigations have indicated an elevated cADPR in response to a glucose stimulated increase in ATP, resulting in calcium release from RyR gated stores, which in turn induces insulin secretion [171].

Recently, other regulators of ADPRC Activity including abscisic acid (ABA) have been identified that provide an example of how CD38 is regulated via phosphorylation [172-174]. The signaling pathway triggered by ABA, a pro-inflammatory cytokine, in granulocytes involves engagement of adenylyl cyclase, cAMP production, and PKA-mediated phosphorylation of the ADPRC CD38 [175, 176]. Furthermore, investigators have shown that the calcium signaling mediated by ABA has been implicated in lytic vs. chronic stage growth [177].

Inflammatory mediators such as interleukin-8 have been shown to induce the association of non-muscle myosin heavy chain IIA (MHCIIA) with CD38 via PKG-mediated phosphorylation leading to increased calcium concentration, cADPR, and LAK cell migration as a result of increased CD38 internalization and activation [178]. Also, recent evidence indicates that $NAADP^+$ acts as a pro-inflammatory cytokine that mediates

calcium increases via activation of P2Y11 purinergic receptors in granulocytes leading to cellular activation [179]. Further, it has been shown that a SR associated cyclase distinct from CD38 is inhibited by PKC-dependent phosphorylation and may participate in modulation of cADPR levels [129].

From this it is not only clear that ADPRC are regulated, but also ADPRC activity is implicated in a diverse set of cellular processes. Thus, it is imperative to further elucidate the mechanisms by which ADPRCs are regulated in order to better understand these cellular processes. We have shown that a novel ADPRC present in heart cytosol is regulated via a PKC-mediated phosphorylation mechanism and its inhibited by zinc, providing evidence that it is indeed a novel ADPRC distinct from previously identified ADPRCs.

Significance

The ADPRC family produces three molecules (cADPR, ADPR and NAADP) known to raise intracellular calcium in multiple cell types [17, 180, 181]. Intracellular calcium is known to regulate key biological functions [182]. Identification and characterization of the enzymes that generate these molecules and knowledge regarding the regulation of these enzymes is important to our overall understanding the mechanisms by which basic biological processes are controlled.

One product of ADPRCs, cADPR, has been shown to play an important role in a variety of cellular processes including: long-term synaptic signaling and memory formation [101], insulin secretion from beta cells [100], contractility in arterial smooth muscles [73, 111], calcium ion dynamics and contractility in airway smooth muscles [145], calcium homeostasis in cardiac myocytes [120, 151], myocyte contraction [183, 184], and ischemia/reperfusion injury of the heart [185], oxytocin release [186-188], cellular metabolism and cell cycle control [189, 190]. Another product of ADPRCs, NAADP, has also been shown to play an important role in vasoconstriction of coronary arteries [131].

The ADPRC signaling pathway has also been implicated in multiple biological processes including neurodevelopmental disorders [186], circadian timekeeping mechanism in plants [191, 192], diabetic nephropathy [193], long-term hypoxia [194], social behavior [173, 188, 195, 196], spatial learning ability [197, 198], cell adhesion events [199, 200] and chemotaxis [201-205], cell signaling [206], antibody responses [207], regulation of energy and fat metabolism [208], hydrogen peroxide-induced beta cell death [209], renal blood flow [159] and urine output [210], osteoclastogenesis [211], cytokine production upon antibody ligation [212, 213], apoptosis [214-216], phagocytosis [217], and microglial activation [218].

There are multiple forms of mammalian ADPRC, many of which have not yet been identified or characterized [11, 12, 72-79]. By performing an in depth characterization of novel ADPRCs, insight will be provided into the function and regulation of ADPRCs and

the complexities of calcium signaling be further elucidated. A better understanding of these regulatory mechanisms can provide a foundation for the intelligent design of drugs and as a prognostic marker for prominent diseases including cardiovascular disease [128], coronary artery disease [131], hypertension [158], pulmonary hypertension [162, 163, 219], diabetes [100, 138], cancer [220, 221], multiple sclerosis [222], neurodegeneration [186, 223-225], Huntington's disease [224], HIV-1 and AIDS [223, 226, 227] , asthma [146, 228], inflammatory diseases [178, 204] and those implicated in cellular damage [173]. Thus, it is imperative to identify novel ADPRCs and elucidate the mechanisms by which the members of this complex family of enzymes are regulated. The purpose of the studies highlighted in this thesis was to develop a sensitive, high-throughput assay for more accurate detection of ADPRC activity to allow for better characterization and identification of ADPRCs. Further, this assay was employed to screen $CD38^{-/-}$ mouse tissues for ADPRC activity and to characterize the novel ADPRC activity identified in the cytosol of various mouse tissues as well as to test novel ADPRC candidates unveiled using a molecular approach to search the genome to identify novel ADPRC candidates based on protein structure.

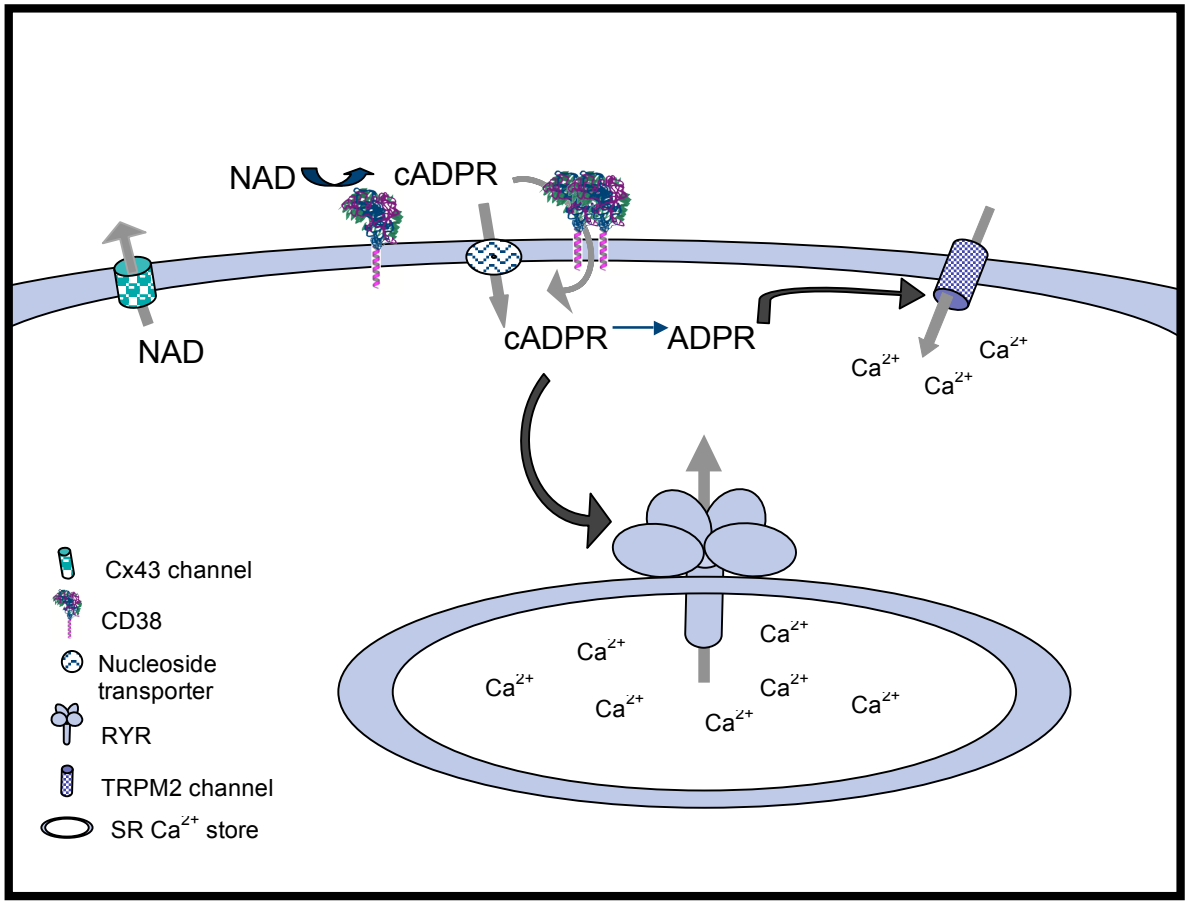

Figure 1. **Role of ADP-Ribosyl Cyclases/cADPR in Cellular Calcium Ion Dynamics**

CD38 is an ectoenzyme that displays discrete activities at the cell surface and is switched off in the absence of NAD^+. NAD^+ is exported from the cell via Cx43 channels to reach the extracellular CD38 target, where it is metabolized to cADPR, which needs to reach its intracellular target to release calcium from the SR. CD38 dimers and nucleoside transporters have both been shown to act as cADPR-transporting proteins that allow cADPR to reach the intracellular RYR gated calcium stores. Altogether this scheme presents a solution for what has previously been described as a topological paradox in the ADPRC mediated calcium-signaling pathway.

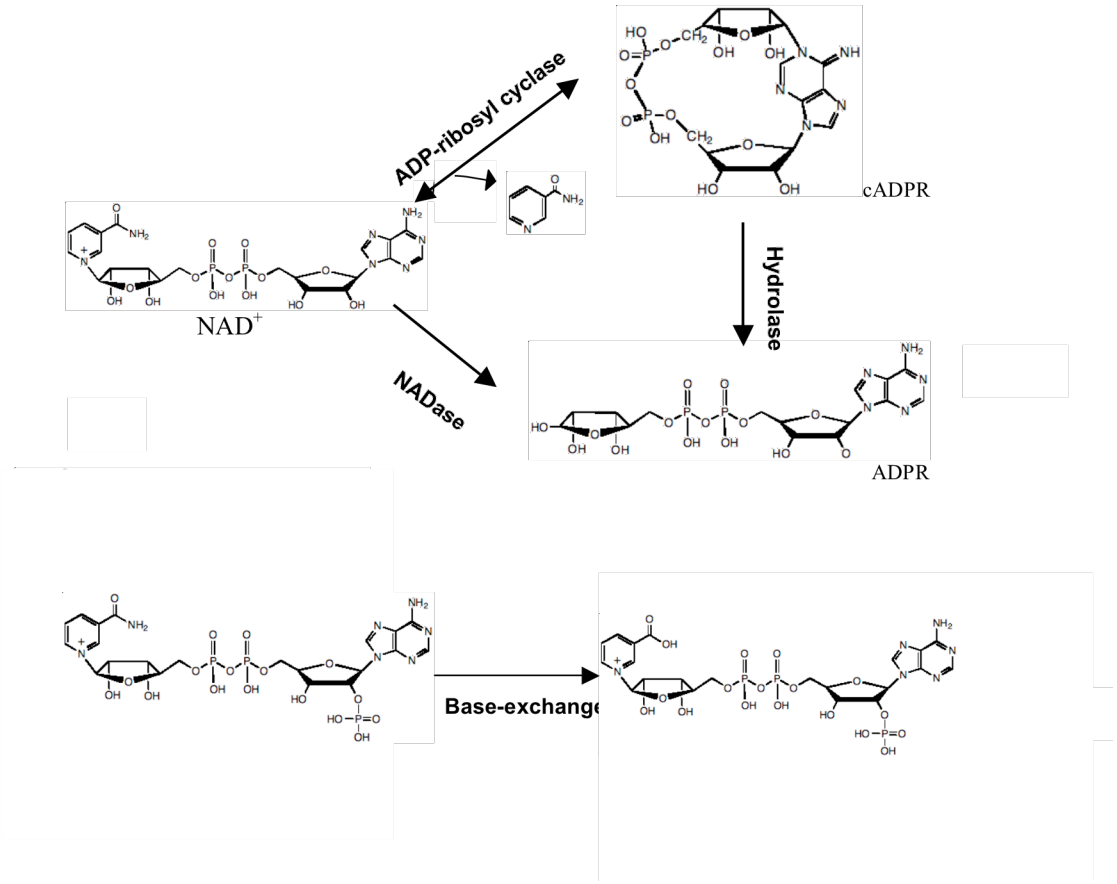

Figure 2. **Enzymatic Activities of the ADP-ribosyl Cyclase Family**

ADPRCs are responsible for the catalytic production of three metabolites, cADPR, ADPR, and NAADP, which are involved in calcium signaling. NAD^+ is converted to cADPR via ADPRC activity, which can be hydrolyzed to NAD with the addition of water. ADPR can also be produced from NAD^+ via NADase activity. Finally, a base-exchange reaction is responsible fro the catalytic conversion of NAD to NAADP.

Chapter 2

Reverse Cyclase Assay:

a sensitive cycling assay for ADP-ribosyl cyclase activity

ADP-ribosyl cyclases (ADPRCs) are multi-functional enzymes responsible for the catalytic production of at least three calcium-mobilizing messengers including cADPR, ADPR, and NAADP. Among the reactions catalyzed by ADPRC is the reaction that involves the cyclization of the linear nucleotide NAD into cADPR and nicotinamide, which is a potent calcium releasing second messenger. Recent evidence suggests that there are novel ADPRCs with low basal activity, which have not been characterized or identified. Given their low basal activity, a highly sensitive assay is required for in-depth studies to characterize and identify the novel ADPRCs. In this study, a previous cycling method for the determination of cADPR was modified to develop a highly sensitive, high-throughput assay that does not involve the timely processing demands of earlier methods. The assay is based on the reversibility of ADPRCs. In the presence of cADPR and high concentration of nicotinamide, ADPRCs catalyze the production of NAD from cADPR. This unique feature contributes to the high specificity of this assay for accurate detection of ADPRC activity. This reaction was coupled to a cycling assay for NAD, which utilized alcohol dehydrogenase (ADH) and diaphorase, to amplify the NAD produced in the first step and convert it to a fluorescent product resorufin. This assay has been shown to measure NAD produced by ADPRC in concentrations as low as the femtomolar range. Using this assay, we were able to show that the timecourse and kinetics of ADPRC of *Aplysia* cyclase and CD38 were in agreement with previously used methods. The specificity, sensitivity and high-throughput nature of this assay will provide a powerful tool useful in identifying and characterizing novel ADPRCs.

Introduction

The ADPRC family of enzymes is composed of several multi-catalytic members including *Aplysia* cyclase [1], CD38 [2-7], CD157 [8, 9], and three sea urchin ADPRCs [10-12]. ADPRCs play a key role in calcium homeostasis [13, 14, 15] as they catalyze the production of three important calcium mobilizing metabolites namely cADPR, ADPR and NAADP [16, 81]. Current methods used for detection of ADPRC activity include HPLC [229], a bioassay [230], radioimmunoassay [231, 232], and the NGD assay [233]. Interestingly, despite that the well-characterized members are known to be membrane bound proteins, recent evidence shows that novel forms of both membrane bound and cytosolic forms of ADPRC exist [11, 12, 72-79]. However, these novel members of the ADPRC family have been a challenge to identify and characterize due to the low basal enzymatic activity [79]. In order to better characterize and identify these novel ADPRCs, a more sensitive assay to detect their enzymatic activities is necessary. Among the reactions catalyzed by ADPRC is the conversion of NAD to cADPR and nicotinamide [1, 2, 5-7, 108]. We have developed a sensitive assay, which from here on will be referred to as the reverse cyclase assay (RCA), for ADPRC activity based on the reverse of this reaction (Figure 3). Previous studies have shown that a high concentration of nicotinamide pushes the reaction in reverse to form NAD as a product [124]. We have taken advantage of this property of nicotinamide to develop an assay in which NAD is produced by the reverse ADPRC reaction, and the NAD produced is detected by a cycling system that includes ethanol, alcohol dehydrogenase (ADH), FMN, diaphorase, and resazurin. The produced NAD is converted to NADH by ADH, which is utilized by

diaphorase to reduce resazurin to produce a fluorescent product resorufin in this reaction scheme. The resorufin fluorescence serves as an indicator of ADPRC activity. The cycling method amplifies NAD over a thousand fold, which enables ready detection of ADPRC activity through the indicator reaction whereby fluorescence is produced [234]. The RCA is conducted both in the absence and presence of nicotinamide so that any contaminating NAD(H) can be accounted for. This assay is the most sensitive method for measuring ADPRC activity shown to detect as low as 25 femtomoles of NAD and may have the degree of sensitivity required to identify and characterize novel ADPRCs. A better understanding of the ADPRC family of enzymes and it's members will provide insight into the function and regulation of ADPRCs, further elucidate the complexities of calcium signaling and with provide useful information about the diseases implicated in the ADPRC/cADPR mediated signaling pathways.

Materials and Methods

Reverse Cyclase Assay

Samples were incubated at 25ºC for a set period of time with cADPR (0.046-5.0 mM) and an excess nicotinamide (0.062-8.0 mM), which facilitated the conversion of cADPR

to NAD in the presence of ADPRC. The reactions were carried out in 96-well plates (Sarstedt) with a total reaction volume of 50 µl. The samples were filter stopped with Millipore IP membranes using a vacuum manifold prior to proceeding to the next reaction step. These IP membranes were made of PVDF and effectively removed protein from the sample. The samples were diluted with 0.1 M sodium phosphate (J.T. Baker) and transferred to 384-well plates (Corning). The initiation of the second step involved the addition of 40 µl of the filtered reaction mixture diluted in 0.1 M sodium phosphate pH 8.0, to 40 µl of the RCA reagent to amplify NAD produced and convert it to the fluorescent product resorufin (Figure 1). The RCA reagent composed of final concentrations of 0.76% ethanol (Pharmco), 40 µg/ml ADH (Sigma), 0.04 µg/ml diaphorase from *Clostidium klyveri* (Sigma), 4 µM FMN (Sigma) and 2 µM resazurin (Sigma) in sodium phosphate pH 8.0. NAD is converted to NADH by ADH, which was utilized by diaphorase to reduce resazurin to produce the fluorescent product resorufin. The resorufin fluorescence served as an indicator of NAD produced in the first step as a result of ADPRC activity. The time dependent increase in resorufin fluorescence was measured for 25 cycles with fluorescence plate reader (*FLUO*star *Galaxy*) set with the excitation at 544 nm and emission at 590 nm. As the cycling method employed to amplify NAD was incredibly potent, the diaphorase was treated with activated charcoal (Sigma) 1:1 for 20 minutes, followed by removal of the charcoal via centrifugation (13,000 x g) to eliminate any contaminant NAD. Upon removal of contaminant NAD, the presence of ADPRC was required for the production of NAD. The difference in fluorescence produced by samples incubated in the presence and absence of

nicotinamide, which is also necessary for NAD production, served as a control to identify background resultant of background NAD or NADH present in the samples.

NAD Standard Curve

The RCA was verified and calibrated by generating a standard curve with varying NAD concentrations. 40 µl samples containing known concentrations of NAD from 0-1500 fmol in sodium phosphate pH 8.0 were added to 40 µl of RCA reagent in a 384-well plate. The RCA reagent consisted sodium phosphate pH 8.0, 0.76% ethanol, 40 µg/ml alcohol dehydrogenase, 2 µM resazurin, 0.04 µg/ml diaphorase, and 4 µM FMN. The cycling reaction was allowed to proceed for 25 cycles on a fluorescent plate reader with the excitation at 544 nm and emission at 590 nm. The slope of the linear regression line of time dependent increase in resorufin fluorescence was used to determine the rate of resorufin fluorescence increase. A typical NAD standard curve is shown in Figure 4. The equation of the linear regression of the NAD concentration dependent increase in fluorescence was used to determine concentrations of NAD in unknown samples in all future RCA.

Aplysia Cyclase and CD38 cADPR RCA Timecourse

Aplysia Cyclase and rCD38 were incubated in 96-well plates with 0.42 mM cADPR in

the presence or absence of 8.0 mM nicotinamide at 25°C for various time frames up to 5 minutes. Also, varying concentrations of rCD38 (0-0.04 μg) were incubated with 0.42 mM cADPR in the presence or absence of 8.0 mM nicotinamide at 25°C for 2.5 minutes. The samples were filtered with Millipore IP membranes with a vacuum manifold to stop the reaction and the RCA carried out under the conditions described already.

Aplysia Cyclase and rCD38 HPLC Timecourse

HPLC was used to verify the timecourse of *Aplysia* cyclase and rCD38 measured by the RCA. A master reaction with 160 μl of 20 mM Tris-HCl (Fisher Scientific) buffer, 160 μl of sample (2.1 nM *Aplysia* cyclase or rCD38), 40 μl 20 mM nicotinamide, and 40 μl of 4.25 mM cADPR was incubated at 25ºC for various timepoints from 30 seconds to 60 minutes. 50 μl of the reaction was removed at each timepoint and 25 μl of ice-cold 1M HCl was added to stop the reaction. The samples were filtered with Millipore IP membranes. 15 μl of 2M Tris-base was added and samples were diluted to 200 μl with ddH_20. Samples were run on a 0.46 x 15 cm LC18T (Supilco) reverse phase column using an ammonium formate gradient system. 150 μl of each sample was added to an equal volume of 5.0 mM NH_4 formate and 200 μl of 20 mM Tris-HCl and the total 500 μl sample was injected to the column. The A solvent constituted of 5.0 mM NH_4 formate and the B solvent was 100% methanol. A gradient from 0%-70% B was initiated over 10 minutes and the column was eluted at a flow rate of 1 mL/minute with fractions collected every three minutes. Injecting known amounts of NAD onto the system under identical

conditions, a standard curve of NAD was generated and the NAD concentration of the unknown samples was calculated from peak integration.

Aplysia Cyclase and CD38 Kinetics for cADPR and Nicotinamide

Kinetic properties of *Aplysia* cyclase and CD38 for cADPR and nicotinamide were measured using the RCA. The nicotinamide kinetics of *Aplysia* cyclase and rCD38 were determined by incubating 2.5 nM of each with 0.371 mM cADPR and varying concentrations of nicotinamide (0-4 mM) at 25°C for 30 seconds and 90 seconds respectively. Also, the cADPR kinetics of *Aplysia* cyclase and rCD38 were determined by incubating 2.5 nM of each with 7.5 mM nicotinamide and varying concentrations of cADPR (0-4 mM) at 25°C for 30 seconds and 90 seconds respectively. The samples were filtered with Millipore IP membranes with a vacuum manifold to stop the reaction and the RCA carried out under the conditions described already. Further, the difference in fluorescence produced by samples incubated in the presence and absence of nicotinamide, which is also necessary for NAD production, served as a control to identify background, which was routinely subtracted. The V_{max} and K_m values of *Aplysia* cyclase and rCD38 were calculated using non-linear regression Michaelis-Menten Kinetics with GraphPad Prism software.

Results

NAD Standard Curve

Samples containing varying concentrations of NAD in sodium phosphate pH 8.0 were incubated with the RCA reagent and rate of resorufin production was measured with a fluorescence plate reader (excitation 544 nm, emission at 590 nm) for 25 cycles. The rate of increase in resorufin fluorescence as a function of time was derived from the slope of a linear regression line (Figure 4). The rate of resorufin production as a function of NAD concentrations measured was linear (r^2 value = 0.999) for NAD concentrations ranging from 0-1500 fmol. The equation of the linear regression line of the NAD standard curve was used to calculate NAD concentrations of unknown samples.

Aplysia Cyclase and rCD38 RCA and HPLC Timecourse

Aplysia cyclase and rCD38 were incubated with cADPR in the presence or absence of nicotinamide followed by the RCA reagent. The resulting resorufin fluorescence as an indicator of NAD produced was determined using a fluorescence plate reader (excitation 544 nm, emission at 590 nm). The RCA was successfully used to detect ADPRC activity of *Aplysia* cyclase and rCD38. A timecourse of *Aplysia* cyclase (Figure 5) and rCD38 (Figure 6) activity showed that NAD formation is time dependent and linear up to 5

minutes as measured by the RCA. The RCA timecourse data of *Aplysia* cyclase was confirmed using an HPLC based method, which also showed NAD formation to be time dependent and linear (Figure 5). Further, increasing rCD38 protein concentrations resulted in a linear increase of NAD production as measured by the RCA (Figure 7).

Aplysia Cyclase and CD38 Kinetics

Aplysia cyclase and rCD38 samples were incubated with cADPR in the presence or absence of varying concentrations of nicotinamide followed by the RCA reagent. The resulting resorufin fluorescence was measured using a fluorescence plate reader as an indicator of NAD produced. At high cADPR, rCD38 was found to have a V_{max} of 2458 pmol NAD/min*µg and Km for nicotinamide of 0.46 mM (Figure 8), and *Aplysia* cyclase was found to have a V_{max} of 1837 µmol NAD/min*mg and K_m for nicotinamide of 0.26 mM (Figure 9). At high nicotinamide, rCD38 was found to have a V_{max} of 3019 pmol NAD/min*µg and K_m for cADPR of 0.63 mM (Figure 8), and *Aplysia* cyclase was found to have a V_{max} of 1922 µmol NAD/min*mg and K_m for cADPR of 0.42 mM (Figure 11).

Discussion

Previous methods to measure ADPRC activity include HPLC [229], a bioassay [230, 235], a radioimmunoassay [231, 232], and the NGD assay [233]. Currently, the assays that have been previously developed to detect ADPRC activity are not sensitive enough to accurately detect the low basal enzymatic activities of novel ADPRCs [79], presenting a challenge in the successful identification and characterization of these novel ADPRCs. In order to better characterize and identify novel ADPRCs and have a more complete understanding of this complex family of multi-functional enzymes, the development of a more sensitive assay to measure the enzymatic activities of ADPRCs is imperative. In this report, the RCA has been described as a sensitive assay, with its detection limit in the femtomolar range (detecting NAD levels as low as 25 fmol), useful for measurement of ADPRC activity and was developed by a minor modification of the previous cycling assay for determination of cADPR levels [234]. The RCA is a two-step reaction, which couples a cycling reaction to amplify NAD with an indicator reaction to produce a fluorescent product [234]. In the first step, the unique feature of the reversibility of the ADPRC reaction was employed contributing to the high specificity of this assay. If ADPRC was present, NAD was produced from cADPR and an excess of nicotinamide, which at high concentrations drives the classic ADPRC reaction in reverse [124]. In the second step, the NAD produced in the first step was amplified over a thousand-fold. The amplified NAD was coupled to a reaction that resulted in the production of resorufin, the fluorescent product [234], which led to a linear increase in fluorescence with time. Slopes of initial rates of resorufin produced were used to determine ADPRC velocity,

which was linear with respect to protein concentration and time. The ability to monitor increasing resorufin fluorescence with a plate reader lends this assay to be a convenient high-throughput technique capable of measuring 384 samples simultaneously. In samples incubated with cADPR and an excess of nicotinamide, we have shown that the rate of resorufin production as a function of time and protein concentration to be linear. Finally, we have shown that the nicotinamide and cADPR kinetics of *Aplysia* cyclase and rCD38 as measured by the RCA to be comparable to methods previously reported. The RCA is the most accurate, sensitive assay available for the detection of ADPRC activity with the added feature of being high-throughput with reduced handling of samples than previously reported assays. This assay will be a powerful tool that may be employed to identify and characterize novel ADPRCs. A better understanding of the ADPRC family of enzymes and its members will provide insight into the function and regulation of ADPRCs and further elucidate the complexities of calcium signaling. This will ultimately lead to a better understanding of prognosis and treatment for the diseases implicated in the ADPRC mediated calcium signaling pathways including cardiovascular disease [128, 152], coronary artery disease [131], hypertension [158], pulmonary hypertension [162, 163, 219], diabetes [100, 138], cancer [220, 221], multiple sclerosis [222], neurodegeneration [186, 223, 224], Huntington's disease [224], HIV-1 and AIDS [223, 226, 227] , asthma [146, 228], inflammatory diseases [178, 204] and diseases implicated in cellular damage [173, 236].

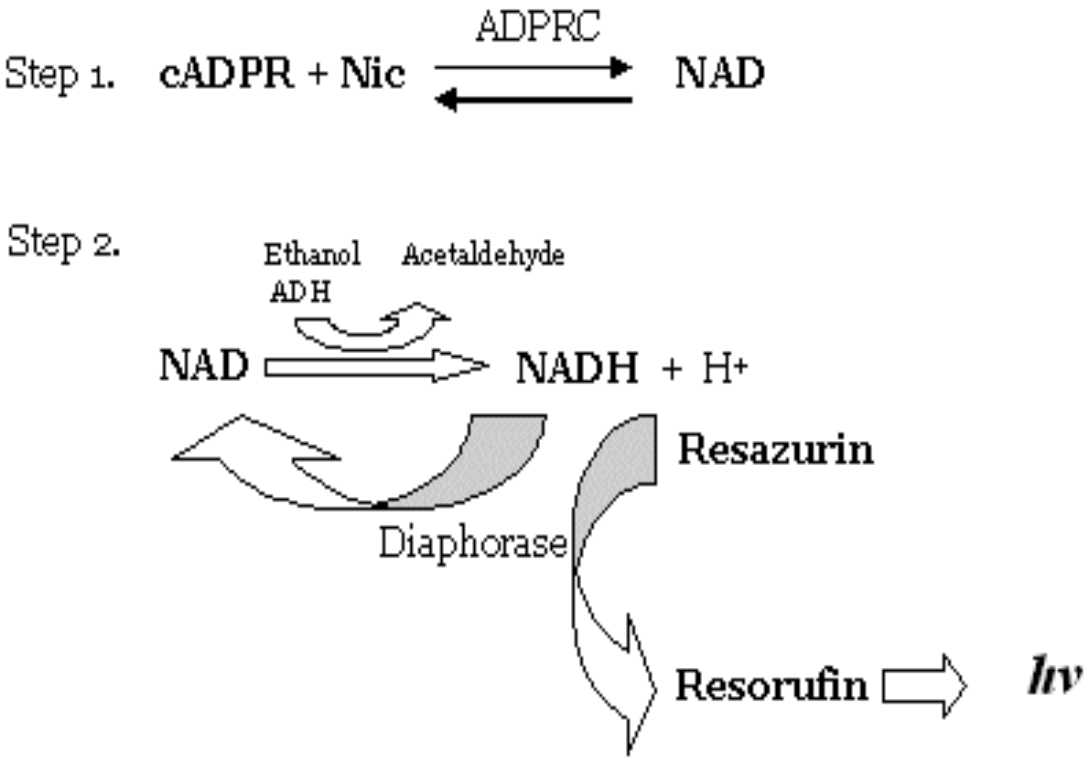

Figure 3. **Reverse Cyclase Assay (RCA) Schematic**

The RCA couples a cycling reaction to amplify NAD with an indicator reaction to produce a fluorescent product resorufin. In step one NAD is produced if ADPRC is present in the sample incubated with cADPR and nicotinamide. The reaction is stopped via IP-membrane filtration before step two is initiated. In the second reaction step NAD is reduced to NADH by ethanol and ADH, a reaction, which is simultaneously coupled with a reaction whereby the fluorescent product resorufin is produced in the presence of NADH. In this reaction scheme, the presence of ADPRC is required for the production of the fluorescent end product.

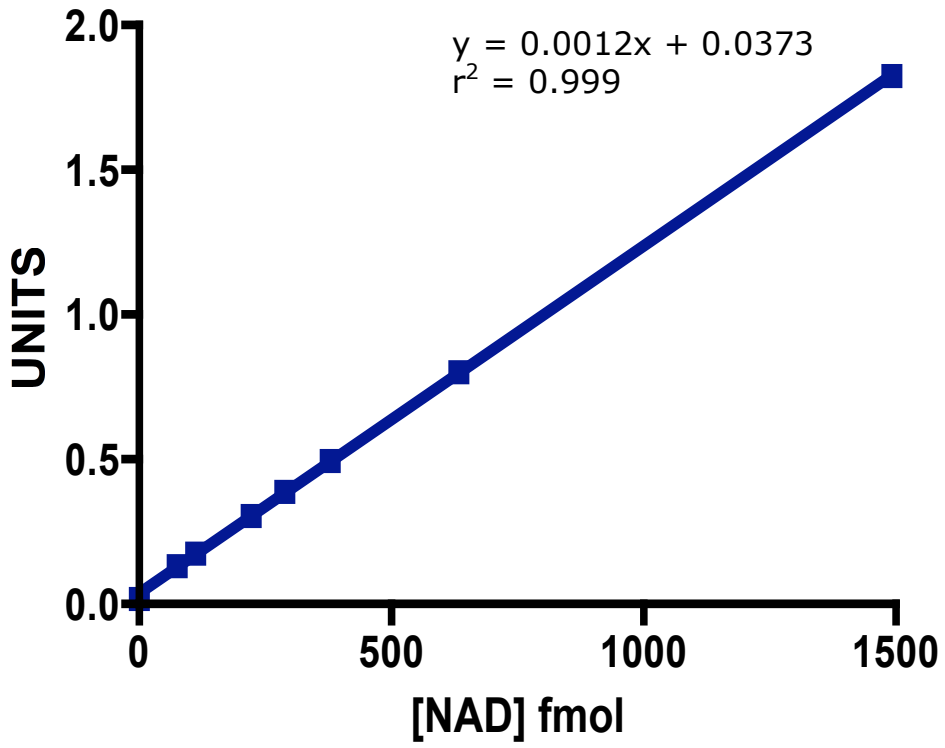

Figure 4. **Standard Curve for NAD**

The reverse cyclase assay reagent was added to varying concentrations of NAD (0-1500 fmol) to generate a standard curve of fluorescence produced as a function of NAD concentration. The rate of fluorescence produced as a function of NAD concentration was shown to be linear with an r^2 value of 0.999.

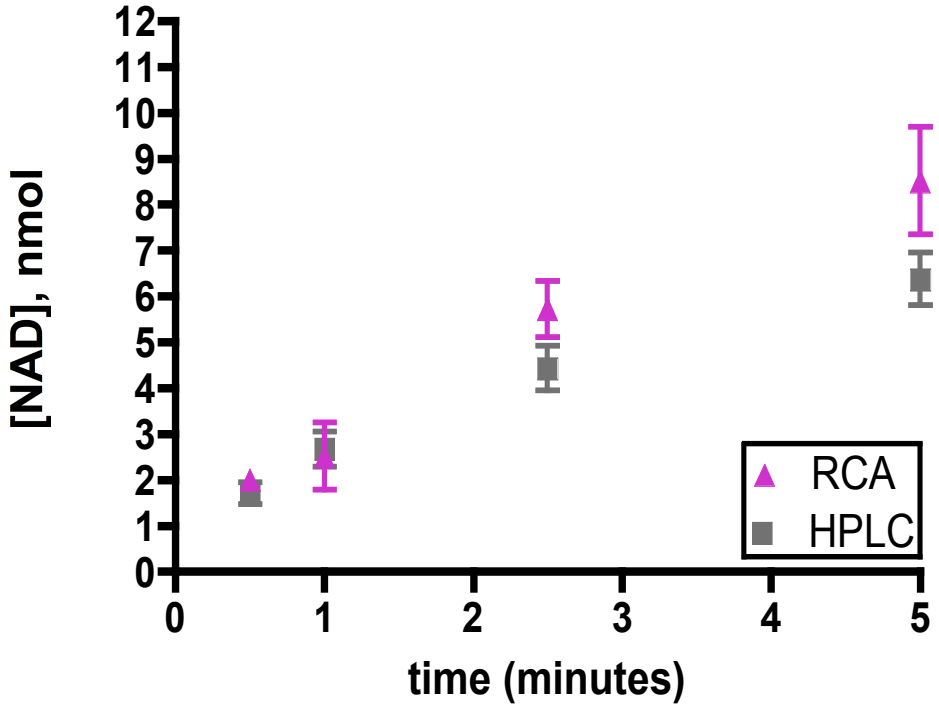

Figure 5. **RCA Timecourse for *Aplysia* Cyclase**

The ADPRC activity of *Aplysia* cyclase was measured as a function of time using both HPLC and the RCA. The formation of NAD was time dependent and linear up to five minutes. The activity ADPRC activity of *Aplysia* cyclase as measured by the RCA was in agreement with the HPLC based method.

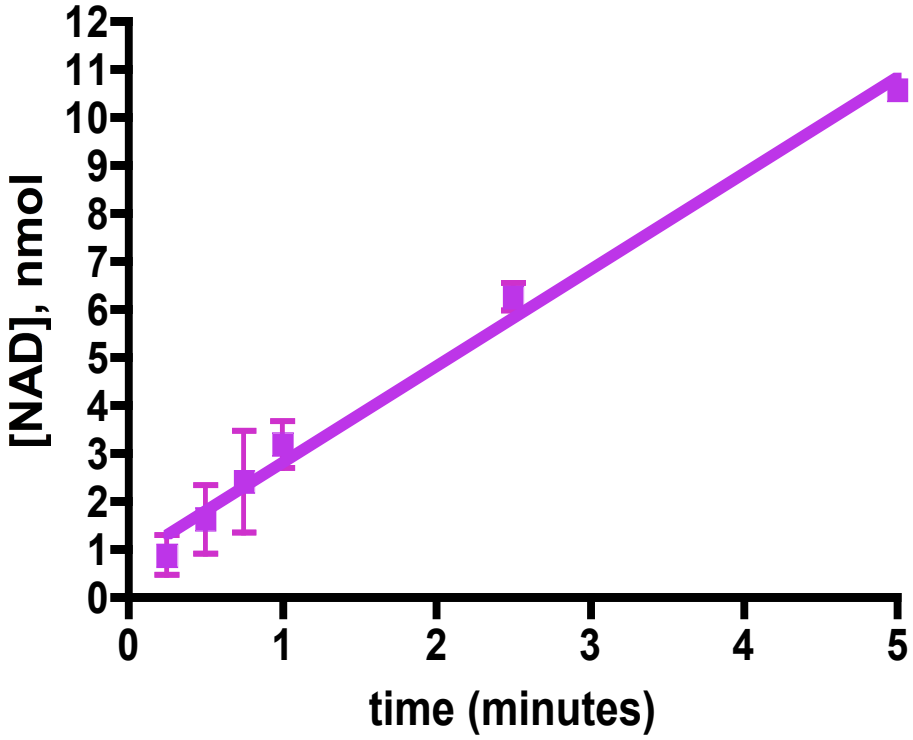

Figure 6. **RCA Timecourse for rCD38**

Samples were incubated with 0.42 mM cADPR in the presence or absence of 8.0 mM nicotinamide and the resulting NAD produced was determined. Controls without nicotinamide were run and have been subtracted. The rCD38 timecourse of ADPRC activity of rCD38 samples incubated with cADPR and nicotinamide for timepoints between 0 and 5 minutes as measured by the RCA was linear with an r^2 value of 0.955.

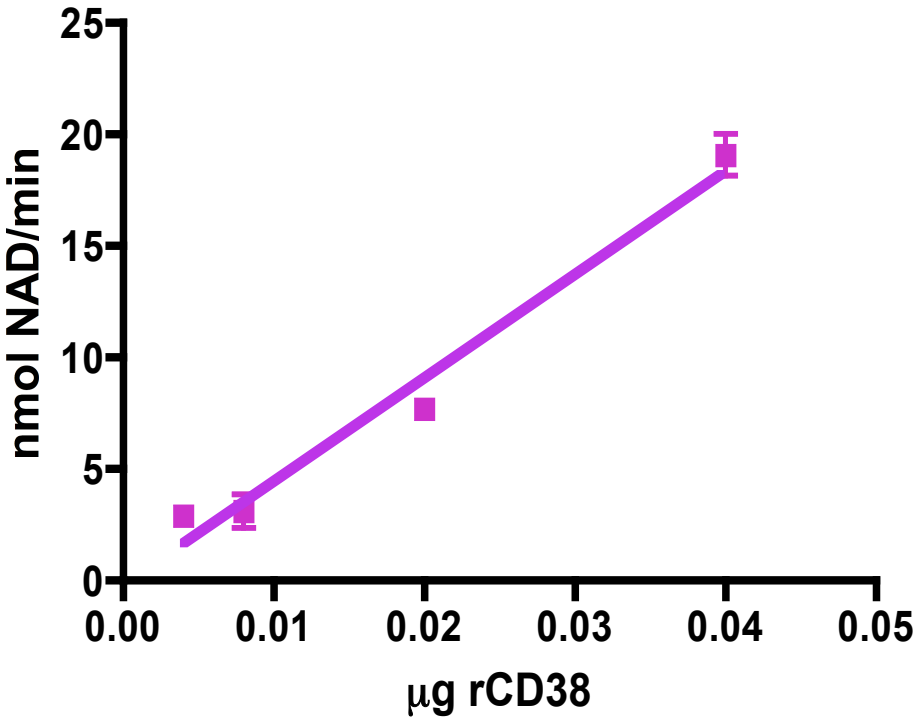

Figure 7. **RCA Activity of rCD38 Protein Concentration Dependence**

The ADPRC activity of varying concentrations of rCD38 (0-0.04 μg) incubated with 0.42 mM cADPR and 8.0 mM nicotinamide was measured with the RCA. The ADPRC activity of rCD38 was shown to be dependent on protein concentration in a linear fashion with an r^2 value of 0.977.

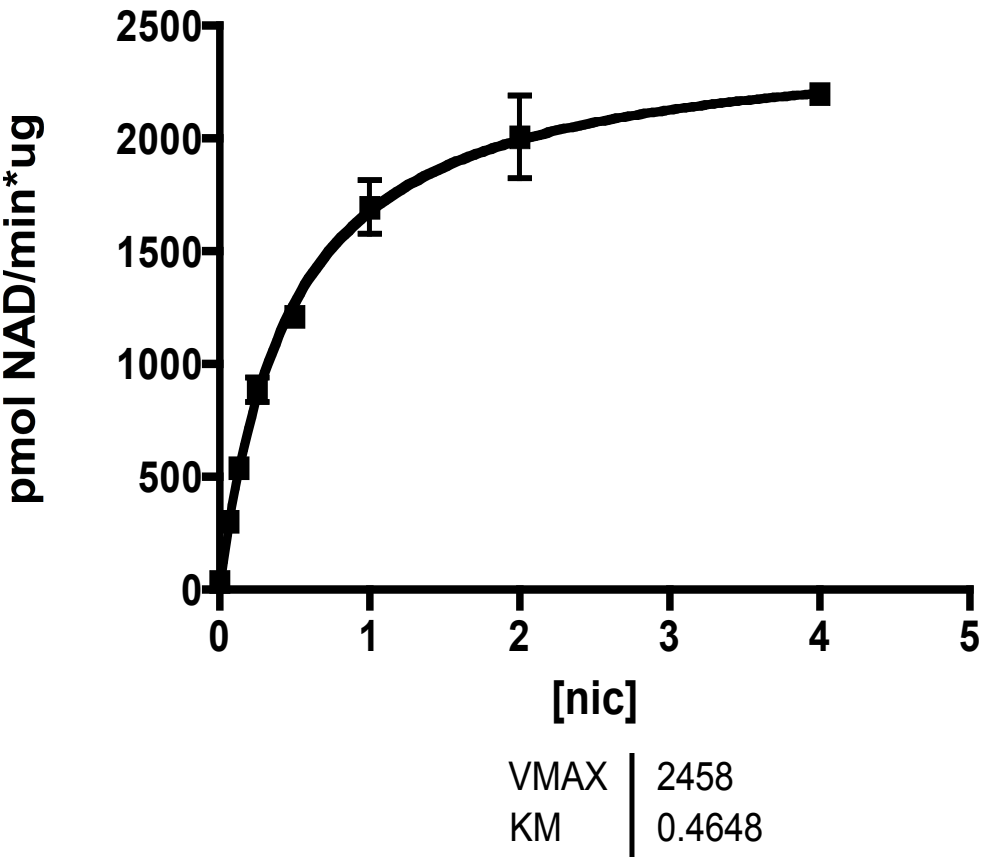

Figure 8. **Nicotinamide Kinetics *for* CD38**

Samples were incubated with cADPR in the presence or absence of varying concentrations of nicotinamide and the resulting NAD produced determined by the RCA. The rCD38 kinetics for nicotinamide were measured by the RCA with a V_{max} of 2458 pmol NAD/min*μg and K_m value of 0.46 mM.

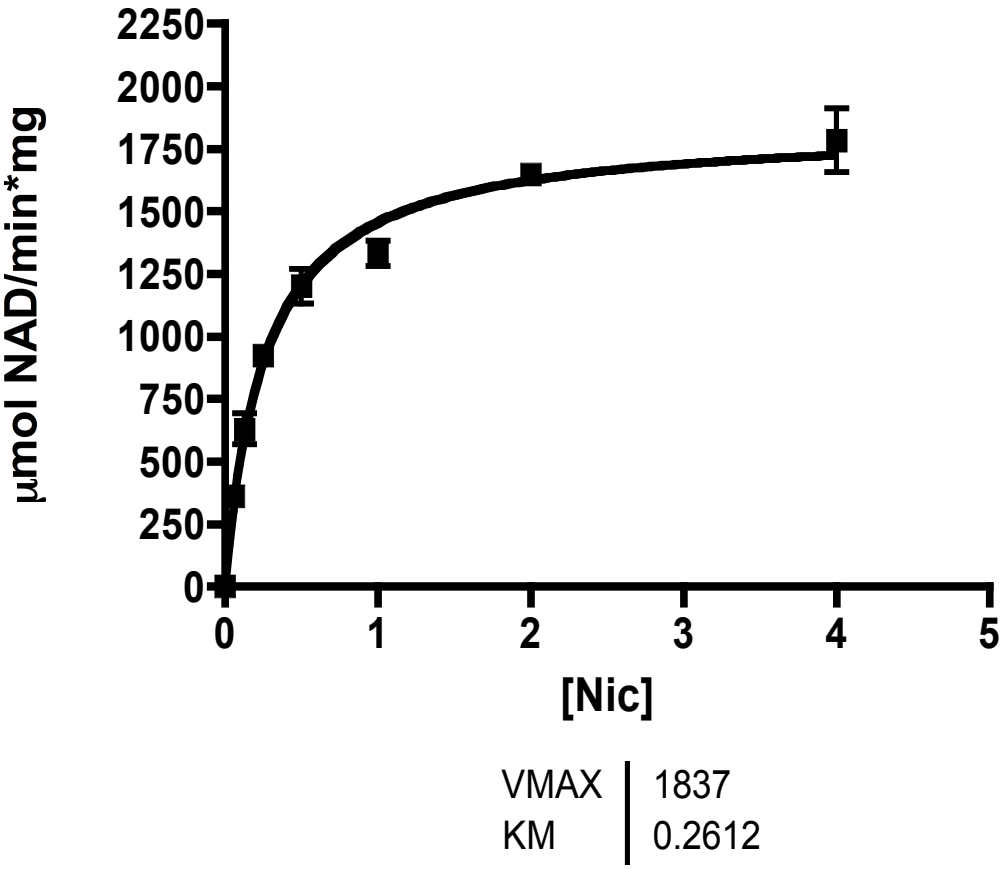

Figure 9. **Nicotinamide Kinetics *for Aplysia* Cyclase**

Samples were incubated with cADPR in the presence or absence of varying concentrations nicotinamide and the resulting NAD produced determined by the RCA. *Aplysia* cyclase had a V_{max} of 1837 µmol NAD/min*mg and K_m value of 0.26 mM.

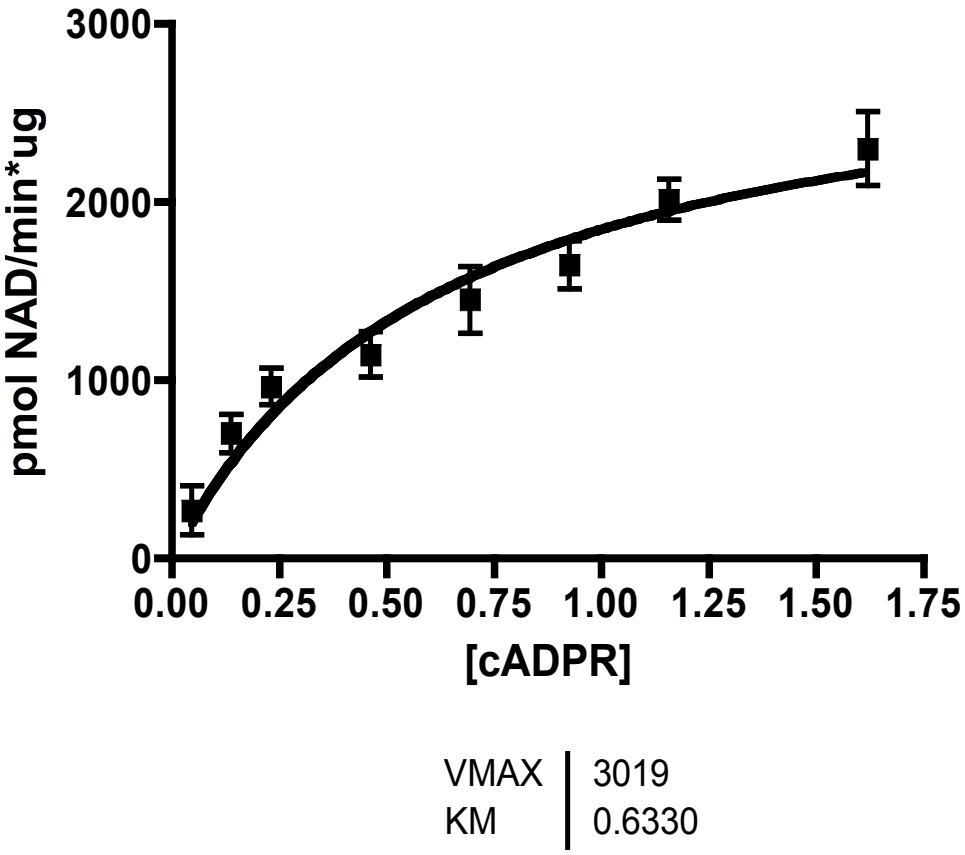

Figure 10. **cADPR Kinetics for rCD38**

Samples were incubated with varying concentrations of cADPR in the presence or absence of nicotinamide and the resulting NAD produced was determined by the RCA. rCD38 had a V_{max} of 3019 pmol NAD/min*μg and K_m value of 0.63 mM.

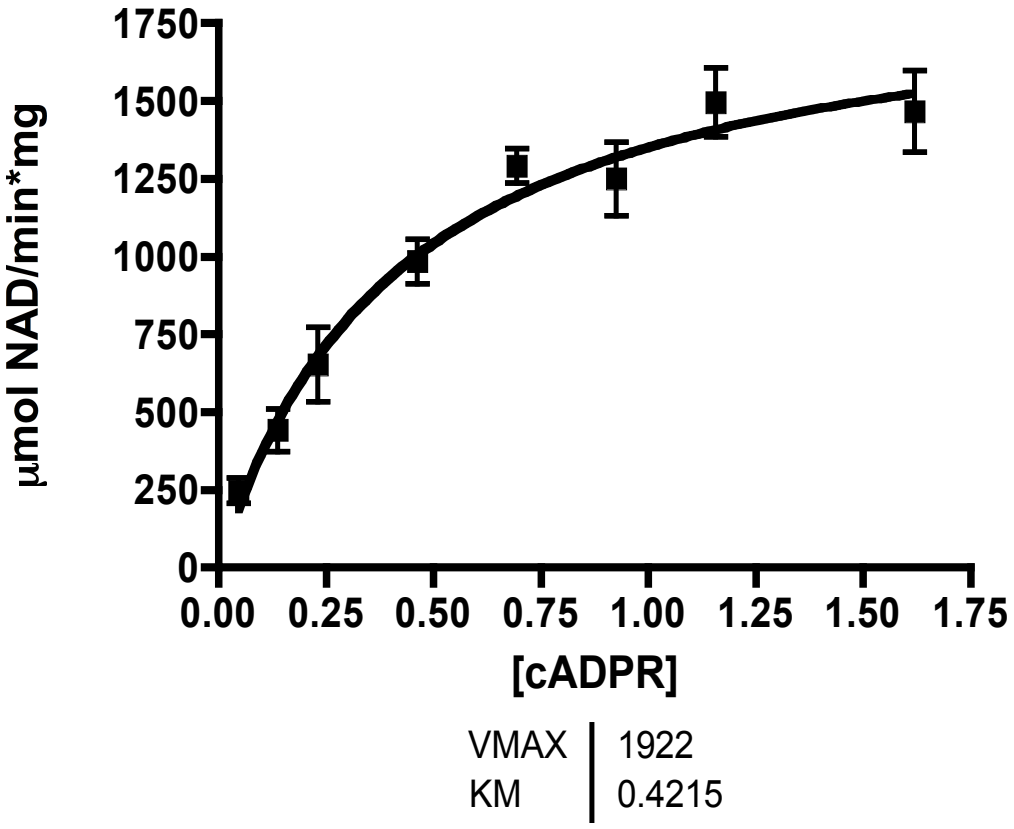

Figure 11. **cADPR Kinetics for *Aplysia* Cyclase**

Samples were incubated with varying concentrations of cADPR in the presence or absence of nicotinamide and the resulting NAD produced determined. *Aplysia* cyclase kinetics for nicotinamide were measured by the RCA with a V_{max} of 1837 µmol NAD/min*mg and K_m value of 0.26 mM.

Chapter 3

Characterization and Identification of Novel Cytosolic ADPRC(s)

CD38 and CD157 have been identified as mammalian forms of ADP-ribosyl cyclase (ADPRC). Recently novel membrane bound and cytosolic ADPRCs that are distinct from CD38 and CD157 have been identified in various tissues by our laboratory as well as others. From this it is clear that there are multiple forms of mammalian ADPRC, many of which have not yet been identified or characterized. The overall goal of the research presented in this chapter is to identify and characterize the novel cyclase(s) present in heart cytosol and determine the mechanism(s) by which cytosolic cyclase(s) are regulated. The existence of novel cyclases(s) localized in the cytosol has implications for a broad range of cellular processes that are influenced by calcium signaling. Characterization of the novel cytosolic cyclase(s) may provide insight into the function and regulation of ADPRCs and further elucidate the complexities of calcium signaling. A more comprehensive understanding of calcium signaling mediated by ADPRCs has implications in better prognosis and treatment methods for diseases implicated in this signaling pathway.

Introduction

The members of the ADPRC family of enzymes [1-12] are responsible for the catalytic production of calcium mobilizing metabolites [10, 14, 16-20] including cADPR, ADPR, and NAADP [13, 14, 15]. CD38 and CD157 are the two well-characterized mammalian membrane bound ADPRCs [2-9]. Previous studies have revealed the existence of membrane bound and cytosolic ADPRCs that are distinct from CD38 [11, 12, 72-79]. Although there are multiple reports of novel ADPRCs in various tissue types, the protein(s) responsible for this enzymatic activity are not yet identified. Characterization and identification of the ADPRC(s) present in the cytosol may provide key insights into the function of the novel cyclase as well as its interaction with and relationship to other members of the ADPRC family. In this study, we further substantiated the claim that novel non-CD38 cyclase(s) exists in various wild-type ($CD38^{+/+}$) and CD38 knock-out ($CD38^{-/-}$) mouse tissues. Using the reverse cyclase assay (RCA), we have shown that there are ADPRC(s) present in the cytosol of both $CD38^{+/+}$ and $CD38^{-/-}$ mouse tissues. Identification and characterization of the novel ADPRC(s) present in the cytosol will increase the understanding of soluble cyclases in mammalian models and their specific roles in these systems. Isolation and purification of the novel cytosolic cyclase(s) is imperative for identification. Conventional purification approaches were utilized to purify the novel cyclase(s) including: size exclusion, ion exchange, dye-conjugated affinity, and hydrophobic chromatography methods. The enzymatic activity of the fractions was examined using a variety of approaches including the RCA and the NGD assay [233]. In order to characterize the novel cytosolic cyclase(s), its properties were

compared to those of known mammalian ADPRCs (CD38 and CD157) [2-9]. Previous studies have revealed that CD38 and CD157 possess multiple activities including ADPRC [1, 2, 5-7, 108] and nicotinic acid adenine dinucleotide phosphate (NAADP) synthesis by base-exchange [19]. Differences in cyclase characteristics have been observed in other known ADPRCs [73], which can be used to compare the properties of the cytosolic activity to the known mammalian cyclases. In this study, we have shown that zinc, a known activator of CD38 and CD157 activity [126], inhibits the ADPRC activity of the novel cytosolic cyclase(s). Furthermore, alternative substrates, including NGD were used as CD38, CD157 and the *Aplysia* cyclase utilize this substrate [237] while a novel membrane ADPRC from brains of $CD38^{-/-}$ mice cannot [127]. Thus, NGD has been useful in distinguishing between cADPR and classical NADase activities [233]. Previous studies have shown that although they are constitutively active, ADPRCs are highly regulated [129, 164-166, 171-173, 175-178, 238]. Further, it has been shown that glycosylation [239], PseudocarbaNAD [240], and DTT [124] inhibit CD38 activities, whereas retinoic acid [4], zinc [126], and serine phosphorylation [175] activate CD38 enzyme activities. It has also been shown that ATP selectively blocks cADPR hydrolase activity [5], and that gangliosides [241, 242] selectively block NADase activity of CD38. Numerous pathways have been shown to activate the cADPR-pathway including metabolic factors, G-protein coupled receptors (GPCRs), and agonists that target intracellular receptors [20, 139, 140, 145, 146, 149, 154, 155, 158]. A most interesting question that remains to be elucidated is how the multiple functions of novel ADPRCs are regulated. Utilizing the RCA, we have shown that a variety of substrates stimulate

cytosolic cyclase activity including MgATP and phorbol 13-myristate 12-acetate (PMA). From this it is not only clear that novel ADPRC(s) are regulated, but also ADPRC activity is implicated in a diverse set of cellular processes. Thus, it is imperative to further elucidate the mechanisms by which ADPRCs are regulated in order to better understand these cellular processes. The data presented here provides evidence that suggests the novel ADPRC(s) present in the heart cytosol is regulated via a protein kinase C (PKC) dependent phosphorylation mechanism.

Materials and Methods

Reverse Cyclase Assay

Samples were incubated at 37ºC for a set period of time with cADPR (0.046-5.0 mM) and an excess nicotinamide (0.062-8.0 mM), which facilitated the conversion of cADPR to NAD in the presence of ADPRC. The reactions were carried out in 96-well plates (Sarstedt) with a total reaction volume of 50 µl. The samples were filter stopped with Millipore IP membranes using a vacuum manifold prior to proceeding to the next reaction step. The samples were diluted and transferred to 384-well plates (Corning). The initiation of the second step involved the of the addition of 40 µl of the filtered

reaction mixture diluted in sodium phosphate buffer, pH 8.0 (J.T. Baker), to 40 µl of RCA reagent to amplify the NAD produced and convert it to the fluorescent product resorufin (Figure 3). The RCA reagent was composed of final concentrations of 0.76% ethanol (Pharmco), 40 µg/ml ADH (Sigma), 0.04 µg/ml diaphorase from *Clostidium klyveri* (Sigma), 4.0 µM FMN (Sigma) and 2.0 µM resazurin (Sigma) in sodium phosphate buffer, pH 8.0. NAD was converted to NADH by ADH, which was utilized by diaphorase to reduce resazurin to produce the fluorescent product resorufin. The resorufin fluorescence served as an indicator of NAD produced as a result of ADPRC activity in the first step. The time dependent increase in resorufin fluorescence was measured at 25°C for 25 cycles with a fluorescence plate reader (*FLUO*star *Galaxy*) set with the excitation at 544 nm and emission at 590 nm. As the cycling method employed to amplify NAD was incredibly potent, the diaphorase was treated with activated charcoal (Sigma) to remove any contaminant NAD. Upon removal of contaminant NAD, the presence of ADPRC was required for the production of NAD. The difference in fluorescence produced by samples incubated in the presence and absence of nicotinamide, which was necessary for NAD production, served as a control to identify background resultant of contaminant NAD present in the samples.

NGD Assay

NGD (nicotinamide guanine dinucleotide) is an NAD analog that is cyclized by ADPRC to form the fluorescent product cGDPR [237]. 100 µl of 100 µM NGD was added to 100

µl of sample and the cGDPR produced was quantified fluorometrically using a fluorescence plate reader at 25°C for 25 cycles with excitation set at 300 nM and emission at 405 nM (Figure 12). The difference in cGDPR fluorescence produced in samples incubated in the presence and absence of NGD served as a control to identify background fluorescence of the samples.

$CD38^{+/+}$ and $CD38^{-/-}$ Tissue Homogenate Preparation

Adult mouse $CD38^{+/+}$ and $CD38^{-/-}$ pancreas, brain, kidney, uterus, heart, and lung tissues stored at -80ºC were thawed on ice and homogenized with an electric homogenizer in a lysis buffer of 20 mM Tris-HCl (Fisher Scientific), pH 7.5 and protease inhibitor tablets (Roche). Tissue homogenates were centrifuged at 200,000 x g for 30 minutes at 4°C to separate the sample into the cytosolic fraction (supernatant) and the membrane fraction (pellet). The pellet was re-suspended in lysis buffer and sonicated on ice for ten seconds. The cytosolic fraction was dialyzed at 4ºC overnight with 3500 molecular weight cut-off (MWCO) dialysis tubing (Fisher Scientific) against 30 mM Tris-HCl, pH 7.5. The dialysis was followed by a 1:1 treatment of the sample with activated charcoal for twenty minutes to remove any contaminant NAD and other impurities that may interfere with the assay (Figure 13). Finally, the dialyzed and charcoal treated cytosolic fraction was centrifuged at 200,000 x g for 30 minutes at 4°C to ensure complete removal of the membrane fraction. Dialysis and charcoal treatment of the samples effectively removed background activity and the amount of NAD produced in the RCA in the absence of

nicotinamide to negligible levels. The protein concentration of the samples was determined using the Pierce BCA (bicinchoninic acid) Protein Assay [243].

ADPRC Activity of $CD38^{-/-}$ and $CD38^{+/+}$ Tissues

The cytosolic fraction of $CD38^{+/+}$ and $CD38^{-/-}$ mouse pancreas, brain, kidney, uterus, heart and lung tissues were incubated with 100 μM cADPR and 10 mM nicotinamide at 37°C for various time frames up to 24 hours. Immediately upon removal from the incubator, the samples were filtered with Millipore IP membranes with a vacuum manifold to stop the reaction and the RCA carried out under conditions described already.

Subcellular Fractionation of $CD38^{-/-}$ and $CD38^{+/+}$ Heart Tissue Homogenate

In order to identify the subcellular localization of ADPRC activity, $CD38^{+/+}$ and $CD38^{-/-}$ mouse heart tissue was fractionated into seven subcellular fractions, including membrane fractions (P1-P6) and a cytosolic fraction (S6), via differential centrifugation. Membrane fractions P1-P6 were obtained by centrifuging the mouse heart homogenate with sequential centrifugations at 4˚C for 10 minutes at 1000 x g, 2000 x g, 3000 x g, 6000 x g, 10,000 x g, 20,000 x g, and 200,000 x g (Table 1). The supernatant was removed with each subsequent centrifugation and each of the pellets was re-suspended in 200 μl of lysis buffer and sonicated on ice for ten seconds. The supernatant from the 200,000 x g

ultracentrifugation, the cytosolic fraction, was dialyzed with 3500 MWCO dialysis tubing against 30 mM Tris-HCl, pH 7.5 at 4°C overnight. Following dialysis, the cytosol fraction was centrifuged at 200,000 x g for 30 minutes three more consecutive times to ensure complete removal of the membrane fractions. The protein concentration of the samples was determined using the BCA Protein Assay [243]. ADPRC activity of the subcellular fractions was measured by the RCA. Further, the cADPR hydrolase and NADase activities of the subcellular fractions were measured using ^{32}P labeled substrates. cADPR hydrolase activity was measured by incubating 20 ul of each subcellular with 5 ul of ^{32}P-cADPR, which was prepared by adding ^{32}P-cADPR to 5.8 ul of 4.35 mM cADPR for a final volume of 50 ul of 100 uM cADPR. NADase activity was measured by incubating 20 ul of each subcellular fraction with 5.0 ul of ^{32}P-NAD, which was prepared by adding ^{32}P-NAD to 5.0 ul of 2.5 mM NAD to for a final volume of 50 ul of 50 uM NAD. The cADPR hydrolase and NADase reactions were stopped at various timepoints (2-120 minutes) by adding 5 ul of the reaction mixture to 5 ul of 150 mM trifluoroacetic acid TFA (Sigma). 1.0 ul of the stopped reaction was spotted on PEI-cellulose thin layer chromatography (TLC) plates (EMD Chemicals) and dried for two minutes. The TLC plates were developed in a solution containing 0.2 M NaCl and 30% ethanol and the conversion of ^{32}P labeled substrates was quantified with a Packard Cyclone Phosphor-Imager.

Zinc Regulation of $CD38^{+/+}$ Heart Cytosol ADPRC(s)

There are a variety of agents known to activate and inactivate CD38. In order to better characterize the cytosolic ADPRC, we utilized zinc, a known activator of murine CD38 and CD157 ADPRC activities [126]. $CD38^{+/+}$ mouse heart cytosol and rCD38 were incubated with 0-10 mM $ZnCl_2$ for five minutes at 25°C. Upon completion of the pre-incubation, the samples were incubated with 100 μM cADPR and 10 mM nicotinamide at 37°C for various times up to 60 minutes. Immediately upon removal from the incubator, the samples were filtered with Millipore IP membranes with a vacuum manifold to stop the reaction and the RCA carried out under conditions described already.

$CD38^{+/+}$ Heart Cytosol ADPRC Activity is Increased by ATP

Previous studies have shown that ADPRCs are regulated by phosphorylation mechanisms [129, 175]. To determine if the novel cytosolic ADPRC(s) was regulated via a phosphorylation mechanism, $CD38^{+/+}$ mouse heart cytosol samples were pre-incubated with 500 mM ATP in the presence of Mg^{2+} for 5 minutes, which has been shown as the optimal incubation time (data not shown). Upon completion of the pre-incubation, the samples were incubated with 100 μM cADPR and 10 mM nicotinamide at 37°C for various times up to 60 minutes. Immediately upon removal from the incubator, the samples were filtered with Millipore IP membranes with a vacuum manifold to stop the reaction and the RCA carried out under conditions described already.

$CD38^{+/+}$ Heart Cytosol ADPRC Activity is Increased by PMA

Previous studies have shown that ADPRCs can be regulated via an intracellular mechanism involving the phosphorylation of PKC [129]. To determine if the novel cytosolic heart ADPRC(s) are regulated via a mechanism involving this pathway we utilized PMA, a known activator of PKC [129]. $CD38^{+/+}$ mouse heart cytosol was pre-incubated for 5 minutes in the presence of $Mg^{2+}$and 500 mM ATP in the absence or presence of 0.1 μM PMA. Upon completion of the pre-incubation, the samples were incubated with 100 μM cADPR and 10 mM nicotinamide at 37°C for various times up to 60 minutes. The samples were filtered with Millipore IP membranes with a vacuum manifold to stop the reaction and the RCA carried out under conditions described already.

$CD38^{+/+}$ Heart Cytosol ADPRC Activity is Increased by Sodium Fluoride (NaF)

In order to confirm the novel cytosolic ADPRC(s) are indeed regulated by a phosphorylation mechanism, we studied the affect of a known phosphatase inhibitor, sodium fluoride (NaF), on ATP stimulated ADPRC activity of the cyclase(s) present in $CD38^{+/+}$ mouse heart cytosol. The cytosolic fraction of $CD38^{+/+}$ mouse heart was pre-incubated for 5 minutes with varying concentrations of NaF (0-36 mM) in the presence of Mg^{2+} and 100 μM ATP. Upon completion of the pre-incubation, the samples were incubated with 100 μM cADPR and 10 mM nicotinamide at 37°C for various times up to 60 minutes. Immediately upon removal from the incubator, the samples were filtered

with Millipore IP membranes with a vacuum manifold to stop the reaction and the RCA carried out under conditions described already.

G3000SW Gel Filtration of CD38$^{+/+}$ Heart Cytosol

Based on the finding of ADPRC activity in the cytosolic fraction of mouse tissues, we investigated the molecular size of the novel cyclase(s) responsible for the activity. CD38 $^{+/+}$ mouse heart cytosol was run over a G3000SW (0.8 x 30 cm) size exclusion chromatography column with a solvent of 20 mM Tris-HCl, pH 7.5 and 100 mM NaCl. Fractions were collected for 1 minute (0.5 mL) from 10-30 minutes and each fraction was screened for ADPRC activity using the RCA and the NGD assay. The CD38$^{+/+}$ mouse heart G3000SW Gel filtration fractions were incubated with 100 μM cADPR and 10 mM nicotinamide at 37°C for 60 minutes. The samples were filtered with Millipore IP membranes with a vacuum manifold to stop the reaction and the RCA carried out under conditions described already.

DEAE Fractionation of CD38 $^{+/+}$ Heart Cytosol

CD38 $^{+/+}$ rat heart cytosol was fractionated on an anion-exchange column (DEAE 5PW) using an HPLC based method with an elution gradient of NaCl (0-1000 mM). The RCA was utilized to determine in which fractions ADPRC activity was present. 40 μl of each

fraction was incubated with 100 µM cADPR and 10 mM nicotinamide at 37°C for various times up to 60 minutes. The samples were filtered with Millipore IP membranes with a vacuum manifold to stop the reaction and the RCA carried out under conditions described already.

Phenyl-Sepharose Column Chromatography of CD38$^{+/+}$ Heart Cytosol

CD38$^{+/+}$ heart cytosol was fractionated using Phenyl-Sepharose column chromatography. The Phenyl-Sepharose columns (0.6 x 3 cm) were equilibrated with 10 mL of 2.0 M KCl. 2.0 mL of rCD38 or CD38$^{+/+}$ heart cytosol was loaded onto the respective columns. The columns were washed with 15 mL of 2.0 M KCl and 3.0 mL fractions were collected. 15 mL of elution buffer (25 mM Tris-HCl) was added and 3.0 mL fractions were collected. The RCA and the NGD assay were used to determine which fractions had ADPRC to reveal if the novel cytosolic ADPRC(s) bound to the hydrophobic column.

Affinity Dye-Conjugated Column Chromatography of CD38$^{+/+}$ Heart Cytosol

CD38$^{+/+}$ rat heart cytosol was fractionated using dye-conjugated affinity column chromatography. Blue, Orange, Red, and Green Matrex-Gel, Affi-gel Blue, Red 2, Red 3, Orange1, Orange2, Orange3, Yellow1, Yellow2, Blue1, BlueSA and Green1 PIXI M Test Kit dye-conjugated columns (0.6 x 3 cm) were all tested. Columns were

equilibrated with 10 mL of 20 mM Tris-HCl pH 7.2. 1.0 mL of $CD38^{+/+}$ rat heart cytosol was loaded onto each column. The columns were washed with 5.0 mL of 20 mM Tris-HCl, pH 7.2 and 2.5 mL fractions were collected. 5.0 mL of elution buffer (2.0 M NaCl pH 7.2 or 1.0 mM cADPR) was added to each column and 2.5 mL fractions were collected. The ADPRC activity of the fractions was measured by the RCA and the NGD assay to determine if the novel cytosolic ADPRC(s) had a high enough affinity with the dye to bind to the columns.

Results

ADPRC Activity in Membrane and Cytosol of $CD38^{+/+}$ and $CD38^{-/-}$ Tissues

Using the RCA with optimized concentrations of reagents, the specific activity of the non-CD38 cyclase in the $CD38^{-/-}$ mouse tissues was investigated. The $CD38^{+/+}$ cytosolic fractions of mouse pancreas, brain, kidney, uterus, heart and lung all displayed ADPRC activity. Furthermore, the $CD38^{-/-}$ cytosolic fractions of mouse heart, brain and lung cytosol had appreciable, however reduced amounts of cytosolic cyclase activity when compared to the $CD38^{+/+}$ tissues (Figure 14). Similar results were observed in $CD38^{+/+}$ rat heart cytosol (data not shown). Although the cytosolic cyclase activity was reduced

compared to the membrane activity of $CD38^{+/+}$ tissues, it was retained throughout four subsequent ultra-centrifugations at 200,000 x g (Figure 15), which strongly suggests the cytosolic ADPRC activity was indeed the result of a cytosolic enzyme. Interestingly, it was shown that while ADPRC activity was observed in all the subcellular fractions of $CD38^{+/+}$ mouse heart tissue, this activity was only present in the cytosolic fraction of the $CD38^{-/-}$ mouse heart subcellular fractions (Figure 16). Hydrolase and NADase activities were also measured of the $CD38^{+/+}$ mouse heart subcellular fractions using ^{32}P labeled substrates. The enzyme activities measured using ^{32}P labeled demonstrated that membrane fractions (P1-P6) and the cytosolic fraction (S6) had cADPR hydrolase activity, and that the membrane fractions (P1, P2, P3, P5, P6) and the cytosolic fraction (S6) had NADase activity (Figure 17).

$CD38^{+/+}$ Heart Cytosol *ADPRC Activity is Inhibited by $ZnCl_2$*

There are a variety of agents known to activate and inactivate CD38. In order to better characterize the cytosolic ADPRC, we utilized zinc, a known activator of murine CD38 and CD157 ADPRC activities [126]. ADPRC activity of $CD38^{+/+}$ mouse heart cytosol and rCD38 were measured at pH 7.0 in the presence of 0-10 mM $ZnCl_2$. We observed that $ZnCl_2$ inhibited the partially purified mouse heart cytosol ADPRC activity, while it stimulated the activity of rCD38 (Figure 18), which suggests this heart cyclase is a novel ADPRC distinct from CD38 and CD157.

CD38 $^{+/+}$ Heart Cytosol ADPRC *Activity is Increased by ATP, PMA & NaF*

Previous studies have shown that ADPRCs can be regulated via phosphorylation mechanisms [129, 175]. We have shown the ADPRC activity found in the cytosolic fraction of CD38$^{+/+}$ mouse heart tissues was increased by 500 mM MgATP (Figures 19 & 20), which suggests the novel heart cytosolic cyclase(s) may be regulated via phosphorylation. To further substantiate evidence that the novel heart cytosolic ADPRC(s) are regulated via phosphorylation mechanisms, we have shown that there was an increase in activity of the novel mouse heart ADPRC(s) upon pre-incubation with PMA, a known activator of PKC mediated phosphorylation (Figure 19). This data suggests that PKC-dependent phosphorylation may represent one of the mechanisms by which the novel cytosolic ADPRC(s) in mouse heart tissue is regulated. To further investigate the potential mechanisms of regulation of the cytosolic cyclase(s) and to confirm that this cyclase is indeed regulated by a phosphorylation mechanism, we studied the affect of a known phosphatase inhibitor NaF, on ADPRC activity of CD38$^{+/+}$ mouse heart cytosol. The cytosolic fraction of CD38$^{+/+}$ mouse heart homogenate was pre-incubated with varying concentrations of NaF (0-36 mM) in the presence of 100 μM MgATP before initiating the RCA reaction. As predicted, the novel heart cytosolic cyclase activity was increased at low concentrations of NaF (5-10 mM) and decreased at high concentrations of NaF (>17mM) in the presence of MgATP (Figure 20). Activity also increased with an increase in pre-incubation time with low concentrations of NaF (data not shown). These results further suggest that the novel heart cytosolic ADPRC(s) may be regulated via a phosphorylation mechanism.

G3000SW Gel Filtration of CD38$^{+/+}$ Heart Cytosol

The CD38$^{+/+}$ mouse heart cytosol was fractionated by G3000SW size exclusion gel filtration (Figure 21). ADPRC activity of the fractions was measured using the RCA and the NGD assay. In both assays the peak ADPRC activity correlated with the same gel filtration fractions #3-7 (Figure 22). This finding was interesting as previous data suggested that the novel heart ADPRC(s) was unable to cyclize NGD [127]. To further investigate this, the mouse heart cytosol fraction was added to mouse heart membrane fraction and rCD38 samples and the NGD assay was used to show that the cytosolic fraction inhibited the NGD activity present in the mouse heart membrane (Figure 23) and rCD38 (Figure 24) samples. The active fraction (Fraction #5) of heart cytosol partially purified by G3000SW fractionation was not able to inhibit the NGD activity of heart membrane (Figure 25) or rCD38 (Figure 26), suggesting an inhibitor was removed during this procedure. Indeed, inhibition of NGD activity in heart cytosol was observed to be due to a component found in fractions #14-18 (Figure 27), which suggests a cytosolic protein of 12-66 kDa was responsible.

DEAE Fractionation of CD38$^{+/+}$ Mouse Heart Cytosol

The CD38$^{+/+}$ mouse heart cytosol was fractionated using an anion-exchange column (DEAE 5PW). The RCA was utilized to determine in which fractions ADPRC activity was present. A majority of the activity bound to the DEAE anion exchange column and

was eluted at concentrations between 50 and 500 mM of NaCl (Figure 28).

Phenyl-Sepharose Column Chromatography of CD38$^{+/+}$ Heart Cytosol

CD38$^{+/+}$ rat heart cytosol was fractionated via hydrophobic Phenyl-Sepharose column chromatography. The ADPRC activity of the fractions as measured by the RCA and the NGD assay, revealed that the novel mouse heart cytosolic ADPRC(s) do not bind Phenyl-Sepharose (Figure 29), which was distinctly different from CD38 that binds to the hydrophobic column (Figure 30). This data demonstrates that conventional purification methods are useful for isolating the cytosolic ADPRC and that this activity can be distinguished from CD38 by comparing how the two activities run on different chromatography systems.

Affinity-Dye Conjugated Column Chromatography of CD38$^{+/+}$ Heart Cytosol

CD38$^{+/+}$ rat heart cytosol was fractionated using dye-conjugated column chromatography and the ADPRC activity of the fractions was measured by the RCA. It was shown that the novel ADPRC(s) bound to the Green Matrex-gel column and can be eluted with 2.0 M NaCl and 1.0 mM cADPR (Figure 31). Further, the novel cytosol ADPRC activity bound to the Blue A and Red Matrex-Gel columns (Figure 32) as well as to the Red2, Red3, Orange1, Orange2, Orange3, Yellow1, Yellow2, and Green1 PIXI M Test Kit dye-

conjugated columns (Figure 33). However, the percentage of activity recovered was low. The novel heart cytosolic ADPRC activity did not bind any of the other dye-conjugated columns tested. The activity was present in the void volume fractions of Blue1 and BlueSA PIXI M Test Kit columns with a high percentage of recovery (Figure 34). The novel heart cytosolic ADPRC activity was found in the void volume of the Affi-gel Blue column (data not shown) as well as the Blue B and Orange Matrex-Gel columns (Figure 35). The columns with a high recovery of activity in the void volume could potentially be useful as a clean-up step, as a majority of the other protein including hemoglobin stuck to the column.

Discussion

In this study, we have confirmed recent evidence that suggests novel ADPRC(s) independent of CD38 and CD157 exist in both $CD38^{-/-}$ and $CD38^{+/+}$ tissues. As metabolites of ADPRCs have been shown to be key players in calcium regulation and homeostasis [16, 206, 244], the need for an in-depth investigation of these enzymes is clear. In these studies we have provided evidence that ADPRC(s) distinct from CD38 are present in $CD38^{-/-}$ and $CD38^{+/+}$ cytosol. Using the highly sensitive RCA, we have demonstrated that various mouse tissues have ADPRC activity in the $CD38^{-/-}$ membrane fractions as well as in $CD38^{+/+}$ and $CD38^{-/-}$ cytosolic fractions. We have shown that the

$CD38^{+/+}$ cytosolic activity was not only excluded from the membrane fractions of $CD38^{+/+}$ mouse heart, but that it was also distinct from that of rCD38 as it was inhibited by zinc, whereas rCD38 was stimulated by zinc. We further provided evidence that novel heart cytosolic ADPRC(s) are regulated via a PKC-dependent phosphorylation mechanism. Another characteristic that distinguishes the novel heart cytosol ADPRC(s) from CD38 was the elution of the cytosolic cyclase(s) in the void volume of the Phenyl-Sepharose column which binds CD38. The novel mouse heart cytosol ADPRC activity eluted in the void volume of G3000SW size exclusion column chromatography suggesting a size of greater than 300 kDa, which is far different from the 90 kDa dimer CD38 [45] runs as on the same system. Perhaps a quite important finding in the midst of these experiments was that a component of the cytosolic fraction was inhibiting NGD activity. Initial experiments suggested that cytosolic cyclase did not have NGD activity, which was in agreement with previous studies that suggested certain novel ADPRCs were distinct based on their inability to cyclize NGD [79]. However, further investigations have revealed that the quench of cGDPR fluorescence was removed by G3000SW gel filtration, which further exemplifies the need for a more sensitive assay to investigate novel cyclases that were overlooked with previous methods. Despite being able to characterize the enzyme activity of the novel cytosolic ADPRC(s) as being distinct from previously identified forms of ADPRC CD38 and CD157 [2-9], isolation and purification of the enzyme to a state sufficient for sequence analysis by mass spectrometry to determine the identity of the novel cyclase has proven to be challenging. One limitation that has contributed to this difficulty in purification of was the stability of the novel

cytosolic ADPRC. Further, the basal activity was relatively low and the recovery of activity was not 100% during the purification process. Despite keeping the protein as concentrated as possible and taking every precaution during purification to prevent loss of activity by keeping stabilizing agents such as protease inhibitors in all buffers, we have been unable to purify the novel cytosolic ADPRC(s). Even if successful in purifying the enzyme, obtaining adequate sequence information may also be a technical limitation. There are multiple forms of mammalian ADPRCs [11, 12, 72-79], many of which have not yet been identified or characterized. The identification of novel ADPRC family members and elucidation of the regulation of ADPRCs will lead to a better knowledge of a number of cell-specific processes. A better understanding of these regulatory mechanisms can provide a foundation for the intelligent design of drugs for prominent diseases implicated in the ADPRC mediated signaling pathways [100, 131, 138, 155, 158-162, 164, 171, 172, 176, 178, 186, 220-224, 226, 227, 236], thus it is imperative to continue with careful analysis, identification and purification of novel ADPRC(s).

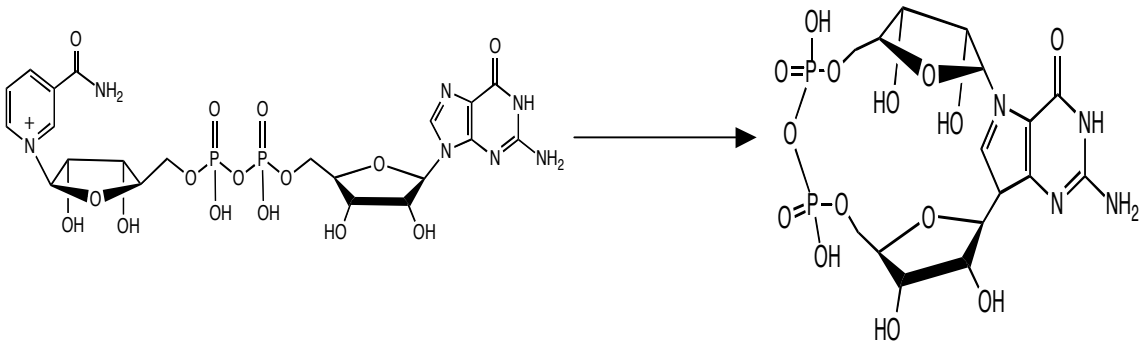

Figure 12. **NGD Assay Reaction Scheme**

In this assay designed to measure ADPRC activity, an NAD analogue NGD, was used as a substrate by ADPRC and converted to a fluorescent product cGDPR. The increase in fluorescence of cGDPR was measured with a fluorescent plate reader as and indicator of ADPRC activity.

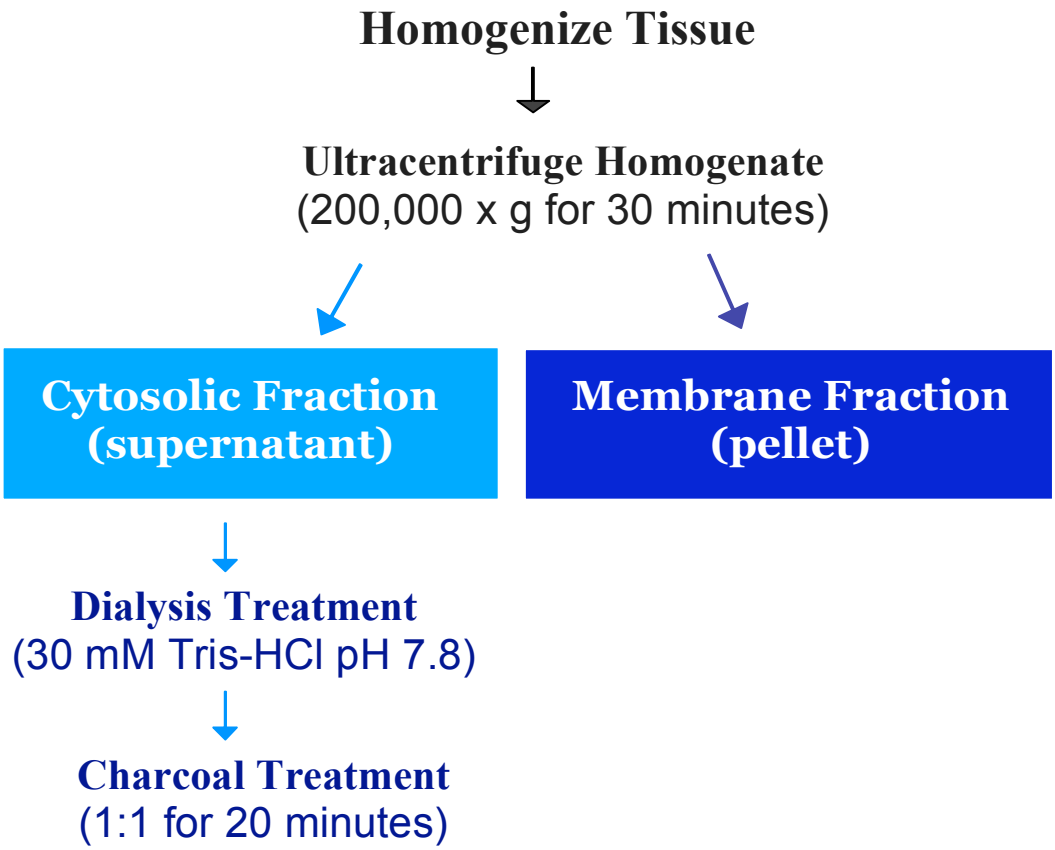

Figure 13. **Tissue Homogenate Fractionation into Cytosol and Membrane Fractions**

The Homogenates from various mouse and rat tissues were fractionated into cytosolic and membrane fractions via ultracentrifugation. Samples were homogenized in lysis buffer (20 mM Tris-HCl pH 8.0 + protease inhibitors) on ice using an electric homogenizer. The homogenate was centrifuged at 200,000 x g for 30 minutes. The supernatant was removed (cytosolic fraction) and the pellet was re-suspended in 20 mM Tris-HCl sucrose pH 8.0. The cytosol was dialyzed with 3500 molecular weight cut-off dialysis tubing against 30 mM Tris-HCl pH 7.8 at 4°C overnight. The dialyzed samples were further charcoal treated to ensure removal of any contaminant NAD.

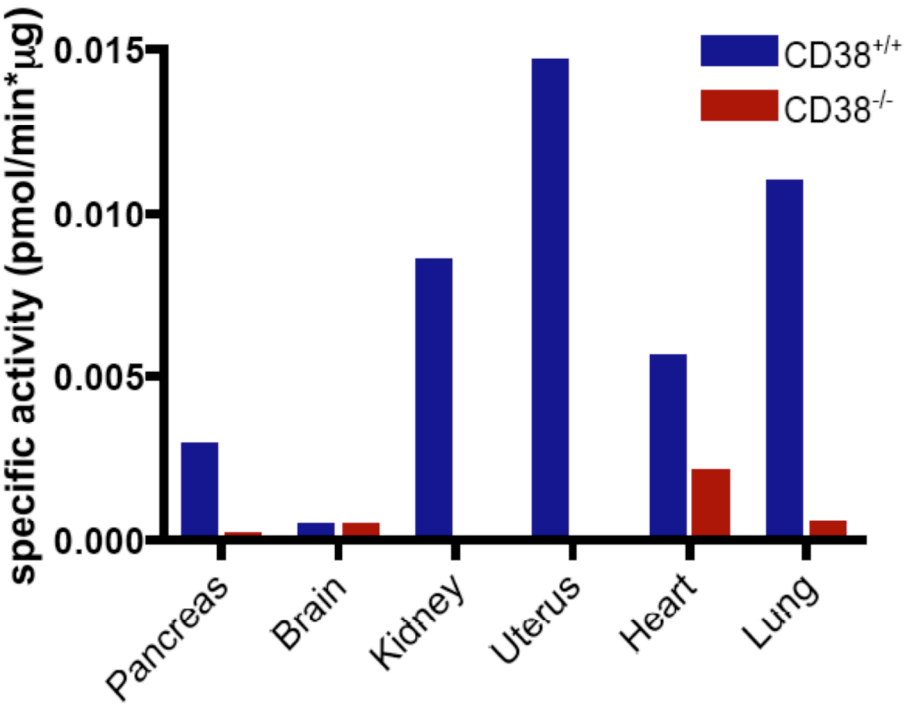

Figure 14. **ADPRC Activity of CD38$^{+/+}$ and CD38$^{-/-}$ Mouse Tissue Cytosol**

The ADPRC activity of the cytosolic fraction from CD38$^{+/+}$ and CD38$^{-/-}$ tissues was measured via the RCA. There was ADPRC activity in the cytosol of all CD38$^{+/+}$ tissues as well as in certain CD38$^{-/-}$ tissues.

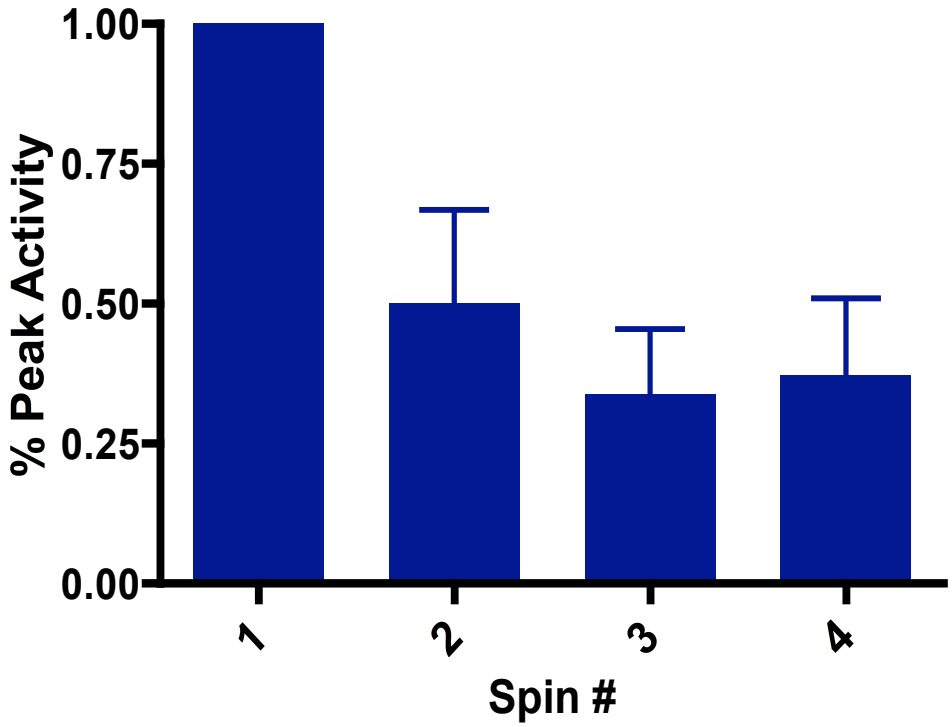

Figure 15. **Subsequent Centrifugations of CD38$^{+/+}$ Heart Cytosol**

CD38$^{+/+}$ mouse and rat heart cytosol was centrifuged at 200,000 x g four consecutive times following dialysis to ensure complete removal of the membrane fraction. Sucrose could function as a cushion and excluding light membranes from the pellet in the initial ultracentrifugation following dialysis removal of sucrose results in formation of a second pellet as opposed to being a result of membrane contamination of the cytosol. The cytosolic fraction retains cyclase activity with subsequent centrifugations, which suggests activity is indeed localized in the cytosol.

Table 1. **Fractionation of Mouse Heart Homogenate via Centrifugation**

P1	**1,000**	**x g**	**(nuclei, heavy mitochondria, PM sheets)**
P2	**3,000**	**x g**	**(heavy mitochondria, pm fragments)**
P3	**6,000**	**x g**	**(mitochondria, lysosomes, peroxisomes, intact golgi)**
P4	**10,000**	**x g**	**(mitochondria, lysosomes peroxisomes, intact gm)**
P5	**20,000**	**x g**	**(lysosomes, peroxisomes, gm, large dense vesicles)**
P6	**200,00 0**	**x g**	**(all vesicles from ER, pm, Golgi, endosomes etc.)**
S6	**200,000**	**x g**	**(cytosol)**

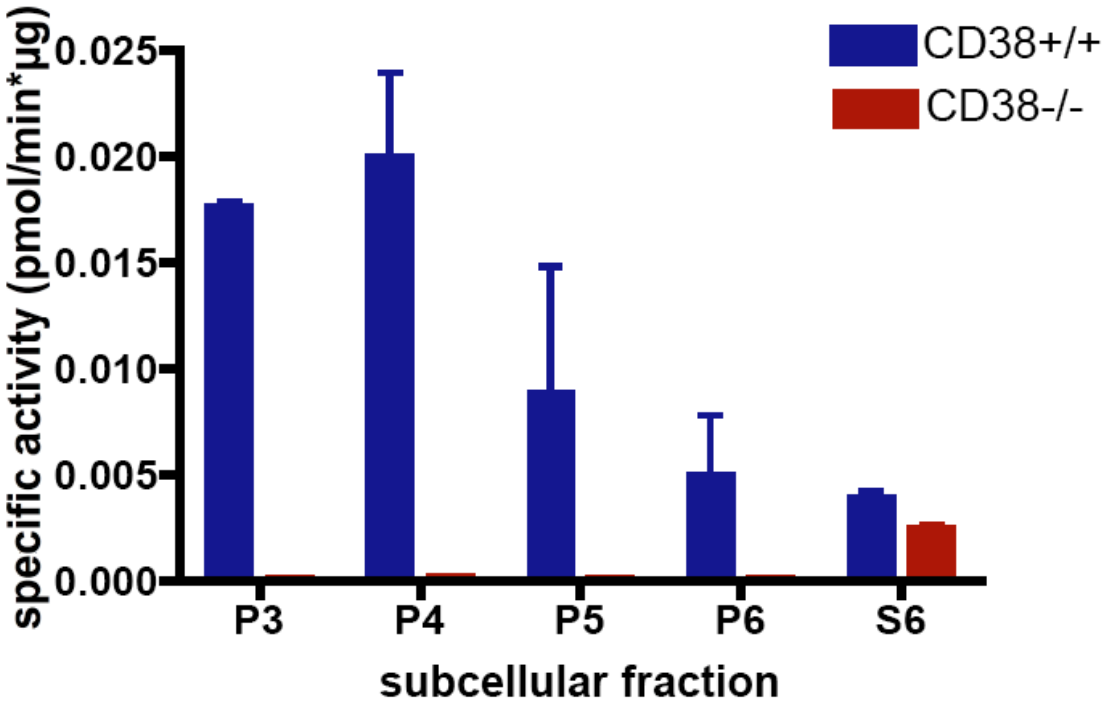

Figure 16. **ADPRC Activity in CD38$^{+/+}$ and CD38$^{-/-}$ Subcellular Fractions**

Mouse heart homogenate was fractionated using centrifugation. ADPRC activity was present in all subcellular fractions of CD38$^{+/+}$ samples. Also, ADPRC activity was present in the cytosolic (S6) fraction in CD38$^{-/-}$ samples, but was absent from the membrane fractions (P3-P6).

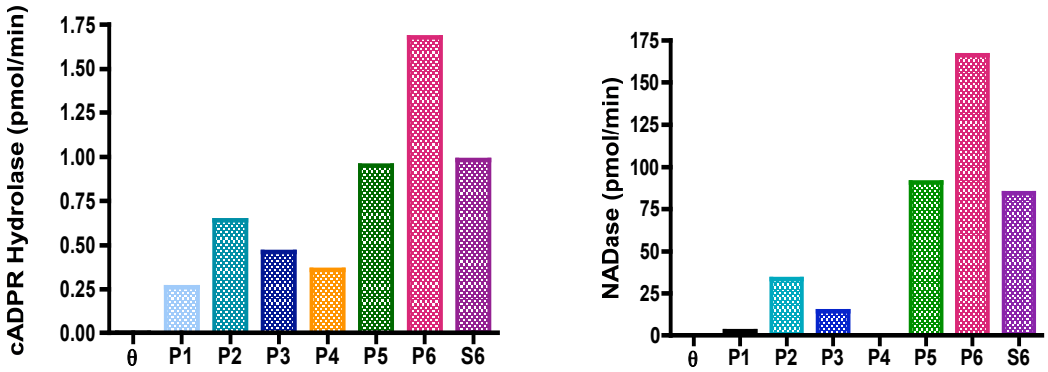

Figure 17. **NADase and Hydrolase Activity in CD38$^{+/+}$ Mouse Heart Cytosol**

CD38$^{+/+}$ mouse heart homogenate was fractionated into various subcellular fractions using centrifugation. The membrane fractions (P1-6) and the cytosolic fraction (S6) had cADPR hydrolase activity. The CD38$^{+/+}$ membrane fractions (P1, P2, P3, P5, P6) and the cytosolic fraction (S6) exhibited NADase activity.

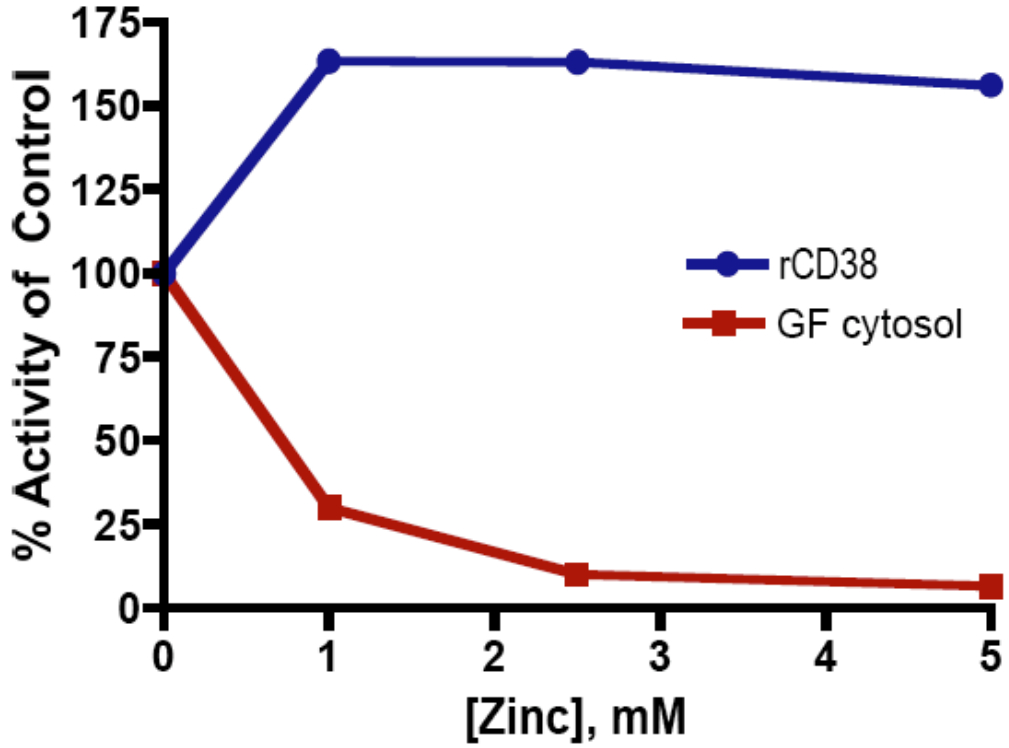

Figure 18. **Zinc Inhibits CD38$^{+/+}$ Heart Cytosolic ADPRC Activity**

The ADPRC activity of CD38$^{+/+}$ heart cytosol partially purified by gel filtration (see Figure 11) and rCD38 was measured at pH 7.0 in the presence of $ZnCl_2$ (0□10 mM). $ZnCl_2$ inhibited the cytosolic ADPRC activity, whereas it stimulated rCD38 ADPRC activity, which suggests this heart cyclase is not CD38 or CD157.

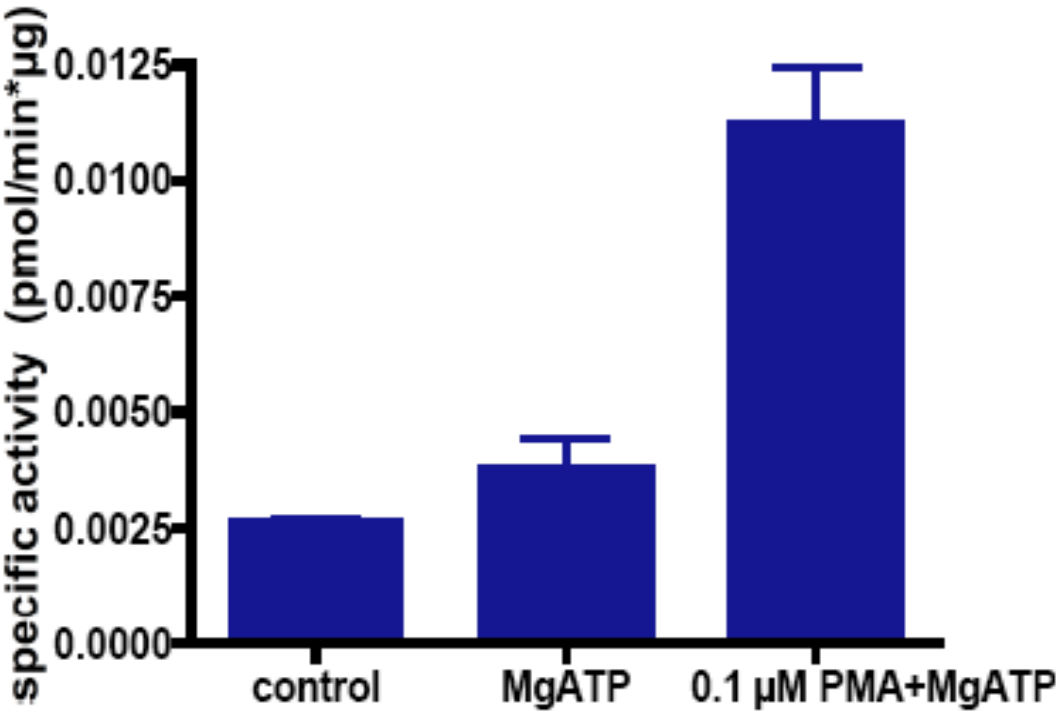

Figure 19. **CD38$^{+/+}$ Heart Cytosolic Cyclase Activity is Increased by ATP and PMA**

CD38$^{+/+}$ mouse cytosol samples pre□incubated with 500 mM MgATP exhibited increased RCA activity. Further, CD38$^{+/+}$ mouse heart cytosol pre□incubated with PMA further increased ADPRC activity of the mouse heart cytosol as measured by the RCA.

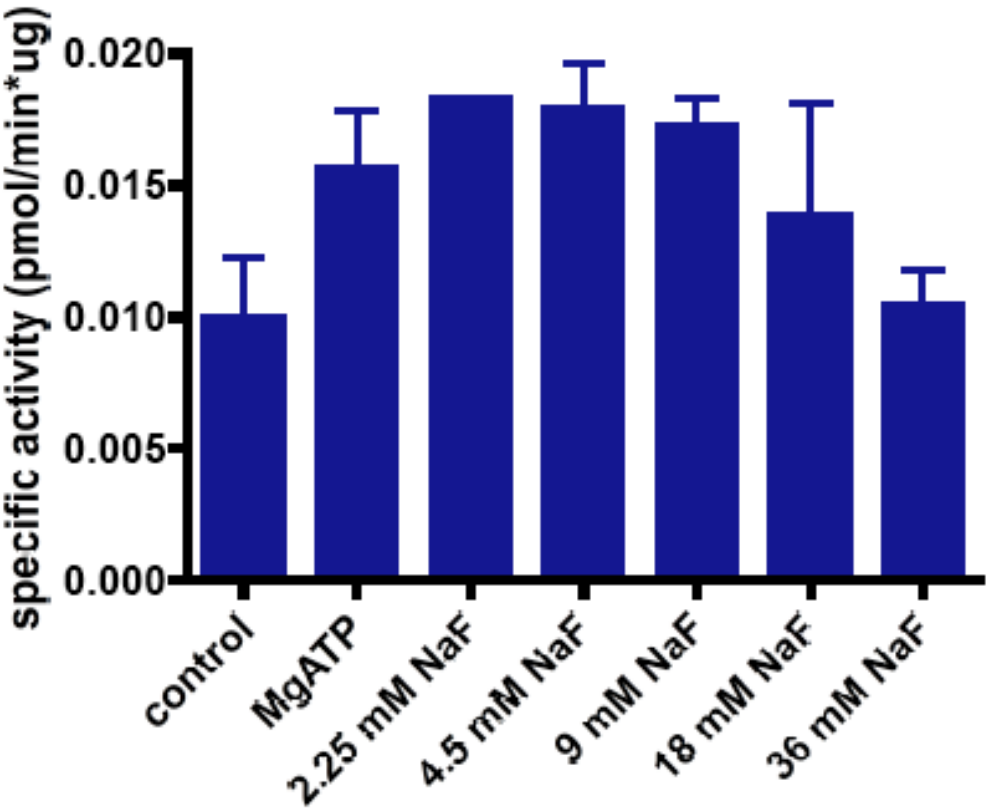

Figure 20. **CD38$^{+/+}$ Heart Cytosolic Cyclase Activity is Increased by NaF**

The ADPRC activity of CD38$^{+/+}$ mouse heart mouse cytosol was increased at low concentrations (5.0□10 mM) and decreased at high concentrations (>17mM) of NaF.

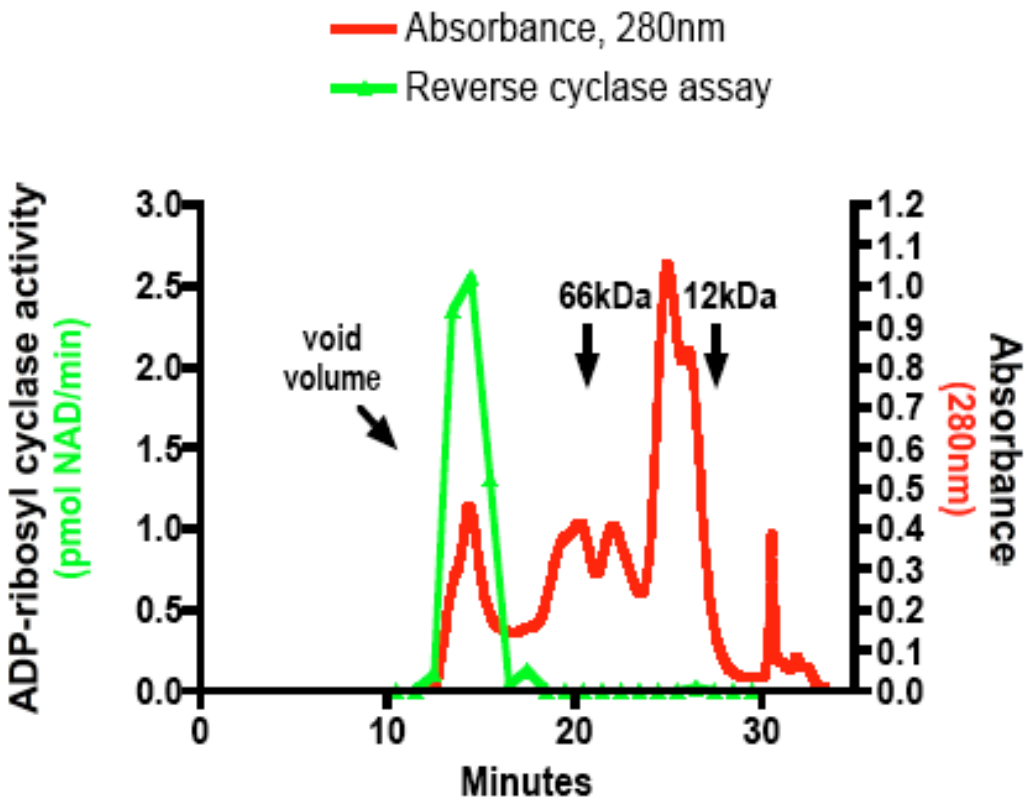

Figure 21. **G3000SW Fractionation of CD38$^{+/+}$ Heart Cytosol**

RCA of the size exclusion G3000SW fractionation of CD38$^{+/+}$ mouse heart cytosol showed a majority of the activity was eluted in the void volume (>300kDa).

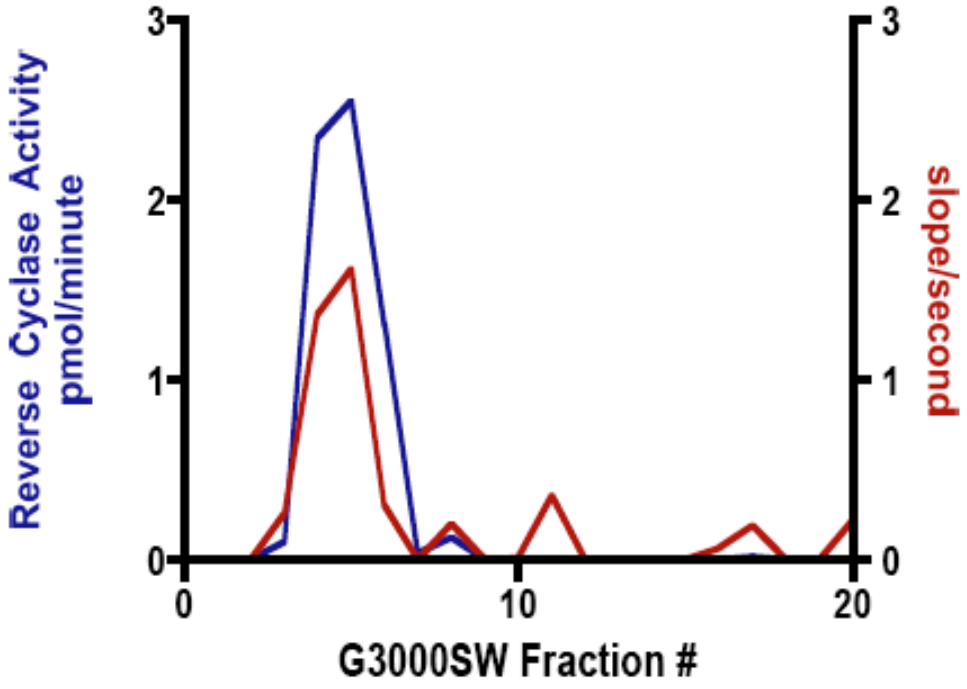

Figure 22. **ADPRC Activity of GS3000SW Fractionated CD38$^{+/+}$ Heart Cytosol**

CD38$^{+/+}$ mouse heart homogenate was fractionated via GS3000SW column chromatography. Peak RCA and NGD activities correlated with fractions #3□7.

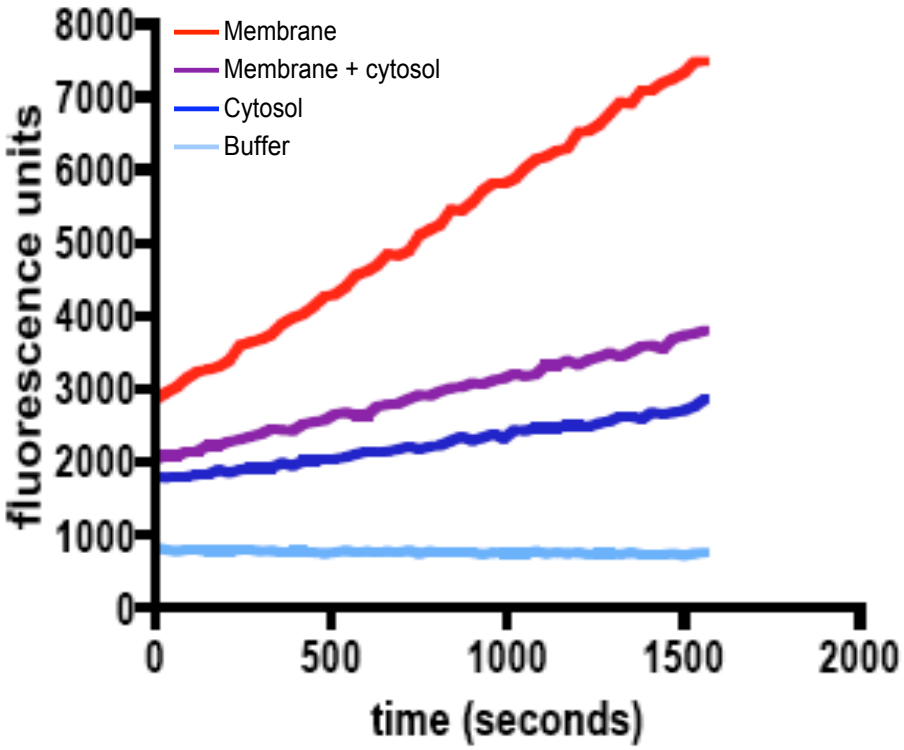

Figure 23. **CD38$^{+/+}$ Heart Cytosol Inhibits CD38$^{+/+}$ Heart Membrane NGD Activity**

The ADPRC activity of CD38$^{+/+}$ mouse heart membrane and cytosol fractions was measured with the NGD assay. The cytosol fraction had negligible NGD activity. Further, the cytosol fraction when added to the membrane fraction, inhibited membrane NGD activity.

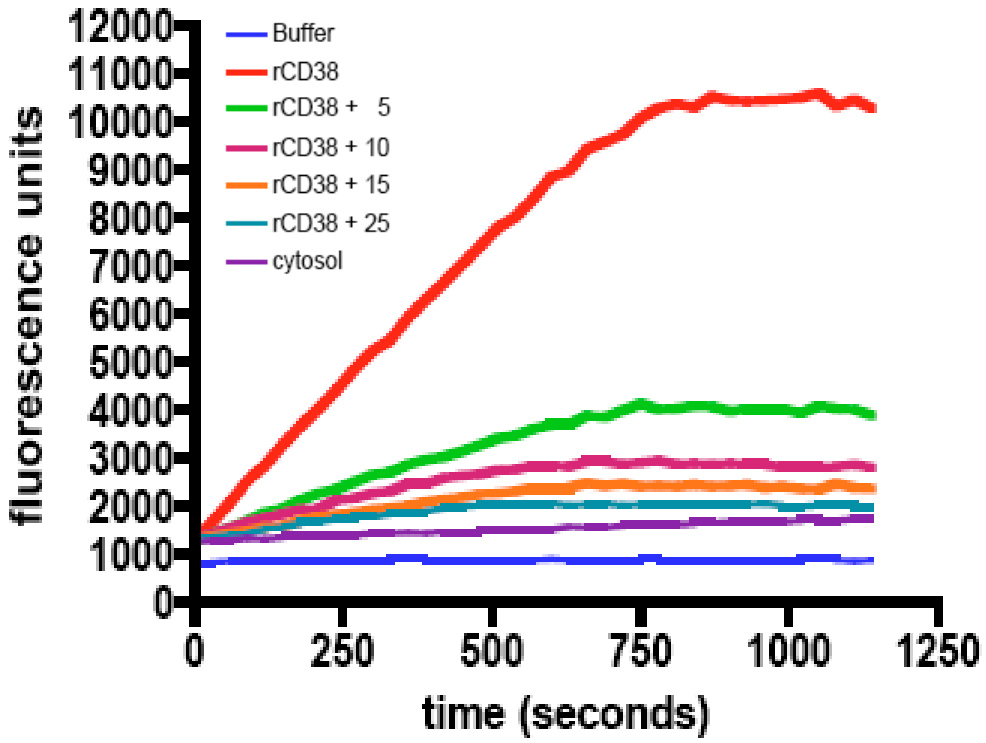

Figure 24. **CD38$^{+/+}$ Heart Cytosol Inhibits NGD Activity of rCD38**

The CD38$^{+/+}$ mouse heart cytosol fraction had negligible NGD activity. Further, the addition of 0-25 µl of the mouse heart cytosol to 2.5 nM rCD38 inhibited the robust NGD activity of rCD38 in a concentration dependent manner.

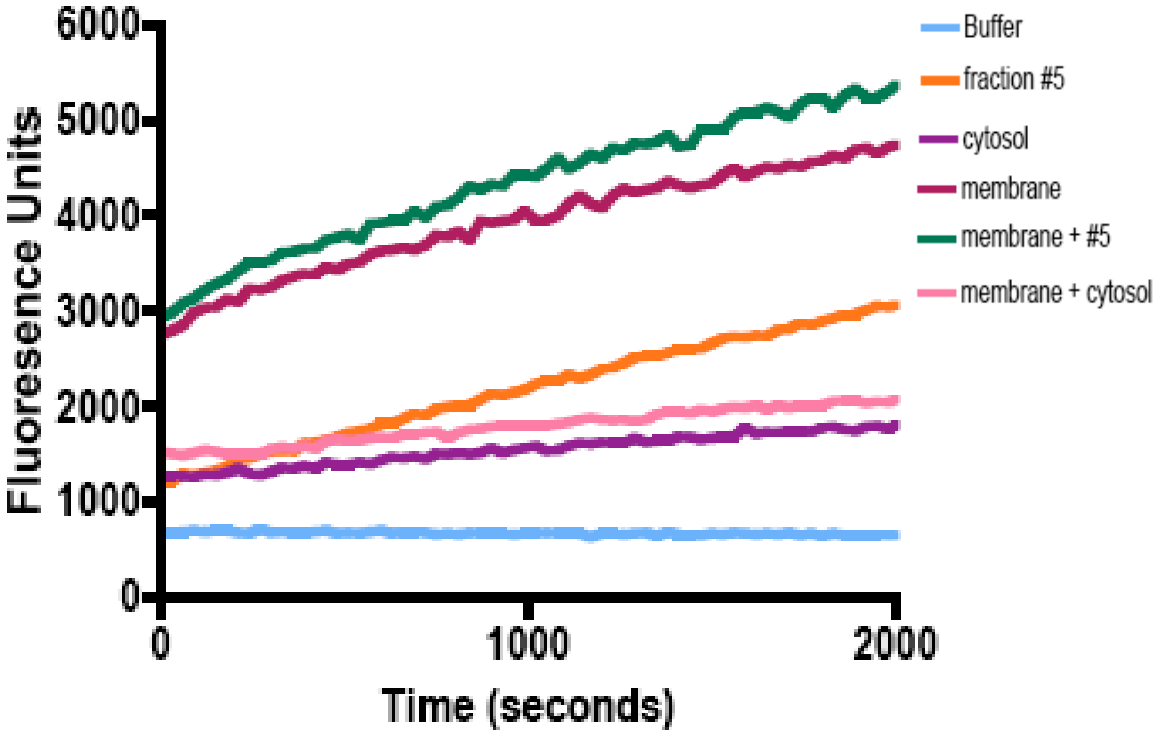

Figure 25. **Removal of CD38$^{+/+}$ Heart Cytosol Inhibition of CD38$^{+/+}$ Heart Membrane NGD Activity**

NGD activity of the CD38$^{+/+}$ mouse heart membrane fraction was inhibited by the addition of CD38$^{+/+}$ heart cytosol. The mouse heart cytosol filtered via GSW3000 column chromatography (fraction #5) had NDG activity. Further, GSW3000 fraction #5 did not quench NGD activity of the membrane fraction.

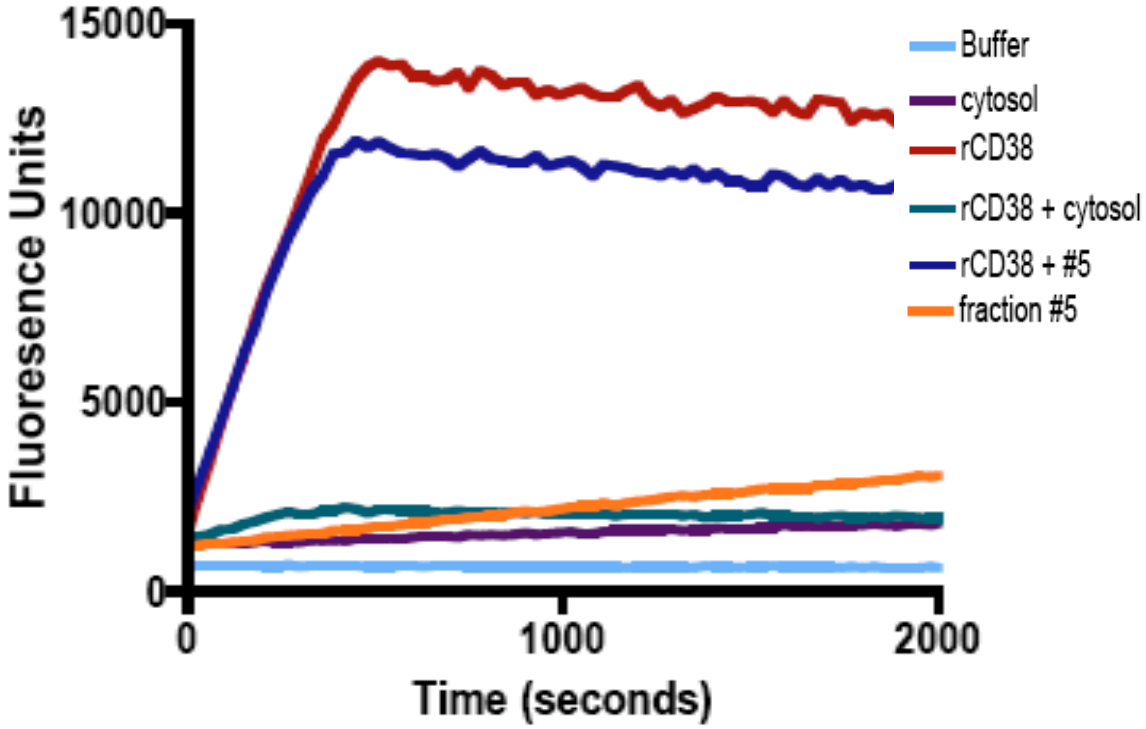

Figure 26. **Removal of CD38$^{+/+}$ Heart Cytosol Inhibition of rCD38 NGD Activity**

The CD38$^{+/+}$ heart cytosol had negligible levels of NGD activity. Further, the robust NGD activity of rCD38 was inhibited by the addition of CD38$^{+/+}$ heart cytosol. The mouse heart cytosol filtered via GSW3000 column chromatography (fraction #5) had NDG activity and also did not quench NGD activity rCD38.

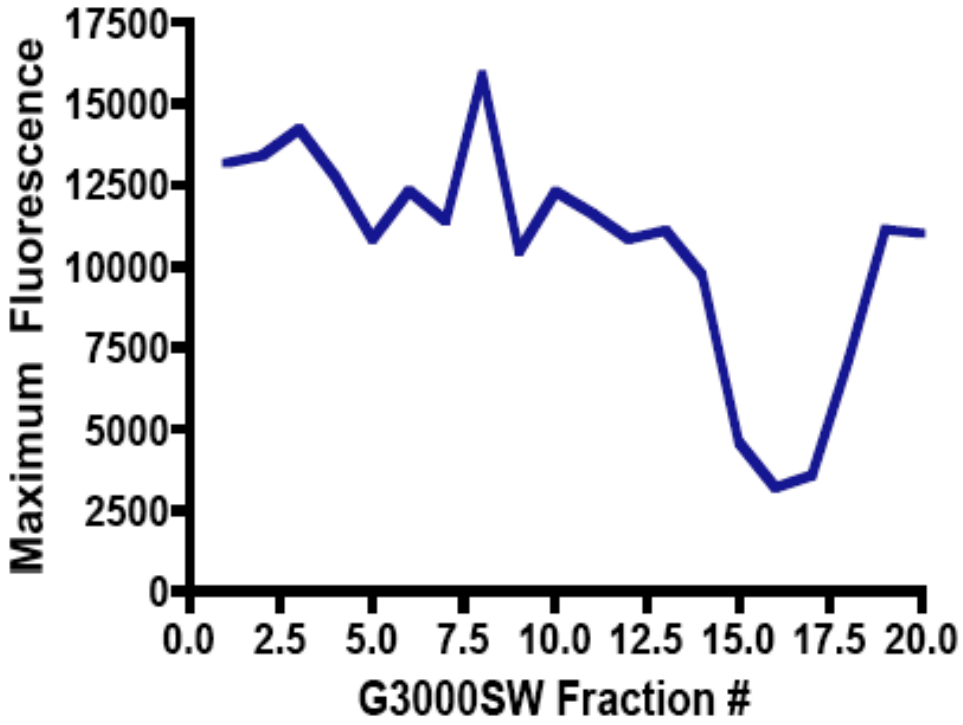

Figure 27. **Removal of an Inhibitor of NGD Activity from CD38$^{+/+}$ Mouse Heart Cytosol by GSW3000SW Fractionation**

The NGD assay was used to measure ADPRC activity of rCD38 incubated with CD38$^{+/+}$ mouse heart cytosol fractionated via GSW3000SW column chromatography. Fractions 1-13 & 19-20 did not have any effect on the ADPRC activity of rCD38. However, fractions #14□18 inhibited NGD activity, which suggests a cytosolic protein of 12□66 kDa is responsible for the observed cytosolic inhibition of membrane and rCD38 NGD activity.

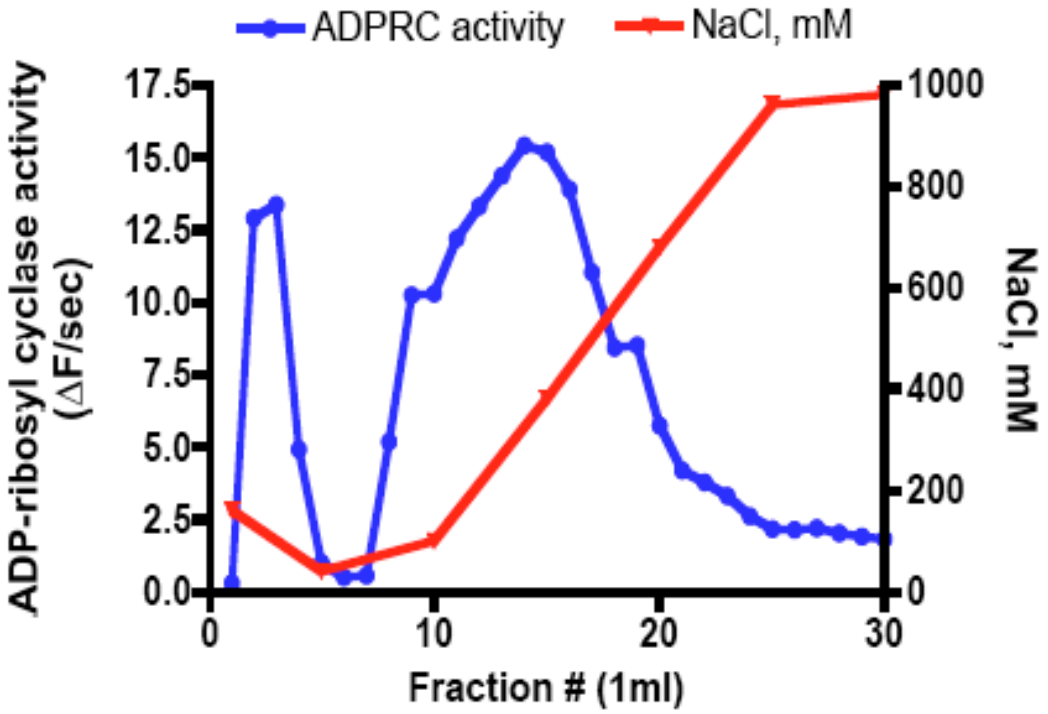

Figure 28. **DEAE Fractionation of CD38$^{+/+}$ Mouse Heart Cytosol**

CD38$^{+/+}$ mouse heart cytosol was fractionated on an anion□exchange column (DEAE 5PW). A majority of the CD38$^{+/+}$ heart cytosol ADPRC activity bound to this column and eluted from about 50 to 500 mM NaCl.

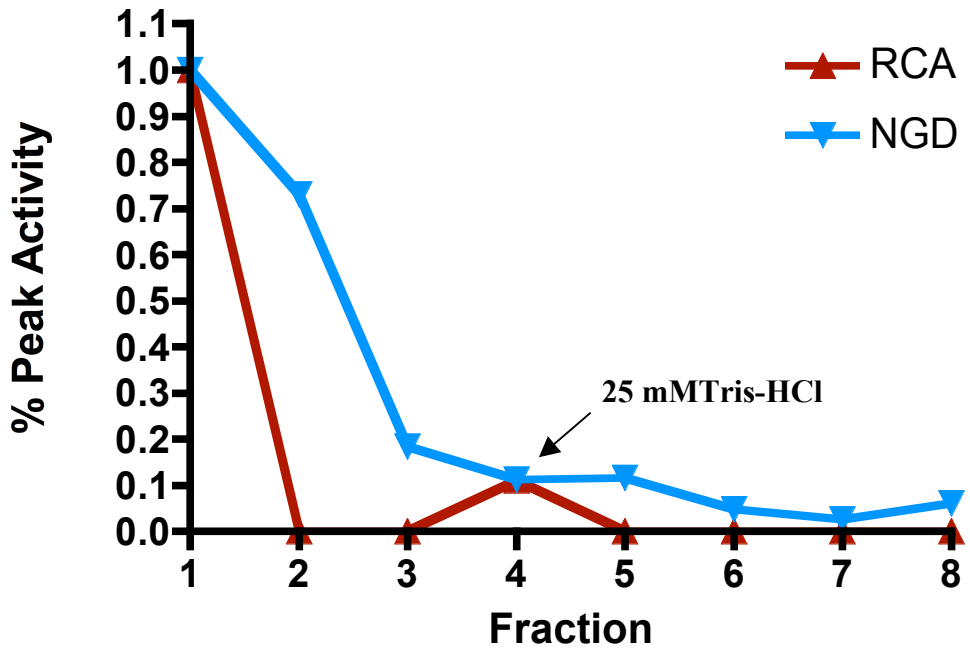

Figure 29. **CD38$^{+/+}$ Heart Cytosol Fractionation with Phenyl-Sepharose Chromatography**

CD38$^{+/+}$ rat heart cytosol was fractionated via Phenyl-Sepharose chromatography. The majority of ADPRC activity as measured by both the RCA and NGD assay was eluted in the void volume fraction with the KCl equilibration buffer, which suggests the novel cytosol ADPRC activity does not bind to Phenyl-Sepharose column.

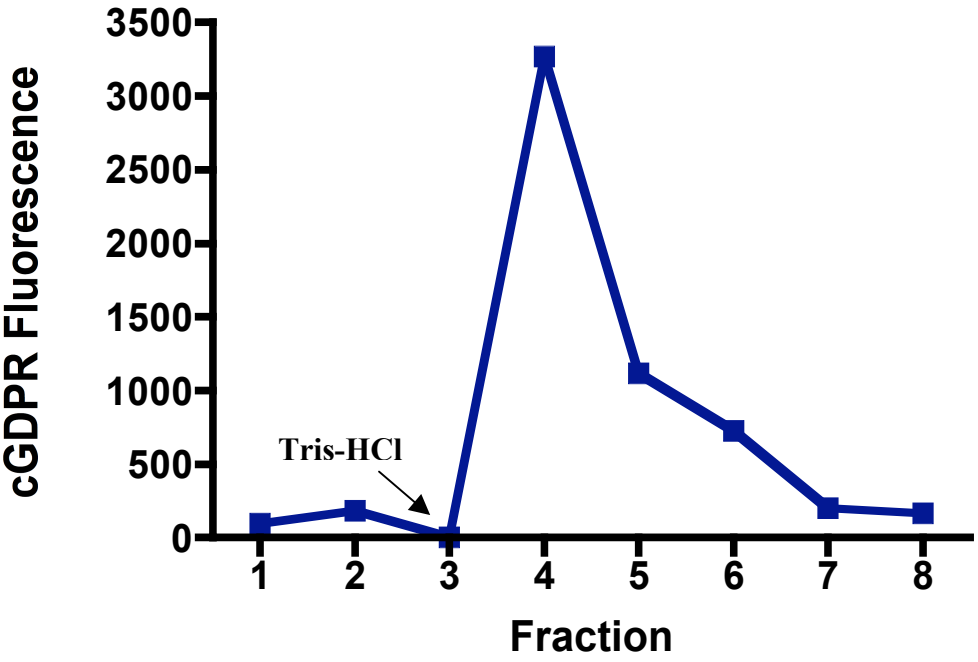

Figure 30. **rCD38 Fractionation with Phenyl-Sepharose Column Chromatography** rCD38 was fractionated via Phenyl-Sepharose chromatography. The majority of cGDPR fluorescence is eluted in the first fraction following the addition of the 25 mM Tris-HCl to the Phenyl-Sepharose column.

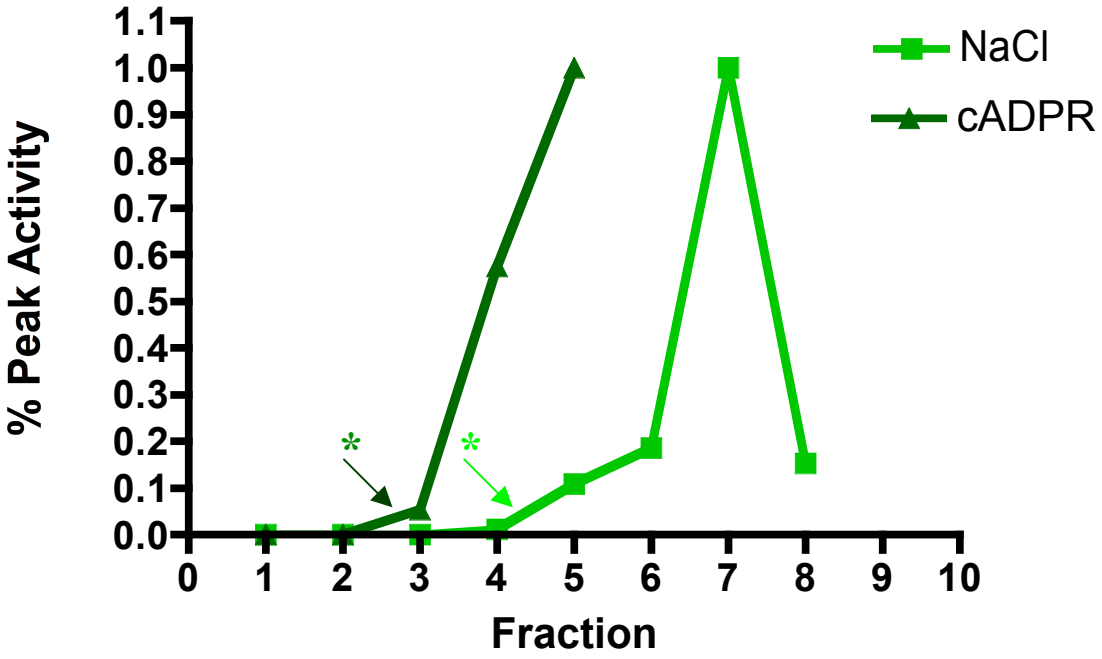

Figure 31. **CD38$^{+/+}$ Heart Cytosol Fractionation with Matrex-Gel Green Dye Affinity Chromatography**

CD38$^{+/+}$ heart cytosol binds to the Green Matrex-gel column and was eluted with 2.0 M NaCl*, which was added prior to collecting fraction four, and 1.0 mM cADPR*, which was added immediately prior to collecting fraction five.

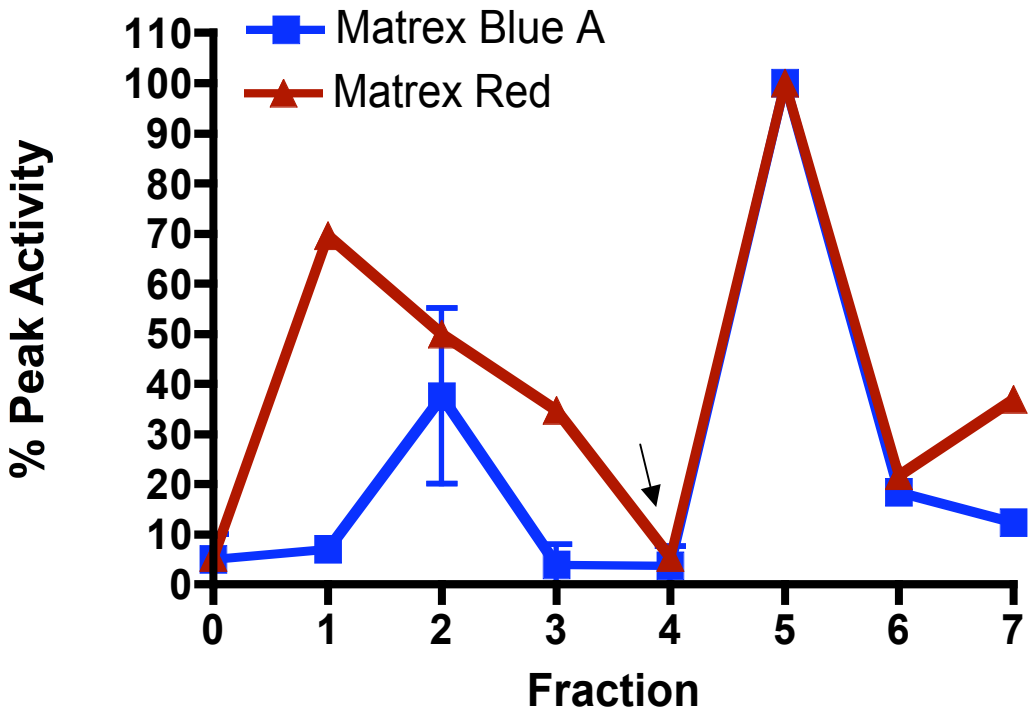

Figure 32. **CD38$^{+/+}$ Heart Cytosol Fractionation with Blue A & Red Matrex-Gel Affinity Chromatography**

CD38$^{+/+}$ heart cytosol was fractionated with Matrex-Gel blue A and Red columns and seven fractions were collected. The CD38$^{+/+}$ heart cytosol activity fractionated with the Matrex-Gel Blue A and Matrex-Gel Red columns had a small peak in the void volume, however a majority of the activity bound to the column and was eluted with the addition of 1.0 mM NaCl.

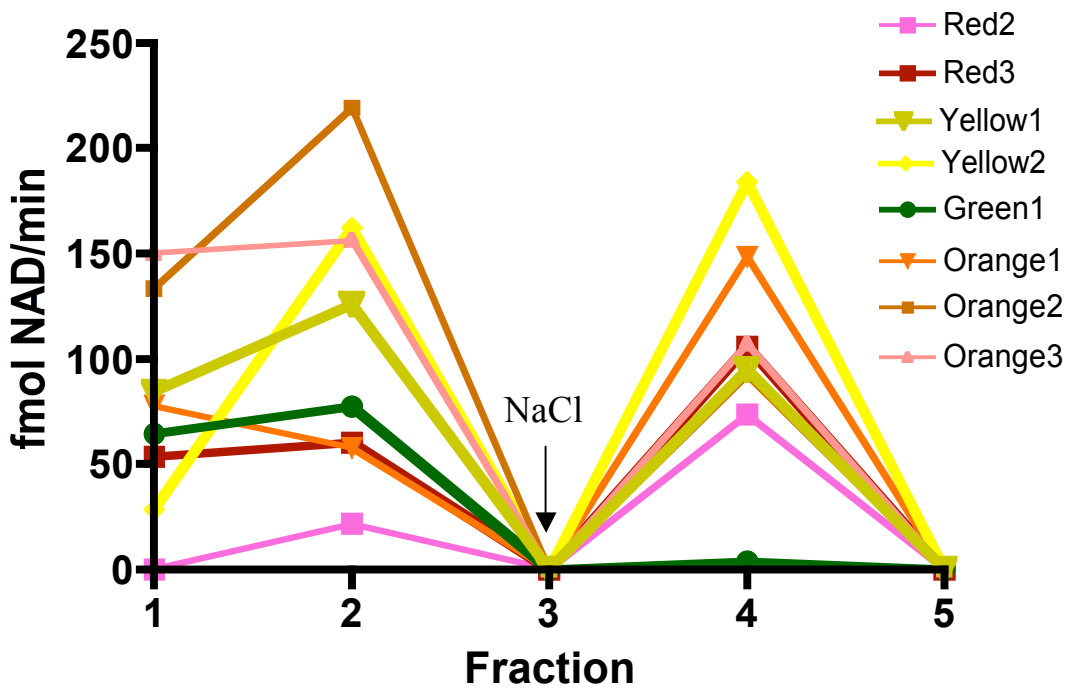

Figure 33. **CD38$^{+/+}$ Heart Cytosol Fractionation with Red 2, Red3, Yellow1, Yellow2, Green1, Orange1, Orange2, & Orange3 PIXI M Test Kit Affinity Chromatography**

The CD38$^{+/+}$ heart cytosol was fractionated using different dyes conjugated to a gel matrix column and the fractions were analyzed using the RCA. A portion of the ADPRC activity of the CD38$^{+/+}$ heart cytosol was eluted in the void volume, but a majority of the activity also bound to the columns with Red2, Red3, Orange1, Orange2, Orange3, Yellow1, Yellow2, and Green1 PIXI M Test Kit columns. The bound ADPC activity was eluted with 2.0 M NaCl, however the percent of activity recovered was very low.

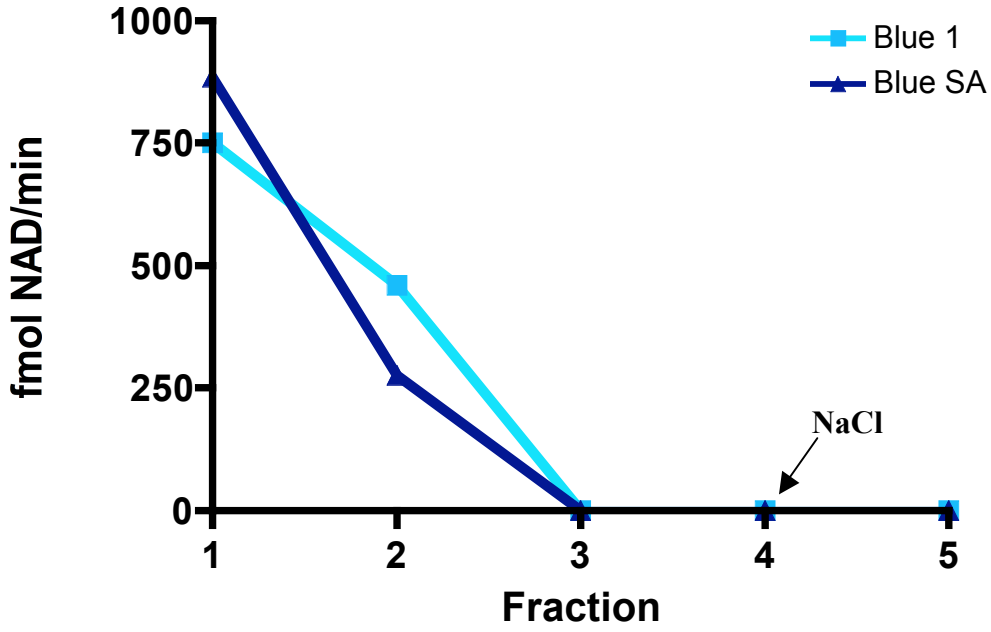

Figure 34. **CD38$^{+/+}$ Heart Cytosol Fractionation with Blue1 & BlueSA PIXI M Test Kit Affinity Chromatography**

The CD38$^{+/+}$ heart cytosol was fractionated using different dyes conjugated to a gel matrix column and the fractions were analyzed using the RCA. The ADPRC activity of the CD38$^{+/+}$ heart cytosol was eluted in the void volume of fractions from columns with Blue1 and BlueSA dye.

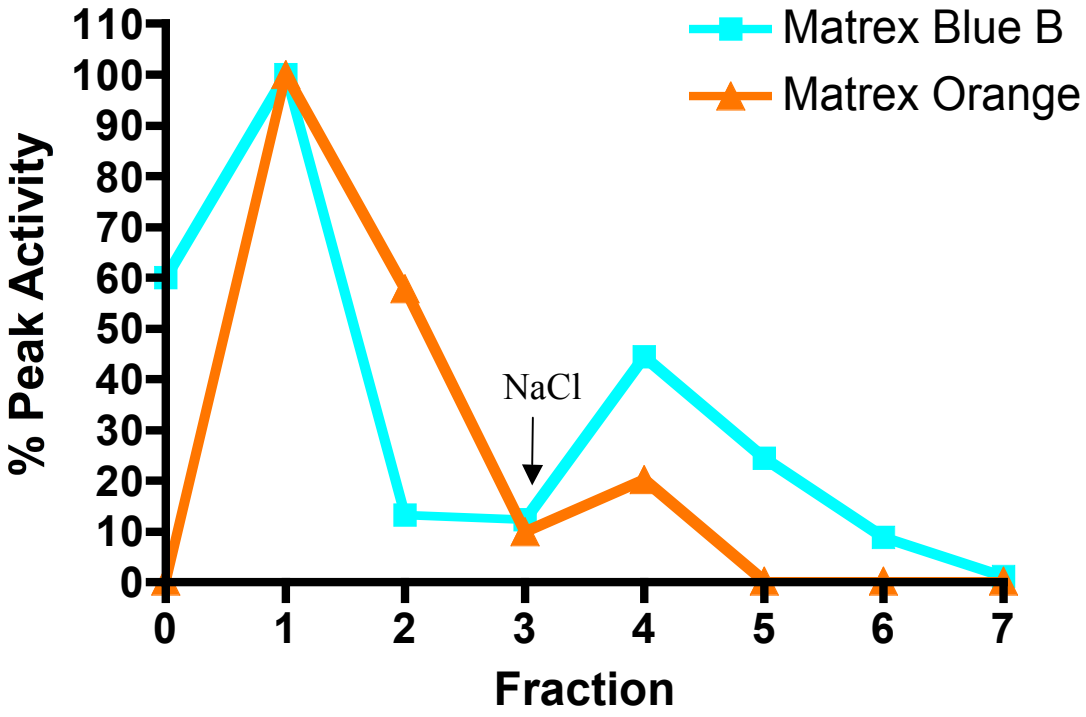

Figure 35. **CD38$^{+/+}$ Heart Cytosol Fractionation with BlueB & Orange Matrex-Gel Affinity Chromatography**

CD38$^{+/+}$ heart cytosol was fractionated with Blue B and Orange Matrex-Gel columns and seven fractions were collected. The columns were washed with equilibration buffer for the first three fractions. Elution buffer (1.0 M NaCl) was added immediately prior to collection of the fourth fraction. The majority of CD38$^{+/+}$ heart cytosol ADPRC activity did not bind to either column.

Chapter 4

Discovery of a Novel ADP-ribosyl Cyclase UC1212:

A Molecular Approach

The members of the ADP-ribosyl (ADPRC) family CD38, CD157, and *Aplysia* cyclase have been classified into the same protein family based on structure and function. There are two main features shared by all of these ADPRCs including a conserved region near the center and ten cysteine residues with conserved spacing alignment. Recently this family of enzymes has expanded with the discovery and characterization of numerous novel ADPRCs. Although evidence suggests that there are novel ADPRCs distinct from the well-known mammalian forms CD38 and CD157, it has been a challenge to utilize conventional protein purification strategies to identify the novel cyclases. Furthermore, molecular approaches including BLAST searches have not been useful in identifying the cyclases. In this study, a Hidden Markov Model (HMM) based approach was employed to search the PROSITE database for proteins with matching conservation of the spacing of the cysteine residues in the carboxyl-terminus and six potential ADPRC candidates were identified. The most interesting candidate, UC1212, shared both the cysteine motif of the carboxyl-terminus as well as sequence identity with the conserved "TLEDTL" domain of the well-known cyclases. UC1212 was cloned into histidine (His)-tagged and GFP-tagged plasmids to create mammalian expression vectors (pDEST26-UC1212 and pEGFP-N3-UC1212), which were transfected into HeLa cells and shown to have ADPRC activity. This study has not only led to the discovery and identification of the novel ADPRC UC1212, but has also provided compelling evidence that utilizing a molecular based approach involving multiple sequence alignments to identify novel ADPRC family members is a powerful alternative to conventional purification strategies.

Introduction

The ADPRC family is a protein family composed of proteins that are classified by related enzymatic structure and function. Previously it has been shown that *Aplysia* cyclase, CD38 and CD157 share approximately 30% sequence identity [9, 21, 24-26]. Specifically, there are two main features shared by each of these members of the ADPRC family; the first being the conserved "TLEDTL" region of about 18 amino acids predicted to be part of the active site necessary for catalysis [27-31], and the second being ten cysteine residues with conserved alignment [24] that form disulfide bridges that participate in maintaining the catalytically active structure of ADPRCs [31, 35]. Recent reports have shown that novel ADPRCs also share the ten conserved cysteine residues of the other known ADPRCs [11, 12, 75, 76]. In the past there have been attempts to identify novel members of the ADPRC family by conducting pairwise alignment methods such as BLAST [245] and FASTA [246] to identify proteins sharing high sequence identity with the *Aplysia* cyclase [21], which was met with limited success. While the spacing of the cysteine residues are tightly conserved [24], the amino acids between the cysteine residues are not well conserved . As is demonstrated by the ADPRC family of proteins, different amino acid residues in a functional sequence are subject to different selective pressures. This results in certain residues being tightly conserved, while others are not [247]. It is from this pattern of conservation that the idea of using position specific information, profile methods, from multiple alignments to search databases for homologous sequences was developed [248, 249]. In the past, the limitation of this model was the inability to calculate the multiple sequence alignment scores analytically [247].

However, statistical models for use as profile methods such as HMM have been introduced as an analytical method of searching for homologous proteins using the multiple sequence alignment based methods [250]. In this study, we exploited the structural similarities of the ADPRC family and utilized a HMM method that involved a protein motif search of the PROSITE profiles database [251] to identify potential novel ADPRC family members. We were interested in identifying proteins that share the feature of the conserved cysteine residues observed in all of the ADPRC family members [11, 12, 24, 75, 76]. Interestingly, six uncharacterized candidate proteins were identified that share the protein motif based on the C-terminal cysteine residues of the members of the ADPRC family (Figure 36). Of the six members, one uncharacterized protein candidate in particular that not only retained the conserved C-terminal cysteine residues, but also a tightly conserved leucine and a significant portion of the conserved "TLEDTL" region [31] (Figure 37). The candidate protein was 1212 amino acids in size, which corresponds to a size of approximately 130 kDa. This uncharacterized candidate protein will be referred to as UC1212 from this point forward. We found that the UC1212 gene was cloned as part of the Mammalian Gene Collection (MGC). We obtained the MGC clone and inserted the UC1212 gene into His-tagged and GFP-tagged mammalian expression vectors using gateway technology and molecular cloning techniques. Both the truncated and full-length mammalian expression constructs of UC1212 expressed ADPRC activity when transiently transfected into various cell lines. This study provides evidence that utilizing a molecular based approach to identify novel ADPRC family members is possible.

Material and Methods

Protein Motif Search of the Mammalian Genome

In the past, it has been shown that proteins that share structural features have similar enzyme activities [248]. Previous investigations have revealed that members of the ADPRC family have a conserved cysteine residue motif [11, 12, 24, 75, 76] that may be utilized to reveal other proteins that share ADPRC enzyme activities. In this study, an HMM based method [250] using the structural information of the ADPRC family was utilized to search the PROSITE profile database [251] to identify potential uncharacterized protein candidates possessing ADPRC activity. Candidates were identified based on a protein motif search off the conservation of the spacing of the cysteines in the carboxyl-terminus of well-known ADPRCs *Aplysia* cyclase, CD38 and CD157 [11, 12, 24, 75, 76] (Figure 2).

Construction of Murine UC1212 Expression Clone (pDEST26-His-UC1212)

UC1212, the most lucrative candidate identified using the protein motif search shared the conserved C-terminal cysteine residues, a tightly conserved leucine, and portions of the "TLEDTL" conserved sequence with the known ADPRCs [24, 31]. In order to determine if UC1212 had similar enzyme activities as ADPRCs [2, 19], we first needed to express

the gene of the UC1212 as a functional protein. The murine UC1212 gene (CQ068) was obtained from the MGC collection and cloned into a His-tagged mammalian expression vector via Invitrogen Gateway Cloning Technology (Figure 39). Human UC1212 was PCR amplified from cDNA clone IMAGE:5549770 (Invitrogen) with the forward primer 5'- GGGGACAAGTTTGTACAAAAAAGCAGGCTTAGCCCTGGCAGAGG and the reverse primer 5'- GGGGACCACTTTGTACAAGAAAGCTGGTCCTAAGAC GAA G CAGCAGA. For the PCR amplified products, an attB1 site was created at the N-terminus and an attB2 site was created at the C-terminus. 50 fmol of PEG purified PCR-UC1212 was added to 150 ng of pDONR221 (Invitrogen) in TE buffer, pH 8.0. 2.0 µl of BP Clonase II (Invitrogen) was added to facilitate the lambda (λ) recombination [252] of the attB sites in the linear PCR products and the attP sites in the donor vector pDONR221 to create the attL entry clone (pDONR221-UC1212). The kanamycin resistant construct was transformed in OneShot TOP10 chemically competent E.*coli*. 50 ng of pDONR221-UC1212 was added to 150 ng of the destination vector pDEST26 (Invitrogen). 2.0 µl of LR Clonase (Invitrogen) was added to facilitate the λ recombination [252] reaction of the attL sites of the entry clone and the attR sites of the destination vector (pDEST26) to create the attB expression clone pDEST26-His-UC1212. The ampicillin resistant construct was transformed in OneShot TOP10 chemically competent E.*coli*. The pDONR221 and pDEST26 vectors contained a ccdB insert, which served as a negative selection marker to increase efficiency of recombination and transformation. The plasmids were purified with HiPure Maxi-prep columns (Invitrogen) and the sequences of the constructs were confirmed using M13 sequencing primers (Invitrogen).

Construction of Human UC1212 Expression Clone (pEGFP-N3-UC1212)

The full-length human homologue of UC1212 was obtained from the MGC clone collection and cloned into a GFP- tagged mammalian expression vector using directional cloning. The vector, pEGFP-N3 (Clontech Laboratories) was cut at cloning sites with restriction enzymes, XhoI and SacI and then purified with Qiagen DNA purification kit. The coding sequence of the full-length UC1212 was PCR amplified from cDNA clone IMAGE:4241696 (Open Biosystems) using the forward primer as 5'-CCGCTCGAGCTA TGGCGGCTGGCCGGGCCCAG and reverse primer as 5'-TCCCCGCGGTACAGGA GGAAGCAAGGATCMCCCAGAG. For the PCR amplified products, an XhoI site was created at the N-terminus and a SacII site was created at the C-terminus. The PCR products were cut with restriction enzymes XhoI and SacII and gel-purified. The purified PCR-UC1212 was inserted into the GFP-tagged mammalian expression vector pEGFP-N3 by traditional ligation techniques. The kanamycin resistant pEGFP-N3-UC1212 construct was transformed into OneShot TOP10 chemically competent E.*coli*. The plasmid was purified with HiPure maxi-prep columns and the recombinant DNA constructs were sequenced to determine whether the UC1212 coding sequence was inserted correctly into the vector.

Cell Culture of HeLa, CHO, and 3T3 Cells

HeLa (supplied by Dr. Graeff, U of M Department of Pharmacology), CHO (supplied by

Dr. Graeff), and 3T3 (supplied by Dr. Potter, U of M Department of BMBB) cell lines, all shown to lack endogenous ADPRC activity, were utilized for the transfection experiments. The cell lines were maintained in DMEM (Invitrogen) containing 10% fetal bovine serum (Invitrogen) and 1.0% Penicillin/Streptavidin (Invitrogen). Cells were split and harvested using TrypLE Express (Invitrogen). Cells were maintained at 37ºC with 5.0% CO_2 in a water-jacketed incubator.

Transfection of HeLa Cells with pDEST26-UC1212 and pShuttle-GFP-CD38

The gateway mammalian expression clone with the murine UC1212 insert (pDEST26-UC1212) was transiently transfected into HeLa, 3T3, and CHO cells. Cells were also transfected with pShuttle-GFP CD38 (supplied by Dr. Kannan, U of M Department of Veterinary and Biomedical Sciences) and the pDEST26 empty vector as positive and negative controls for ADPRC expression respectively. 1.0 x 10^6 HeLa cells were plated in 60 mm dishes (Corning) 24 hours prior to transfection. Cells were transfected with a total volume of 500 µl of Opti-MEM media (Invitrogen) containing 2.5 µg of DNA and 7.5 µl of lipofectamine 2000 transfection reagent (Invitrogen). Transfected cells incubated at 37°C and 5.0% CO_2 were harvested with Trypsin LE Express at 48 hours. The harvested cells were dialyzed against 30 mM Tris-HCl (Fisher Scientific) with 3500 MWCO dialysis tubing (Fisher Scientific) for 24 hours at 4ºC to remove any contaminant NAD. The dialyzed samples were centrifuged at 13,000 x g for 10 minutes. The supernatant was removed (cytosol fraction) and the pellet was re-suspended (membrane

fraction) in 200 µl of lysis buffer, containing 20 mM Tris-HCl and protease inhibitor tablets (Roche), and then sonicated for 10 seconds on ice.

Transfection of HeLa Cells

The full-length, GFP-tagged human homologue of UC1212 (pEGFP-N3-UC1212) was transiently transfected into HeLa cells. HeLa cells were also transiently transfected with pShuttle-GFP CD38 and pcDNA3.1-CD38 (supplied by Dr. Kannan), as positive controls as well as with an empty vector negative control for ADPRC activity. 1.0×10^6 HeLa cells were plated in each well of a 6-well plate (Corning) immediately prior to transfection. Cells were split transfected with a total volume of 500 µl of Opti-MEM media containing 5.0 µg of DNA and 15 µl of Megatran 1.0 (Origene Technologies) transfection reagent per well. Transfected cells incubated at 37°C and 5.0% CO_2 were harvested with TrypLE Express at 48 hours. The harvested cells were dialyzed against 30 mM Tris-HCl with 3500 MWCO dialysis tubing for 24 hours at 4ºC to remove any contaminant NAD. The dialyzed samples were centrifuged at 13,000 x g for 10 minutes. The supernatant was removed (cytosol fraction) and the pellet was re-suspended in 200 µl of lysis buffer (membrane fraction) and sonicated for 10 seconds on ice. This investigation was also completed as a set of blind experiments under the same conditions.

Imaging of Transfected HeLa Cells Transfected GFP-constructs

Images of cells transfected with the GFP-tagged pShuttle-GFP CD38 and pEGFP-N3-UC1212 constructs, were obtained using confocal and fluorescence microscopy. 1.0 x 10^6 cells were plated in 35 mm glass bottom dishes (Corning) immediately prior to transfection. Cells were split transfected with a total of 500 µl of Opti-MEM media containing 5.0 µg of DNA and 15 µl of Megatran 1.0 transfection reagent. Transfected cells were incubated at 37°C and 5.0% CO_2 for 48 hours. Images of live cells were obtained using a confocal microscope at excitation wavelength 400 nm. Cells were also fixed with formaldehyde (Sigma), stained with DAPI (Molecular Probes) and images of the cells were obtained using a fluorescence microscope.

Western Blot of pEGFP-N3-UC1212 and pShuttle-GFP-CD38 Transfected HeLa Cells

1.0 x 10^6 cells were plated in 35 mm dishes immediately prior to transfection. Cells were split transfected with a total volume of 500 µl of Opti-MEM media containing 5.0 µg of DNA and 15 µl of Megatran 1.0 transfection reagent. Transfected cells were incubated at 37°C and 5.0% CO_2 and harvested 48 hours. Samples were separated on a 4-12% (w/v) polyacrylamide denaturing gel and electrotransffered to a nitrocellulose membrane (Millipore) for detection. The membrane was incubated in 12% non-fat dry milk with a 1:1000 dilution of the primary antibodies anti-GFP (Santa-Cruz Biotechnology) and anti-β-tubulin (Pierce Scientific) at 4°C overnight. The membrane was washed with

phosphate buffered saline tween-20 (PBST) prior to incubation with 12% non-fat dry milk with a 1:5000 dilution of IRDye800 (Li-Cor Biosciences) for 1 hour at 25°C. After washing the blots, the reactive proteins were detected with Li-Cor Odyssey Infrared Imaging.

Reverse Cyclase Assay of Transfected Cells

Samples were incubated at 37ºC for four hours with cADPR (350-425 μM) and an excess nicotinamide (10 mM), which facilitated the conversion of cADPR to NAD in the presence of ADPRC. The reactions were carried out in 96-well plates (Sarstedt) with a total reaction volume of 50 μl. The samples were filter stopped with Millipore IP membranes using a vacuum manifold prior to proceeding to the next reaction step. The samples were diluted and transferred to 384-well plates (Corning). The initiation of the second step involved the of the addition of 40 μl of the filtered reaction mixture, diluted in sodium phosphate buffer (J.T. Baker) pH 8.0, to 40 μl of RCA reagent to amplify the NAD produced and convert it to the fluorescent product resorufin (Figure 3). The RCA reagent was composed of final concentrations of 0.76% ethanol (Pharmco), 40 μg/ml ADH (Sigma), 0.04 μg/ml diaphorase from *Clostidium klyveri* (Sigma), 4.0 μM FMN (Sigma) and 2.0 μM resazurin (Sigma) in sodium phosphate buffer, pH 8.0. NAD was converted to NADH by ADH, which was utilized by diaphorase to reduce resazurin to produce the fluorescent product resorufin. The resorufin fluorescence served as an indicator of NAD produced in the first step as a result of ADPRC activity. The time

dependent increase in resorufin fluorescence was measured at 25°C for 25 cycles with fluorescence plate reader (*FLUO*star *Galaxy*) set with the excitation at 544 nm and emission at 590 nm. As the cycling method employed to amplify NAD was incredibly potent, the diaphorase was treated with activated charcoal (Sigma) to remove any contaminant NAD. Upon removal of contaminant NAD, the presence of ADPRC was required for the production of NAD. The difference in fluorescence produced by samples incubated in the presence and absence of nicotinamide, which was also necessary for NAD production, served as a control to identify background resultant of background NAD present in the samples.

Zinc Regulation of pEGFP-N3-UC1212 and pShuttle-GFP-CD38 ADPRC Activity

There are a variety of agents known to activate and inactivate CD38. Previous studies have shown that zinc activates the ADPRC activity of CD38 and CD157 [126]. In order to better characterize the ADPRC activity of UC1212, we investigated if its enzyme activities were regulated by zinc. The full-length human homologue of UC1212 pEGFP-N3-UC1212 construct was transiently transfected into HeLa cells. HeLa cells were also transiently transfected with pShuttle-GFP CD38 and an empty vector to serve as positive and negative controls for ADPRC activity respectively. The membrane fraction of the harvested cells was incubated with 0-10 mM zinc acetate (Sigma) for ten minutes at 25°C. Upon completion of the pre-incubation, the samples were incubated with 380 μM cADPR and 10 mM nicotinamide at 37°C for four hours. Immediately upon removal

from the incubator, the samples were filtered with Millipore IP membranes using a vacuum manifold to stop the reaction. The second reaction step was initiated with the addition of 40 µl of RCA reagent to 40 µl of sample diluted in sodium phosphate buffer, pH 8.0 in 384-well plates. The cycling reaction was allowed to proceed at 25°C for 25 cycles on a fluorescence plate reader with the excitation at 544 nm and emission at 590 nm. The increase in resorufin fluorescence was used as an indication of cyclase activity. Background, which was determined by incubating the samples without nicotinamide, was subtracted from the fluorescence seen upon incubation of the samples with nicotinamide.

Results

Protein Motif Search of the Mammalian Genome

The HMM based protein motif search [250] was used to search PROSITE profile database [251] to reveal proteins with a similar carboxyl-terminus motif as known ADPRCs [24]. Interestingly, we identified six uncharacterized proteins that have retained the protein motif observed in the carboxyl-terminus of the identified cyclases (Figure 36). One of the candidates in particular, UC1212 (Figure 38), also exhibited a region with sequence identity to the "TLEDTL" conserved region [31], as well as a

tightly conserved leucine (Figure 37), which strongly suggested a high probability it was a novel ADPRC based on structural similarities.

Imaging of HeLa Cells Transfected with GFP-constructs

Images of HeLa cells transfected with pEGFP-N3-UC1212 and pShuttle-GFP- CD38 were obtained using fluorescence and confocal microscopy of both live (Figure 40) and fixed cells (Figure 41). The images indicate efficient transfection with peak GFP expression occurring at 48 hours (data not shown). Further, similar localization of GFP signal, which was clearly ubiquitous, was observed in both CD38 and UC1212 GFP-tagged mammalian expression constructs.

Western Blot of HeLa Cells Transfected with GFP-constructs

Western blot analysis was utilized to confirm the full-length GFP-tagged CD38 and UC1212 protein expression in the HeLa cells transfected with pEGFP-N3-UC1212 and pShuttle-GFP-CD38 constructs. The western blot confirmed the presence UC1212 at 150 KDa in HeLa cells transfected with pEGFP-N3-UC1212. However, the presence of GFP-tagged CD38 (50 KDa) was difficult to detect in the HeLa cells transfected with pShuttle-GFP CD38, as the expected size was very close to the loading control anti-β-tubulin (55 KDa). The anti-β-tubulin loading control indicated the samples had equal amounts of

protein (Figure 42).

ADPRC activity of Murine Truncated Clone pDEST26-UC1212 Transfected Cells

The murine UC1212 gene was cloned into a His-tagged gateway mammalian expression vector to create pDEST26-UC1212. This construct was transiently transfected into HeLa cells, which have been shown to have negligible levels of endogenous ADPRC activity. The HeLa cells transfected with the mammalian vector expressing UC1212, exhibited ADPRC activity as measured by the RCA (Figure 43), which provided compelling evidence that UC1212 is indeed a novel ADPRC that does not require the N-terminus to retain enzyme activity.

ADPRC Activity of Human Full-length Clone pEGFP-N3-UC1212 Transfected Cells

Since murine UC1212 exhibited ADPRC activity, the full-length human homologue was cloned into a GFP-tagged mammalian expression vector. HeLa cells transiently transfected with pEGFP-N3-UC1212 were shown to have ADPRC activity comparable to that of the GFP-tagged CD38 construct as measured by the RCA (Figure 44). The untagged pcDNA3.1-CD38 clone, which was also a positive control, had a substantial amount of ADPRC activity as well, while the negative transfection controls did not express ADPRC activity. Similar results were obtained with the blind transfection

studies (Figure 45). Further, we have shown that both membrane and cytosol fractions of the HeLa cells transfected with pEGFP-N3-UC1212, pShuttle-GFP-CD38, and pcDNA3.1-CD38 constructs had ADPRC activity (Figure 46). This data confirmed the uncharacterized protein UC1212 as a novel member of the ADPRC family of enzymes.

Zinc Regulation of pEGFP-N3-UC1212 and pShuttle-GFP-CD38 ADPRC Activity

Zinc is among the variety of agents known to activate [126] and inactivate [124, 240] CD38 ADPRC activity. In order to better characterize the novel ADPRC UC1212, we utilized zinc, a known activator of CD38 and CD157 ADPRC activities [126]. ADPRC activity of the membrane fraction of HeLa cells transiently transfected with pEGFP-N3-UC1212 and pShuttle-GFP-CD38 constructs was measured at pH 7.0 in the presence of 0-10 mM zinc acetate. Concentrations of zinc from 5.0-10 mM resulted in complete inhibition of the ADPRC activity of UC1212, while it resulted in more than a 200 percent increase in CD38 activity (Figure 47). This data suggests UC1212 is a novel ADPRC regulated in a manner distinct from CD38 and CD157.

Discussion

The ADPRC family is a highly conserved and classified by multi-functional enzyme activities of its members which share approximately 30% sequence identity [9, 21, 24-26]. The two key features shared by each of these members of the ADPRC family include a conserved "TLEDTL" domain [31] and ten conserved cysteine residues that can be perfectly aligned [24]. Although the cysteine residues are tightly conserved, the amino acid sequence between the cysteine residues is not well conserved. Statistical models such as HMM have been introduced as an analytical method of searching for homologous proteins using the multiple sequence alignment based methods [250]. In this study, an HMM based method using the structural information of the ADPRC family was utilized to search the PROSITE profiles database [251] to identify six potential uncharacterized proteins that shared a protein motif based on the C-terminal cysteine residues [11, 12, 75, 76]. The most interesting uncharacterized protein candidate UC1212 not only had the C-terminal region of cysteine residues conserved, but also a tightly conserved leucine and a significant portion of the conserved "TLEDTL" region [31]. Further, the candidate protein was 1212 amino acids in size, which corresponded to the heart cytosolic protein that was predicted to be around 130 KDa. The UC1212 MGC clones were obtained and both the truncated murine UC1212 gene and the full-length human UC1212 homologue were cloned into mammalian expression vectors. HeLa cells transiently transfected with both the full-length and truncated UC1212 constructs were shown to have ADPRC activity as measured by the RCA. Interestingly the truncated version, which lacked the N-terminus, retained ADPRC activity. This is in agreement

with previous studies that indicate the N-terminal cytoplasmic tail and trans-membrane domain are not required for ADPRC activity [53]. The ADPRC activity of the full-length human homologue was comparable to the activity of the GFP-tagged CD38 positive control and this activity was also confirmed using blind transfection studies. Further, we have shown that the ADPRC activity of UC1212 was inhibited by zinc, which is characteristically distinct from the activity of CD38, which was stimulated by zinc. In these studies we have demonstrated that a highly sensitive, high throughput assay to screen for ADPRC activity in combination with a molecular based approach to identify potential ADPRC candidates was successful in uncovering the novel ADPRC UC1212. This indicates it is possible to exploit the structural similarities of ADPRC family members [11, 12, 75, 76] to identify candidate proteins to be screened for ADPRC activity, which will contribute to advances in identification of the proteins responsible for observed novel ADPRC activity.

Entry name	Description	Pattern	Position	AA's
K0562_MOUSE	uncharacterized protein	**C-x (20) -C-x (11) -C.**	813	926
CQ068_MOUSE (UC1212)	uncharacterized protein	**C-x (7) -L-x(12)C-x (11) -C.**	1024	1212
CN130_MOUSE	Uncharacterized protein	**C-x (20) -C-x (11) -C.**	78	425
CA095_MOUSE	uncharacterized protein	**C-x (20) -C-x (11) -C.**	57	141
CA172_MOUSE	uncharacterized protein	**C-x (11) -C-x (8) -C.**	74	397
CT075_MOUSE	uncharacterized protein	**C-x (11) -C-x (8) -C.**	544	733

Figure 36. **Conserved Protein Motif Search Novel ADPRC Candidates**

An HMM based method was utilized to search the PROSITE profiles database using a protein motif search of the C-terminal conserved cysteine residues. Six uncharacterized murine proteins that shared the protein motif observed in the carboxyl-terminus of the known members of the ADPRC cyclase family were identified.

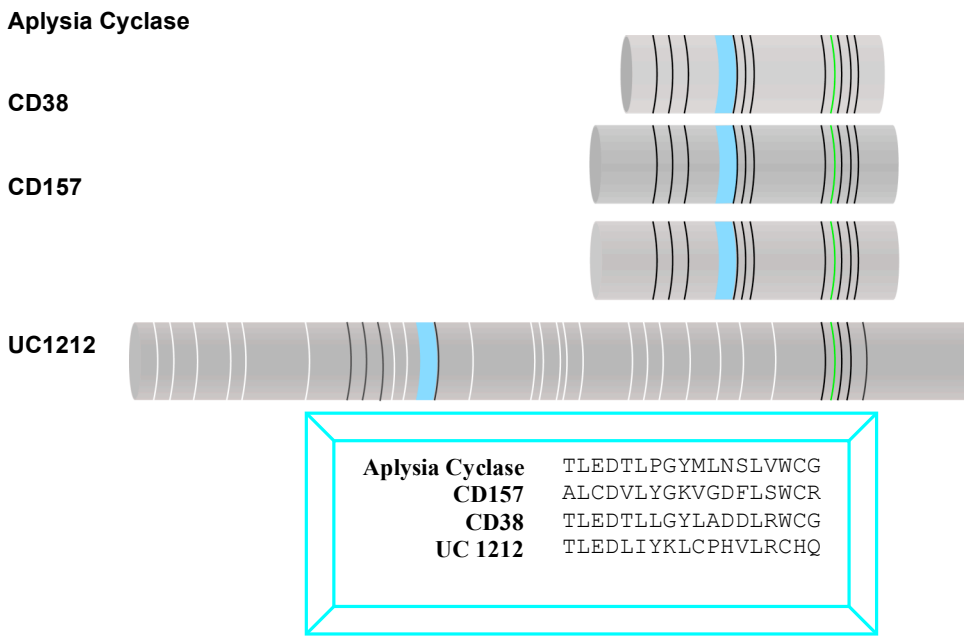

Figure 37. **Structural Similarities of ADPRCs with UC1212.**

The known members of the ADPRC family Aplysia cyclase, CD38 and CD157 share sequence homology. There are two features that are highly conserved throughout the ADPRC family: 10 cysteine residues that can be perfectly aligned (black lines) as well as the conserved "TLEDTL" region (blue), shown in detail. These features were utilized along with a protein motif search of the mouse genome to identify UC 1212 as a potential ADPRC. As depicted in this figure, UC1212 shares three perfectly aligned cysteines (black) and one leucine (green) at the C-terminal region of the genes as well as the conserved region (blue) toward the N-terminus. The sequence of the conserved regions of each is shown. Further there are multiple cysteines (white) that may correspond with other conserved cysteines.

MAACRAQPPT SEQAWLEAAQ TFIQETLCPA GKEVDKELTR SVIACVKETW 50
LSQGENQDLT LPFSYSFVSV QSLKTHQRLP CCSHLSWSQS AYQAWTRGGR 100
PGDGVLPREQ LILLGTLVDL LGDSEQECRS GSLYVRDNTG TLDCELIDLD 150
LSWLGHLFLF PSWSYLPSAK RNSLGEGHLE LWGTPVPVFP LTVSPGPLIP 200
IPVLYPEKAS HLLRYRKKSS IKEINLAGKL VHLSALIITQ NKRYFIMTLG 250
ELAQAGSQVS IIVQIPAQMV WHRVLRPGRA YVLTKLQVTK TRIHLSCIWT 300
TIPSSTLKPL RPGYVQELEL DLEFSKADLK PPPQPTSSKD SRGQEGLVRA 350
SKVLHYLGTV TAVLHESAGL YILDGQLILC LAYQKIHGLR RVIRPGVCLE 400
LRDVHLLQAV GGATTKPVLA LCLHGTVRLQ GFSCLKPLTL PSSKVYGASL 450
YEQLVWKCQL GLPLYLWAAK TLEDLIYKLC PHVLRCHQFL KQPSPGKPSL 500
GLQLLAPSWD VLIPPGSPMR HAYSEILEEP HNCPLQKYTP LQTPYSFPTM 550
LALAEEGQHR AWATFDPKAM LPLPEASHLT SCQLNRHLAW SWVCLPSCVF 600
QPAQVLLGVL VASSRKGCLE LRDLRGSLPC IPLTESSQPL IDPNLVGCLV 650
RVEKFQLVVE REVRSSFPSW EEMGMARFIQ KKQARVYVQF YLADALILPV 700
PRPTFGSEPS QTASSCPEGP HLGQSRLFLL SHKEALMKRN FCLLPGDSSQ 750
PAKPTLSFHV SGTWLCGTQR KEGSGWSPPE SLAVESKDQK VFLIFLGSSV 800
RWFPFLYPNQ VYRLVASGPS QTPVFETEGS AGTSRRPLEL ADCGSCLTVQ 850
EEWTLELGSS QDIPNVLEVP RTLPESSLAQ LLGDNSPDSL VSFSAEILSR 900
ILCEPPLALR RMKPGNAGAI KTGVKLTVAL EMDDCEYPPH LDIYIEDPQL 950
PPQIGLLPGA RVHFSQLEKR ISRSNIVYCC FRSSTSVQVL SFPPETKASA 1000
PLPHIYLAEL LQGDRPPFQA TTSCHIVYVL SLQILWVCAH CTSICPQGKC 1050
SRRDPSCPSQ RAVSQANIRL LVEDGTAEAT VICRNHLVAR ALGLSPSEWS 1100
SILEHARGPG RVALQFTGLG GQTESASKTH EPLTLLLRTL CTSPFVLRPV 1150
KLSFALERRP TDISPREPSR LQQFQCGELP LLTRVNPRLR LVCLSLQEPE 1200
LPNPPQASAA SS

Figure 38. **Amino Acid Sequence of UC1212**

UC1212 was the most interesting uncharacterized candidate protein uncovered using the protein motif search. The amino acid sequence revealed that it had the conserved carboxyl-terminal cysteine residues, a tightly conserved leucine, and the conserved "TLEDTL' region.

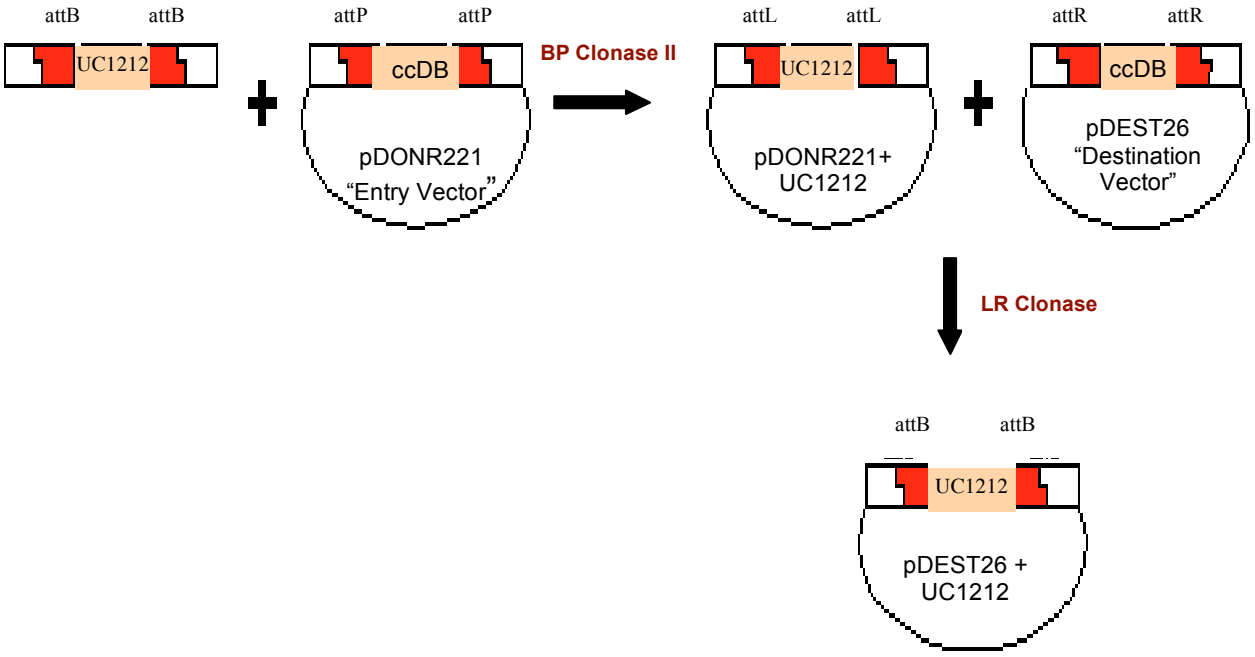

Figure 39. **Gateway Cloning Reaction Schematic**

UC1212 PCR products with attB sites were recombined with pDONR221 vector with attP sites using BP Clonase II to generate pDONR221 UC1212. The pDONR221 plasmid with attL sites was recombined with the pDEST26 vector with attR sites using LR Clonase to produce the histidine-tagged mammalian expression pDEST26 UC1212.

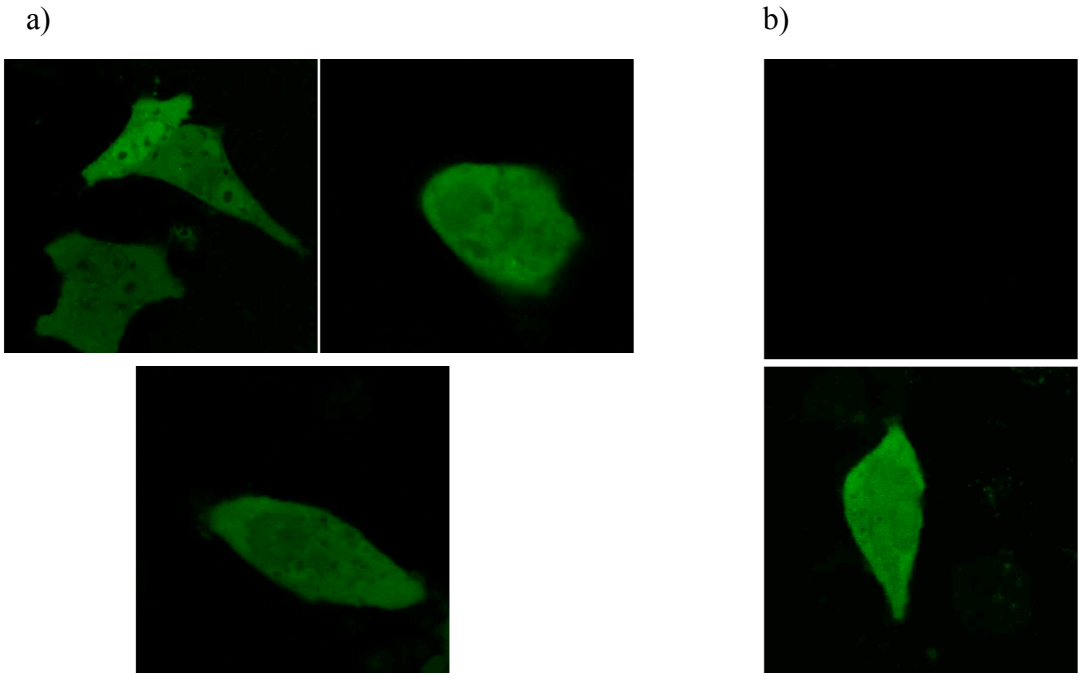

Figure 40. **Confocal Images of HeLa Cells Transfected with GFP-constructs**

a) The GFP-tagged UC1212 construct pEGFP-N3-UC1212 had ubiquitous GFP expression in live cells 48 hours post-transfection. b) The negative transfection control did not have background fluorescence and the GFP-tagged CD38 construct pShuttle-GFP- CD38 had ubiquitous GFP expression.

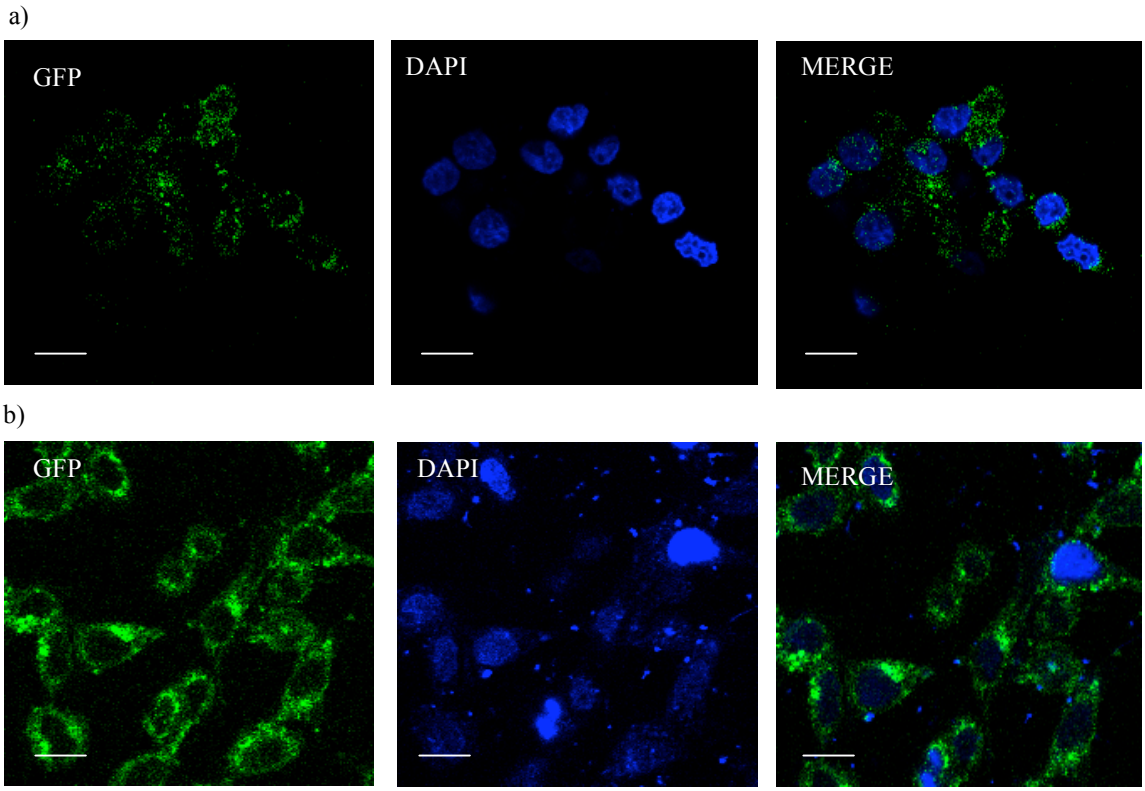

Figure 41. **Fluorescence Images of GFP-construct Transfected HeLa Cells**

a) HeLa cells transiently transfected with the GFP-tagged UC1212 construct pEGFP-N3-UC1212 and b) HeLa cells transiently transfected with the GFP-tagged CD38 construct pShuttle-GFP-CD38 expressed GFP in DAPI stained cells (20 μm in diameter) with intact nuclei 48 hours post-transfection.

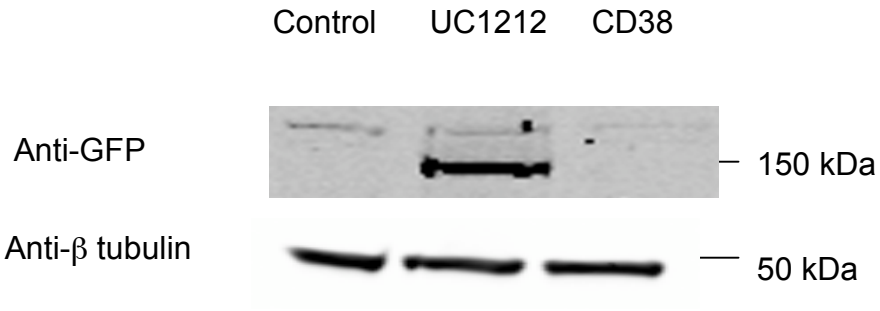

Figure 42. **Western Blot of HeLa cells Transfected with GFP-tagged Constructs** Western blot analysis was used to confirm the expression of GFP-tagged proteins in HeLa cells transfected with pEGFP-N3-UC1212 and pShuttle-GFP-CD38 constructs. The loading control anti-β-tubulin (55 kDa) was used to show that the samples had equal amounts protein. HeLa cells transfected with pEGFP-N3-UC1212 had a GFP-expressing protein that ran at 150 kDa. The expression of the GFP-tagged CD38 (50 KDa) protein was difficult to detect in HeLa cells transfected with pShuttle-GFP-CD38, as it was very close in size to the heavily expressed anti-β-tubulin loading control.

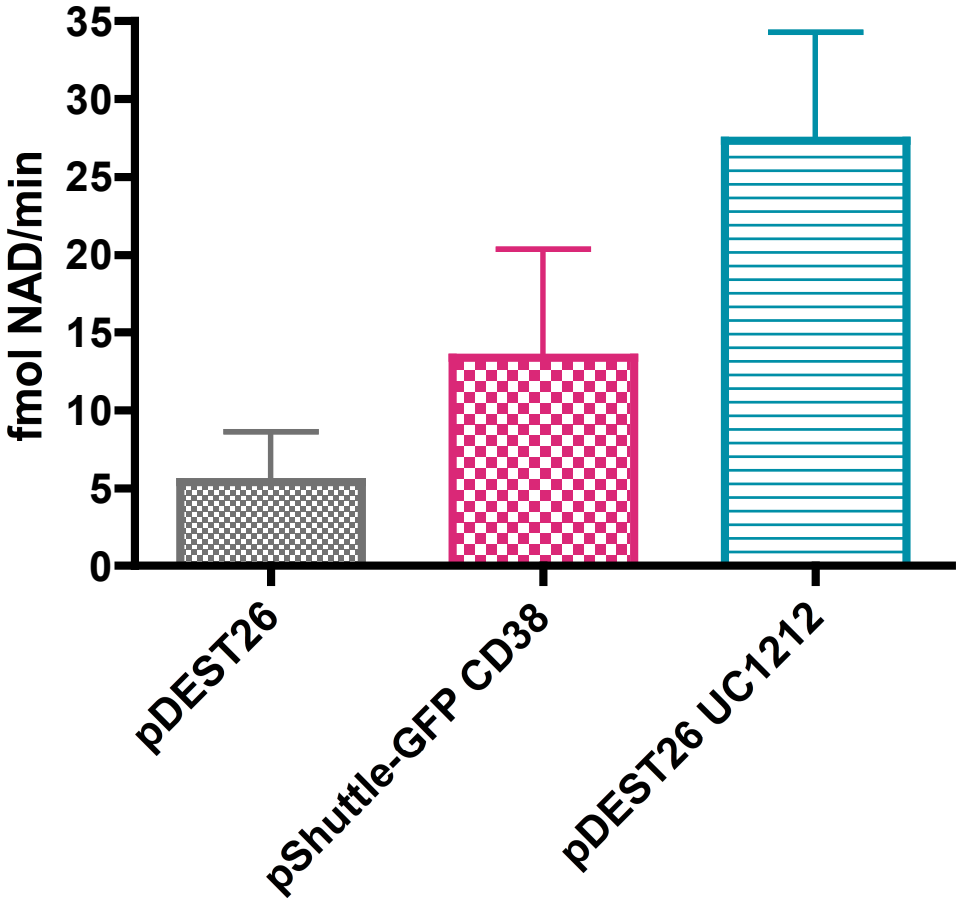

Figure 43. **Murine UC1212 Expression of ADPRC Activity in HeLa Cells**

The pDEST26-His-UC1212, pShuttle-GFP-CD38, and empty pDEST26-His constructs were transiently transfected into HeLa cells. The pDEST26-His-UC1212 and pShuttle-GFP-CD38 both expressed ADPRC activity in HeLa cells as measured by the RCA.

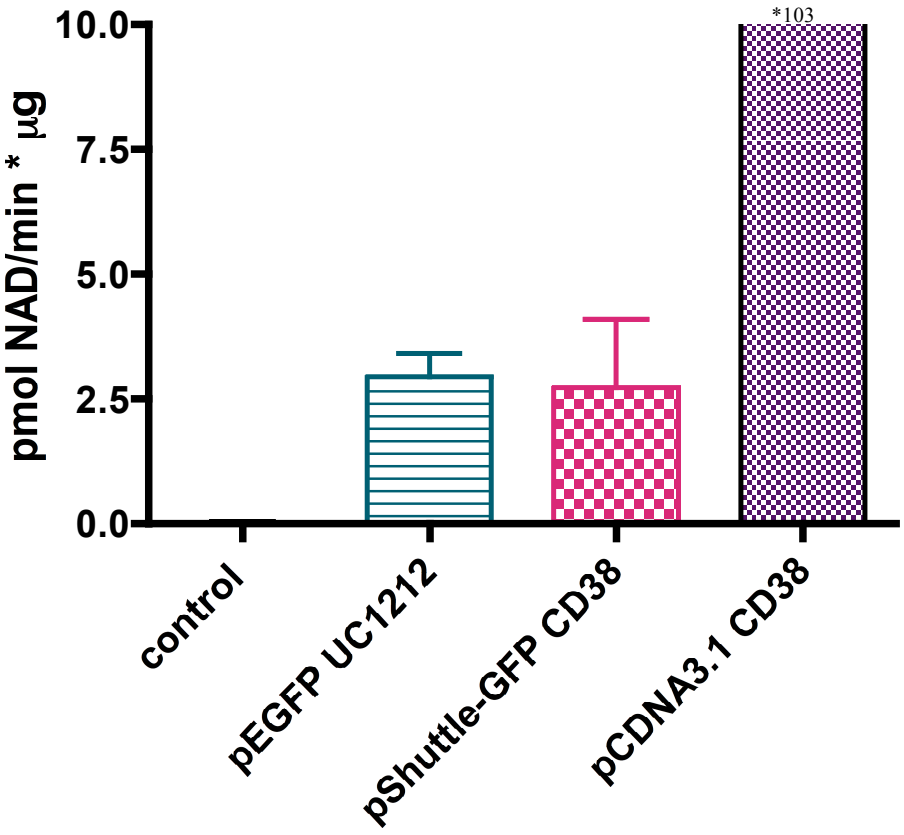

Figure 44. **ADPRC Activity of HeLa Cells Transfected with pEGFP-N3-UC1212**

The membrane faction of HeLa cells transfected with pEGFP-N3-UC1212, pShuttle-GFP-CD38, and pCDNA3.1-CD38 expressed ADPRC activity as measured by the RCA. The negative transfection control did not express ADPRC activity.

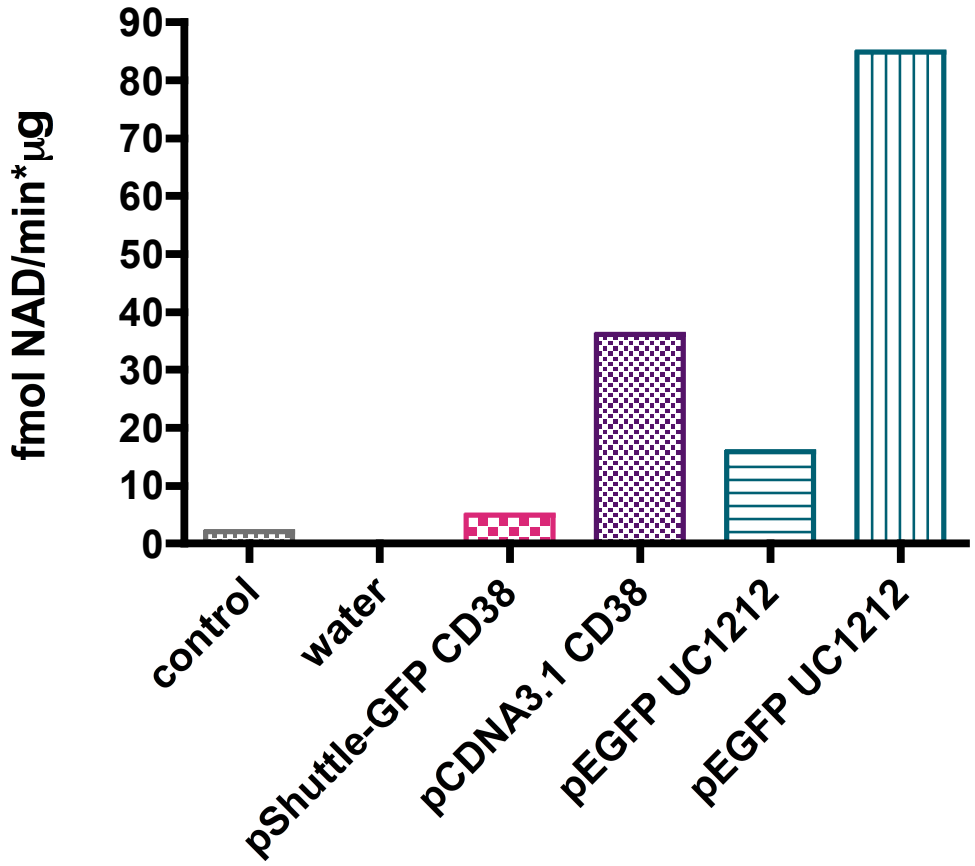

Figure 45. **ADPRC Activity of Blind Transfected HeLa Cells**

HeLa cells were transfected blind with UC1212 and CD38 expressing constructs. The membrane faction of HeLa cells transfected with pEGFP-N3-UC1212, pShuttle-GFP-CD38, and pCDNA3.1-CD38 expressed ADPRC activity as measured by the RCA. The negative transfection control did not express ADPRC activity.

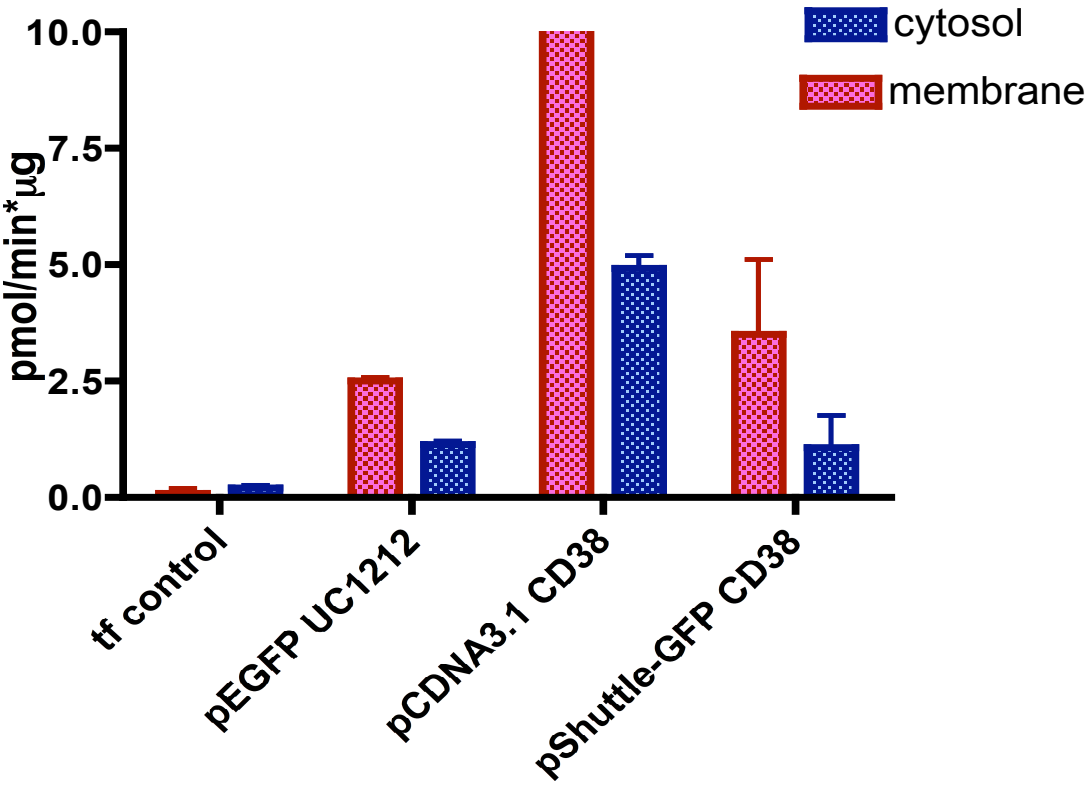

Figure 46. **Membrane and Cytosolic ADPRC Activity of Transfected HeLa Cells** The membrane and cytosolic fractions of HeLa cells transfected with pEGFP-N3-UC1212, pCDNA3.1-CD38, and pShuttle-GFP-CD38 expressed ADPRC activity as measured by the RCA. The negative control transfection did not express ADPRC activity.

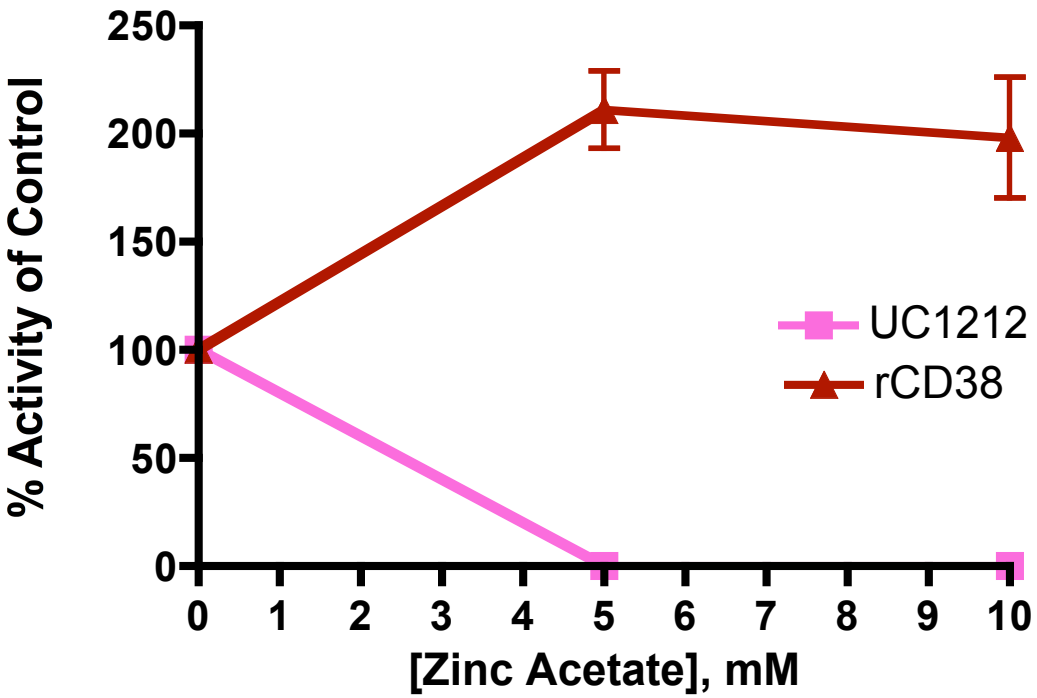

Figure 47. **Zinc Regulation of UC1212**

HeLa cells transfected with UC1212 (pEGFP-N3-UC1212) and rCD38 (pShuttle-GFP-CD38) constructs were incubated with 0-10 mM zinc acetate for 10 minutes prior to initiation of the RCA. The ADPRC activity of UC1212 was fully inhibited with zinc concentrations from 0-10 mM, while the ADPRC activity of CD38 was stimulated by zinc concentrations from 0-10 mM.

Chapter 5

Discussion & Conclusions

Previous investigations have revealed the existence of both cytosolic and membrane-bound ADPRCs that are distinct from the known mammalian cyclases CD38 and CD157 [74, 79, 130]. In these studies we have developed a sensitive assay for ADPRC enzyme activity detection, which has been useful in identifying and characterizing novel ADPRCs. Further, a molecular based protein motif search was utilized to identify potential novel ADPRC candidates.

It has been shown by our group as well as others that the basal activity of the novel ADPRCs is very low [79] and has escaped detection by traditional methods. In these studies, we have provided evidence that the cytosolic fraction of mouse heart tissues contains a component that actually inhibits ADPRC activity as measured by a previous method, the NGD assay [233]. This may have further contributed to the difficulty of detection of novel cyclases in the past, especially those that are soluble. Further, previous studies have suggested the lack of ability to cyclize NGD as a distinguishing characteristic of certain novel cyclases [72], which may actually have been resultant of an inhibitory component of the cytosol.

In order to better characterize and identify the novel ADPRCs the RCA, a highly sensitive, high-throughput assay with detection of ADPRC activity in the femtamolar range was developed. The RCA coupled a reaction that utilized nicotinamide and its

unique ability to drive the ADPRC enzymatic reaction in reverse resulting in the production of NAD [124], with a set of reactions that amplified the NAD produced and converted it to a fluorescent product resorufin [253]. The NAD concentration was determined by quantification of the resultant resorufin fluorometrically. We have shown the timecourse and kinetics of rCD38 and *Aplysia* cyclase as measured by the RCA to be equivalent to previously used methods such as HPLC. Although the RCA is the most sensitive assay available for detection of ADPRC activity, it is limited in that certain buffers and reagents interfere with fluorescence.

Using the RCA, we have shown that $CD38^{+/+}$ and $CD38^{-/-}$ mouse cytosol of various tissues exhibited ADPRC activity, which suggest the presence of novel ADPRC(s). The tissue with highest cytosolic cyclase activity, heart, was investigated to further characterize and identify the protein(s) responsible for this activity. We have provided multiple lines of evidence that point to the presence of novel ADPRC(s) in heart cytosol that is distinct from the known mammalian ADPRCs. First the activity was present in cytosol obtained from $CD38^{-/-}$ mouse hearts. Second, the cytosolic activity was inhibited by zinc, which clearly is distinct from CD38 and CD157 are activated by zinc [126]. Third, the cytosolic activity exhibits a size of greater than 300 kDa using gel filtration, which is also different from CD38 that is a 90 kDa dimer [45] in this system. Fourth, the cytosolic activity does not bind to Phenyl-Sepharose, whereas CD38 does. Further, we have provided evidence that the cytosolic form of ADPRC is regulated by a phosphorylation mechanism, and more specifically a PKC-dependent phosphorylation mechanism.

Despite being able to characterize the novel heart cytosolic cyclase(s), conventional protein purification was not sufficient to isolate and identify the protein(s) responsible for the activity. The key limitation of this approach was the low basal activity of the cytosolic cyclase(s). Although the protein was concentrated as much as possible and stabilizing agents were used in all buffers, the isolation of the cyclase(s) was not achieved. However, in the process of testing numerous column chromatography techniques, we did find the cyclase(s) had an affinity for certain dye-conjugated columns. In the future, certain columns could be used with concentrated protein samples in a sequential fashion utilizing columns the activity did not bind to as a clean-up step and columns the activity had high enough affinity to bind to isolate the novel ADPRC(s) and determine their identity using mass spectrometry.

In an attempt to identify the novel ADPRC(s), we abandoned the conventional protein purification approach and turned to a molecular based approach. Previously it has been shown that *Aplysia* ADPRC, CD38 and CD157 are conserved with approximately 30% sequence identity [9, 21, 24-26]. The two key features shared by the ADPRC family members include the conserved "TLEDTL" region [31] and ten cysteine residues with conserved spacing and alignment [24]. We utilized a HMM based method [250] employed to identify six potential uncharacterized protein ADPRC candidates. The method was based on a protein motif search of the C-terminal cysteine residues conserved among ADPRCs [9, 21, 24-26]. The most interesting candidate UC1212, which at 1212 amino acids correlated with the size of the novel mouse heart cytosolic cyclase, retained the C-terminal cysteine residue conserved motif as well as the

"TLEDTL" region. To confirm that UC1212 was a novel ADPRC, we constructed expression plasmids and introduced them into HeLa cells. The HeLa cells into which the UC1212 expression vector had been introduced exhibited ADPRC activity in both the cytosol and membrane fractions as measured by the RCA.

Both murine UC1212 and its human homologue have been demonstrated to have ADPRC activity. Further investigations of the novel ADPRC UC1212 to distinguish it from the known mammalian cyclases and to provide insight as to whether it was the same novel ADPRC responsible for the mouse heart cytosolic ADPRC activity, the regulation of UC1212 with zinc was studied. Here we have shown that the ADPRC activity of both novel mouse heart cytosolic cyclase and UC1212 were inhibited by zinc, which suggests the novel cyclases are indeed distinct from the known mammalian cyclases [126]. This also points to the possibility that the UC1212 protein is responsible for the cytosolic cyclase activity observed in mouse hearts. In the past evidence has indicated that zinc binds directly to CD38 resulting in changes in enzymatic properties due to a conformational change of the catalytic protein [126]. Although traditional zinc binding motifs are not observed in ADPRCs, the conserved cysteine residues could act as ligands for zinc ions. It has been proposed that zinc induces a conformational change that results in increased accessibility of the hydrophobic domain of CD38 [126]. As the novel mouse heart cytosolic cyclase is not membrane bound and does not bind the Phenyl-Sepharose column, this suggests differences in hydrophobic nature which may explain the differences in zinc regulation of the ADPRCs [72, 73, 79, 126, 254, 255]. These differences in enzymatic properties of the novel cyclases observed could provide insight

into the regulation of ADPRCs and the role of novel cyclases in the ADPRC mediated calcium signaling pathways.

In future experiments, it would be useful to determine if DTT inhibits the activity of the novel cyclases, as it has been predicted that the disulfide bridges formed by the conserved cysteine residues contribute the tertiary structure necessary for enzyme activity are disrupted by the addition of DTT [4]. Currently, this investigation is difficult as DTT interferes with the RCA and the low basal levels of the novel cyclase activity are difficult to detect using other less sensitive methods. Furthermore, studies utilizing silencing RNA (siRNA) against UC1212 to interfere with gene expression as well as investigations to determine the localization of UC1212 may provide insights into novel cyclases and further elucidate the regulatory mechanisms involved in the cADPR/ADPRC calcium mediated signaling pathways. Finally, given evidence the HMM based protein motif search successfully uncovered a novel ADPRC, it is important to continue with molecular cloning of the other uncharacterized protein candidates into mammalian expression vectors to screen for ADPRC activity and potentially lead to the discovery of additional novel ADPRC family members.

The ADPRC family produces cADPR, ADPR and NAADP [16, 81], which are all known to raise intracellular calcium in multiple cell types [10, 14, 16-20]. Intracellular calcium is known regulate several key biological functions [182]. Identification and characterization of the enzymes that generate these molecules and knowledge regarding the regulation of these enzymes is important to our overall understanding the mechanisms

by which basic biological processes are controlled. The ADPRC mediated signaling pathways have been implicated in a variety of biological processes including: long-term synaptic signaling and memory formation [101], insulin secretion from beta cells [100], contractility in arterial smooth muscles [73, 111], calcium ion dynamics and contractility in airway smooth muscles [145], calcium homeostasis in cardiac myocytes [120, 151], myocyte contraction [183], and ischemia/reperfusion injury of the heart [185], oxytocin release [186], cellular metabolism and cell cycle control [189, 190], circadian timekeeping mechanism in plants [191, 256], long-term hypoxia [194], social behavior [188, 195, 196], spatial learning ability [197, 198, 216], cell adheshion events [199, 200] and chemotaxis [201, 204, 205, 236], cell signaling [206], antibody responses [207], regulation of energy and fat metabolism [208], hydrogen peroxide-induced beta cell death [209], renal blood flow and urine output [210], osteoclastogenesis [211], cytokine production upon antibody ligation [212, 213], apoptosis [215, 216], phagocytosis [217], and microglial activation [218]. There are multiple forms of mammalian ADPRC, many of which have not yet been identified or characterized [11, 12, 72-79]. A better understanding of novel ADPRCs will provide a foundation for the intelligent design of drugs and as a prognostic marker for prominent diseases including cardiovascular disease [128], coronary artery disease [131], hypertension [158, 164], pulmonary hypertension [162, 163, 219], diabetes [100, 138], cancer [220, 221], multiple sclerosis [222], neurodegeneration [186, 223, 224, 257], Huntington's disease [224], HIV-1 and AIDS [223, 226, 227] , asthma [146, 228], inflammatory diseases [155, 172, 176, 178] and those implicated in cellular damage [173]. Thus, it is imperative to continue with

identification of novel ADPRCs and elucidation of the mechanisms by which the members of this complex family of enzymes are regulated.

Literature Cited

1. Lee, H.C. and R. Aarhus, *ADP-ribosyl cyclase: an enzyme that cyclizes NAD+ into a calcium-mobilizing metabolite.* Cell Regul, 1991. **2**(3): p. 203-9.

2. Howard, M., J.C. Grimaldi, J.F. Bazan, F.E. Lund, L. Santos-Argumedo, R.M. Parkhouse, T.F. Walseth, and H.C. Lee, *Formation and hydrolysis of cyclic ADP-ribose catalyzed by lymphocyte antigen CD38.* Science, 1993. **262**(5136): p. 1056-9.

3. Gelman, L., P. Deterre, H. Gouy, L. Boumsell, P. Debre, and G. Bismuth, *The lymphocyte surface antigen CD38 acts as a nicotinamide adenine dinucleotide glycohydrolase in human T lymphocytes.* Eur J Immunol, 1993. **23**(12): p. 3361-4.

4. Kontani, K., H. Nishina, Y. Ohoka, K. Takahashi, and T. Katada, *NAD glycohydrolase specifically induced by retinoic acid in human leukemic HL-60 cells. Identification of the NAD glycohydrolase as leukocyte cell surface antigen CD38.* J Biol Chem, 1993. **268**(23): p. 16895-8.

5. Takasawa, S., A. Tohgo, N. Noguchi, T. Koguma, K. Nata, T. Sugimoto, H. Yonekura, and H. Okamoto, *Synthesis and hydrolysis of cyclic ADP-ribose by human leukocyte antigen CD38 and inhibition of the hydrolysis by ATP*. J Biol Chem, 1993. **268**(35): p. 26052-4.

6. Zocchi, E., L. Franco, L. Guida, U. Benatti, A. Bargellesi, F. Malavasi, H.C. Lee, and A. De Flora, *A single protein immunologically identified as CD38 displays NAD+ glycohydrolase, ADP-ribosyl cyclase and cyclic ADP-ribose hydrolase activities at the outer surface of human erythrocytes.* Biochem Biophys Res Commun, 1993. **196**(3): p. 1459-65.

7. Summerhill, R.J., D.G. Jackson, and A. Galione, *Human lymphocyte antigen CD38 catalyzes the production of cyclic ADP-ribose.* FEBS Lett, 1993. **335**(2): p. 231-3.

8. Hirata, Y., N. Kimura, K. Sato, Y. Ohsugi, S. Takasawa, H. Okamoto, J. Ishikawa, T. Kaisho, K. Ishihara, and T. Hirano, *ADP ribosyl cyclase activity of a novel bone marrow stromal cell surface molecule, BST-1.* FEBS Lett, 1994. **356**(2-3): p. 244-8.

9. Itoh, M., K. Ishihara, H. Tomizawa, H. Tanaka, Y. Kobune, J. Ishikawa, T. Kaisho, and T. Hirano, *Molecular cloning of murine BST-1 having homology with CD38 and Aplysia ADP-ribosyl cyclase.* Biochem Biophys Res Commun, 1994. **203**(2): p. 1309-17.

10. Clapper, D.L., T.F. Walseth, P.J. Dargie, and H.C. Lee, *Pyridine nucleotide metabolites stimulate calcium release from sea urchin egg microsomes desensitized to inositol trisphosphate.* J Biol Chem, 1987. **262**(20): p. 9561-8.

11. Churamani, D., M.J. Boulware, T.J. Geach, A.C. Martin, G.W. Moy, Y.H. Su, V.D. Vacquier, J.S. Marchant, L. Dale, and S. Patel, *Molecular characterization of a novel intracellular ADP-ribosyl cyclase.* PLoS One, 2007. **2**(8): p. e797.

12. Churamani, D., M.J. Boulware, L. Ramakrishnan, T.J. Geach, A.C. Martin, V.D. Vacquier, J.S. Marchant, L. Dale, and S. Patel, *Molecular characterization of a novel cell surface ADP-ribosyl cyclase from the sea urchin.* Cell Signal, 2008. **20**(12): p. 2347-55.

13. Lee, H.C., T.F. Walseth, G.T. Bratt, R.N. Hayes, and D.L. Clapper, *Structural determination of a cyclic metabolite of NAD+ with intracellular Ca2+-mobilizing activity.* J Biol Chem, 1989. **264**(3): p. 1608-15.

14. Lee, H.C. and R. Aarhus, *A derivative of NADP mobilizes calcium stores insensitive to inositol trisphosphate and cyclic ADP-ribose.* J Biol Chem, 1995. **270**(5): p. 2152-7.

15. Machida, M., S. Yokoyama, H. Matsuzawa, T. Miyazawa, and T. Ohta, *Allosteric effect of fructose 1,6-bisphosphate on the conformation of NAD+ as bound to L-lactate dehydrogenase from Thermus caldophilus GK24.* J Biol Chem, 1985. **260**(30): p. 16143-7.

16. Guse, A.H. and H.C. Lee, *NAADP: a universal Ca2+ trigger.* Sci Signal, 2008. **1**(44): p. re10.

17. Lee, H.C., *Multiplicity of Ca2+ messengers and Ca2+ stores: a perspective from cyclic ADP-ribose and NAADP.* Curr Mol Med, 2004. **4**(3): p. 227-37.

18. Aarhus, R., D.M. Dickey, R.M. Graeff, K.R. Gee, T.F. Walseth, and H.C. Lee, *Activation and inactivation of Ca2+ release by NAADP+.* J Biol Chem, 1996. **271**(15): p. 8513-6.

19. Aarhus, R., R.M. Graeff, D.M. Dickey, T.F. Walseth, and H.C. Lee, *ADP-ribosyl cyclase and CD38 catalyze the synthesis of a calcium-mobilizing metabolite from NADP.* J Biol Chem, 1995. **270**(51): p. 30327-33.

20. Cancela, J.M., G.C. Churchill, and A. Galione, *Coordination of agonist-induced Ca2+-signalling patterns by NAADP in pancreatic acinar cells.* Nature, 1999. **398**(6722): p. 74-6.

21. Glick, D.L., M.R. Hellmich, S. Beushausen, P. Tempst, H. Bayley, and F. Strumwasser, *Primary structure of a molluscan egg-specific NADase, a second-messenger enzyme.* Cell Regul, 1991. **2**(3): p. 211-8.

22. Hellmich, M.R. and F. Strumwasser, *Purification and characterization of a molluscan egg-specific NADase, a second-messenger enzyme.* Cell Regul, 1991. **2**(3): p. 193-202.

23. Lee, H.C. and R. Aarhus, *Wide distribution of an enzyme that catalyzes the hydrolysis of cyclic ADP-ribose.* Biochim Biophys Acta, 1993. **1164**(1): p. 68-74.

24. States, D.J., T.F. Walseth, and H.C. Lee, *Similarities in amino acid sequences of Aplysia ADP-ribosyl cyclase and human lymphocyte antigen CD38.* Trends Biochem Sci, 1992. **17**(12): p. 495.

25. Nata, K., T. Sugimoto, A. Tohgo, T. Takamura, N. Noguchi, A. Matsuoka, T. Numakunai, K. Shikama, H. Yonekura, S. Takasawa, and et al., *The structure of the Aplysia kurodai gene encoding ADP-ribosyl cyclase, a second-messenger enzyme.* Gene, 1995. **158**(2): p. 213-8.

26. Kaisho, T., J. Ishikawa, K. Oritani, J. Inazawa, H. Tomizawa, O. Muraoka, T. Ochi, and T. Hirano, *BST-1, a surface molecule of bone marrow stromal cell lines that facilitates pre-B-cell growth.* Proc Natl Acad Sci U S A, 1994. **91**(12): p. 5325-9.

27. Munshi, C., D.J. Thiel, Mathews, II, R. Aarhus, T.F. Walseth, and H.C. Lee, *Characterization of the active site of ADP-ribosyl cyclase.* J Biol Chem, 1999. **274**(43): p. 30770-7.

28. Munshi, C., R. Aarhus, R. Graeff, T.F. Walseth, D. Levitt, and H.C. Lee, *Identification of the enzymatic active site of CD38 by site-directed mutagenesis.* J Biol Chem, 2000. **275**(28): p. 21566-71.

29. Lee, H.C., C. Munshi, and R. Graeff, *Structures and activities of cyclic ADP-ribose, NAADP and their metabolic enzymes.* Mol Cell Biochem, 1999. **193**(1-2): p. 89-98.

30. Graeff, R., C. Munshi, R. Aarhus, M. Johns, and H.C. Lee, *A single residue at the active site of CD38 determines its NAD cyclizing and hydrolyzing activities.* J Biol Chem, 2001. **276**(15): p. 12169-73.

31. Prasad, G.S., D.E. McRee, E.A. Stura, D.G. Levitt, H.C. Lee, and C.D. Stout, *Crystal structure of Aplysia ADP ribosyl cyclase, a homologue of the bifunctional ectozyme CD38.* Nat Struct Biol, 1996. **3**(11): p. 957-64.

32. Jackson, D.G. and J.I. Bell, *Isolation of a cDNA encoding the human CD38 (T10) molecule, a cell surface glycoprotein with an unusual discontinuous pattern of expression during lymphocyte differentiation.* J Immunol, 1990. **144**(7): p. 2811-5.

33. Deaglio, S., M. Morra, R. Mallone, C.M. Ausiello, E. Prager, G. Garbarino, U. Dianzani, H. Stockinger, and F. Malavasi, *Human CD38 (ADP-ribosyl cyclase) is a counter-receptor of CD31, an Ig superfamily member.* J Immunol, 1998. **160**(1): p. 395-402.

34. Deaglio, S. and F. Malavasi, *The CD38/CD157 mammalian gene family: An evolutionary paradigm for other leukocyte surface enzymes.* Purinergic Signal, 2006. **2**(2): p. 431-41.

35. Guida, L., L. Franco, E. Zocchi, and A. De Flora, *Structural role of disulfide bridges in the cyclic ADP-ribose related bifunctional ectoenzyme CD38.* FEBS Lett, 1995. **368**(3): p. 481-4.

36. Musso, T., S. Deaglio, L. Franco, L. Calosso, R. Badolato, G. Garbarino, U. Dianzani, and F. Malavasi, *CD38 expression and functional activities are up-regulated by IFN-gamma on human monocytes and monocytic cell lines.* J Leukoc Biol, 2001. **69**(4): p. 605-12.

37. Nishina, H., K. Inageda, K. Takahashi, S. Hoshino, K. Ikeda, and T. Katada, *Cell surface antigen CD38 identified as ecto-enzyme of NAD glycohydrolase has hyaluronate-binding activity.* Biochem Biophys Res Commun, 1994. **203**(2): p. 1318-23.

38. Mizuguchi, M., N. Otsuka, M. Sato, Y. Ishii, S. Kon, M. Yamada, H. Nishina, T. Katada, and K. Ikeda, *Neuronal localization of CD38 antigen in the human brain.* Brain Res, 1995. **697**(1-2): p. 235-40.

39. Verderio, C., S. Bruzzone, E. Zocchi, E. Fedele, U. Schenk, A. De Flora, and M. Matteoli, *Evidence of a role for cyclic ADP-ribose in calcium signalling and neurotransmitter release in cultured astrocytes.* J Neurochem, 2001. **78**(3): p. 646-57.

40. Khoo, K.M. and C.F. Chang, *Characterization and localization of CD38 in the vertebrate eye.* Brain Res, 1999. **821**(1): p. 17-25.

41. Kramer, G., G. Steiner, D. Fodinger, E. Fiebiger, C. Rappersberger, S. Binder, J. Hofbauer, and M. Marberger, *High expression of a CD38-like molecule in normal prostatic epithelium and its differential loss in benign and malignant disease.* J Urol, 1995. **154**(5): p. 1636-41.

42. Fernandez, J.E., S. Deaglio, D. Donati, I.S. Beusan, F. Corno, A. Aranega, M. Forni, B. Falini, and F. Malavasi, *Analysis of the distribution of human CD38 and of its ligand CD31 in normal tissues.* J Biol Regul Homeost Agents, 1998. **12**(3): p. 81-91.

43. Deaglio, S., R. Mallone, G. Baj, D. Donati, G. Giraudo, F. Corno, S. Bruzzone, M. Geuna, C. Ausiello, and F. Malavasi, *Human CD38 and its ligand CD31 define a unique lamina propria T lymphocyte signaling pathway.* FASEB J, 2001. **15**(3): p. 580-2.

44. Koguma, T., S. Takasawa, A. Tohgo, T. Karasawa, Y. Furuya, H. Yonekura, and H. Okamoto, *Cloning and characterization of cDNA encoding rat ADP-ribosyl*

cyclase/cyclic ADP-ribose hydrolase (homologue to human CD38) from islets of Langerhans. Biochim Biophys Acta, 1994. **1223**(1): p. 160-2.

45. Dogan, S., T.A. White, D.A. Deshpande, M.P. Murtaugh, T.F. Walseth, and M.S. Kannan, *Estrogen increases CD38 gene expression and leads to differential regulation of adenosine diphosphate (ADP)-ribosyl cyclase and cyclic ADP-ribose hydrolase activities in rat myometrium.* Biol Reprod, 2002. **66**(3): p. 596-602.

46. Sun, L., O.A. Adebanjo, B.S. Moonga, S. Corisdeo, H.K. Anandatheerthavarada, G. Biswas, T. Arakawa, Y. Hakeda, A. Koval, B. Sodam, P.J. Bevis, A.J. Moser, F.A. Lai, S. Epstein, B.R. Troen, M. Kumegawa, and M. Zaidi, *CD38/ADP-ribosyl cyclase: A new role in the regulation of osteoclastic bone resorption.* J Cell Biol, 1999. **146**(5): p. 1161-72.

47. Yamada, M., M. Mizuguchi, N. Otsuka, K. Ikeda, and H. Takahashi, *Ultrastructural localization of CD38 immunoreactivity in rat brain.* Brain Res, 1997. **756**(1-2): p. 52-60.

48. Sun, L., O.A. Adebanjo, A. Koval, H.K. Anandatheerthavarada, J. Iqbal, X.Y. Wu, B.S. Moonga, X.B. Wu, G. Biswas, P.J. Bevis, M. Kumegawa, S. Epstein, C.L. Huang, N.G. Avadhani, E. Abe, and M. Zaidi, *A novel mechanism for coupling cellular intermediary metabolism to cytosolic Ca2+ signaling via CD38/ADP-ribosyl cyclase, a putative intracellular NAD+ sensor.* FASEB J, 2002. **16**(3): p. 302-14.

49. Adebanjo, O.A., H.K. Anandatheerthavarada, A.P. Koval, B.S. Moonga, G. Biswas, L. Sun, B.R. Sodam, P.J. Bevis, C.L. Huang, S. Epstein, F.A. Lai, N.G. Avadhani, and M. Zaidi, *A new function for CD38/ADP-ribosyl cyclase in nuclear Ca2+ homeostasis.* Nat Cell Biol, 1999. **1**(7): p. 409-14.

50. Liu, Q., R. Graeff, I.A. Kriksunov, H. Jiang, B. Zhang, N. Oppenheimer, H. Lin, B.V. Potter, H.C. Lee, and Q. Hao, *Structural basis for enzymatic evolution from a dedicated ADP-ribosyl cyclase to a multifunctional NAD hydrolase.* J Biol Chem, 2009. **284**(40): p. 27637-45.

51. Graeff, R., Q. Liu, I.A. Kriksunov, M. Kotaka, N. Oppenheimer, Q. Hao, and H.C. Lee, *Mechanism of cyclizing NAD to cyclic ADP-ribose by ADP-ribosyl cyclase and CD38.* J Biol Chem, 2009. **284**(40): p. 27629-36.

52. Hoshino, S., I. Kukimoto, K. Kontani, S. Inoue, Y. Kanda, F. Malavasi, and T. Katada, *Mapping of the catalytic and epitopic sites of human CD38/NAD+ glycohydrolase to a functional domain in the carboxyl terminus.* J Immunol, 1997. **158**(2): p. 741-7.

53. Lund, F.E., H.M. Muller-Steffner, N. Yu, C.D. Stout, F. Schuber, and M.C. Howard, *CD38 signaling in B lymphocytes is controlled by its ectodomain but occurs independently of enzymatically generated ADP-ribose or cyclic ADP-ribose.* J Immunol, 1999. **162**(5): p. 2693-702.

54. Liu, Q., R. Graeff, I.A. Kriksunov, C.M. Lam, H.C. Lee, and Q. Hao, *Conformational Closure of the Catalytic Site of Human CD38 Induced by Calcium.* Biochemistry, 2008. **47**(52): p. 13966-73.

55. Ortolan, E., P. Vacca, A. Capobianco, E. Armando, F. Crivellin, A. Horenstein, and F. Malavasi, *CD157, the Janus of CD38 but with a unique personality.* Cell Biochem Funct, 2002. **20**(4): p. 309-22.

56. McNagny, K.M., P.A. Cazenave, and M.D. Cooper, *BP-3 alloantigen. A cell surface glycoprotein that marks early B lineage cells and mature myeloid lineage cells in mice.* J Immunol, 1988. **141**(8): p. 2551-6.

57. Wimazal, F., M. Ghannadan, M.R. Muller, A. End, M. Willheim, P. Meidlinger, G.H. Schernthaner, J.H. Jordan, W. Hagen, H. Agis, W.R. Sperr, K. Czerwenka, K. Lechner, and P. Valent, *Expression of homing receptors and related molecules on human mast cells and basophils: a comparative analysis using multi-color flow cytometry and toluidine blue/immunofluorescence staining techniques.* Tissue Antigens, 1999. **54**(5): p. 499-507.

58. Okuyama, Y., K. Ishihara, N. Kimura, Y. Hirata, K. Sato, M. Itoh, L.B. Ok, and T. Hirano, *Human BST-1 expressed on myeloid cells functions as a receptor molecule.* Biochem Biophys Res Commun, 1996. **228**(3): p. 838-45.

59. Hernandez-Campo, P.M., J. Almeida, M.L. Sanchez, M. Malvezzi, and A. Orfao, *Normal patterns of expression of glycosylphosphatidylinositol-anchored proteins on different subsets of peripheral blood cells: a frame of reference for the diagnosis of paroxysmal nocturnal hemoglobinuria.* Cytometry B Clin Cytom, 2006. **70**(2): p. 71-81.

60. Ishihara, K., Y. Kobune, Y. Okuyama, M. Itoh, B.O. Lee, O. Muraoka, and T. Hirano, *Stage-specific expression of mouse BST-1/BP-3 on the early B and T cell progenitors prior to gene rearrangement of antigen receptor.* Int Immunol, 1996. **8**(9): p. 1395-404.

61. Todd, R.F., 3rd, J.A. Roach, and M.A. Arnaout, *The modulated expression of Mo5, a human myelomonocytic plasma membrane antigen.* Blood, 1985. **65**(4): p. 964-73.

62. Honczarenko, M., Y. Le, M. Swierkowski, I. Ghiran, A.M. Glodek, and L.E. Silberstein, *Human bone marrow stromal cells express a distinct set of biologically functional chemokine receptors.* Stem Cells, 2006. **24**(4): p. 1030-41.

63. Podesta, M., F. Benvenuto, A. Pitto, O. Figari, A. Bacigalupo, S. Bruzzone, L. Guida, L. Franco, L. Paleari, N. Bodrato, C. Usai, A. De Flora, and E. Zocchi, *Concentrative uptake of cyclic ADP-ribose generated by BST-1+ stroma stimulates proliferation of human hematopoietic progenitors.* J Biol Chem, 2005. **280**(7): p. 5343-9.

64. Shimaoka, Y., J.F. Attrep, T. Hirano, K. Ishihara, R. Suzuki, T. Toyosaki, T. Ochi, and P.E. Lipsky, *Nurse-like cells from bone marrow and synovium of patients with rheumatoid arthritis promote survival and enhance function of human B cells.* J Clin Invest, 1998. **102**(3): p. 606-18.

65. Seki, M., S. Fairchild, O.A. Rosenwasser, N. Tada, and K. Tomonari, *An immature rat lymphocyte marker CD157: striking differences in the expression between mice and rats.* Immunobiology, 2001. **203**(5): p. 725-42.

66. Vicari, A.P., A.G. Bean, and A. Zlotnik, *A role for BP-3/BST-1 antigen in early T cell development.* Int Immunol, 1996. **8**(2): p. 183-91.

67. Ortolan, E., E.V. Tibaldi, B. Ferranti, L. Lavagno, G. Garbarino, R. Notaro, L. Luzzatto, F. Malavasi, and A. Funaro, *CD157 plays a pivotal role in neutrophil transendothelial migration.* Blood, 2006. **108**(13): p. 4214-22.

68. Ghannadan, M., M. Baghestanian, F. Wimazal, M. Eisenmenger, D. Latal, G. Kargul, S. Walchshofer, C. Sillaber, K. Lechner, and P. Valent, *Phenotypic characterization of human skin mast cells by combined staining with toluidine blue and CD antibodies.* J Invest Dermatol, 1998. **111**(4): p. 689-95.

69. McNagny, K.M., R.P. Bucy, and M.D. Cooper, *Reticular cells in peripheral lymphoid tissues express the phosphatidylinositol-linked BP-3 antigen.* Eur J Immunol, 1991. **21**(2): p. 509-15.

70. Kajimoto, Y., J. Miyagawa, K. Ishihara, Y. Okuyama, Y. Fujitani, M. Itoh, H. Yoshida, T. Kaisho, T. Matsuoka, H. Watada, T. Hanafusa, Y. Yamasaki, T. Kamada, Y. Matsuzawa, and T. Hirano, *Pancreatic islet cells express BST-1, a CD38-like surface molecule having ADP-ribosyl cyclase activity.* Biochem Biophys Res Commun, 1996. **219**(3): p. 941-6.

71. Nemoto, E., S. Sugawara, H. Tada, H. Takada, H. Shimauchi, and H. Horiuchi, *Cleavage of CD14 on human gingival fibroblasts cocultured with activated neutrophils is mediated by human leukocyte elastase resulting in down-regulation of lipopolysaccharide-induced IL-8 production.* J Immunol, 2000. **165**(10): p. 5807-13.

72. Ceni, C., N. Pochon, M. Villaz, H. Muller-Steffner, F. Schuber, J. Baratier, M. De Waard, M. Ronjat, and M.J. Moutin, *The CD38-independent ADP-ribosyl cyclase from mouse brain synaptosomes: a comparative study of neonate and adult brain.* Biochem J, 2006. **395**(2): p. 417-26.

73. de Toledo, F.G., J. Cheng, M. Liang, E.N. Chini, and T.P. Dousa, *ADP-Ribosyl cyclase in rat vascular smooth muscle cells: properties and regulation.* Circ Res, 2000. **86**(11): p. 1153-9.

74. Sternfeld, L., E. Krause, A.H. Guse, and I. Schulz, *Hormonal control of ADP-ribosyl cyclase activity in pancreatic acinar cells from rats.* J Biol Chem, 2003. **278**(36): p. 33629-36.

75. Goodrich, S.P., H. Muller-Steffner, A. Osman, M.J. Moutin, K. Kusser, A. Roberts, D.L. Woodland, T.D. Randall, E. Kellenberger, P.T. LoVerde, F. Schuber, and F.E. Lund, *Production of calcium-mobilizing metabolites by a novel member of the ADP-ribosyl cyclase family expressed in Schistosoma mansoni.* Biochemistry, 2005. **44**(33): p. 11082-97.

76. Augustin, A., H. Muller-Steffner, and F. Schuber, *Molecular cloning and functional expression of bovine spleen ecto-NAD+ glycohydrolase: structural identity with human CD38.* Biochem J, 2000. **345 Pt 1**: p. 43-52.

77. Adebanjo, O.A., A. Koval, B.S. Moonga, X.B. Wu, S. Yao, P.J. Bevis, M. Kumegawa, M. Zaidi, and L. Sun, *Molecular cloning, expression, and functional characterization of a novel member of the CD38 family of ADP-ribosyl cyclases.* Biochem Biophys Res Commun, 2000. **273**(3): p. 884-9.

78. Ziegler, M., D. Jorcke, and M. Schweiger, *Identification of bovine liver mitochondrial NAD+ glycohydrolase as ADP-ribosyl cyclase.* Biochem J, 1997. **326 (Pt 2)**: p. 401-5.

79. Ceni, C., H. Muller-Steffner, F. Lund, N. Pochon, A. Schweitzer, M. De Waard, F. Schuber, M. Villaz, and M.J. Moutin, *Evidence for an intracellular ADP-ribosyl cyclase/NAD+-glycohydrolase in brain from CD38-deficient mice.* J Biol Chem, 2003. **278**(42): p. 40670-8.

80. Lee, H.C., *Physiological functions of cyclic ADP-ribose and NAADP as calcium messengers.* Annu Rev Pharmacol Toxicol, 2001. **41**: p. 317-45.

81. Lee, H.C., *Structure and enzymatic functions of human CD38.* Mol Med, 2006. **12**(11-12): p. 317-23.

82. Kraft, R., C. Grimm, K. Grosse, A. Hoffmann, S. Sauerbruch, H. Kettenmann, G. Schultz, and C. Harteneck, *Hydrogen peroxide and ADP-ribose induce TRPM2-mediated calcium influx and cation currents in microglia.* Am J Physiol Cell Physiol, 2004. **286**(1): p. C129-37.

83. Galione, A., *Cyclic ADP-ribose, the ADP-ribosyl cyclase pathway and calcium signalling.* Mol Cell Endocrinol, 1994. **98**(2): p. 125-31.

84. Lee, H.C., *Potentiation of calcium- and caffeine-induced calcium release by cyclic ADP-ribose.* J Biol Chem, 1993. **268**(1): p. 293-9.

85. Galione, A., *Cyclic ADP-ribose: a new way to control calcium.* Science, 1993. **259**(5093): p. 325-6.

86. Galione, A., H.C. Lee, and W.B. Busa, *Ca(2+)-induced Ca2+ release in sea urchin egg homogenates: modulation by cyclic ADP-ribose.* Science, 1991. **253**(5024): p. 1143-6.

87. Li, P.L., W.X. Tang, H.H. Valdivia, A.P. Zou, and W.B. Campbell, *cADP-ribose activates reconstituted ryanodine receptors from coronary arterial smooth muscle.* Am J Physiol Heart Circ Physiol, 2001. **280**(1): p. H208-15.

88. Thomas, J.M., R. Masgrau, G.C. Churchill, and A. Galione, *Pharmacological characterization of the putative cADP-ribose receptor.* Biochem J, 2001. **359**(Pt 2): p. 451-7.

89. Ozawa, T., *Ryanodine-sensitive Ca2+ release mechanism in non-excitable cells (Review).* Int J Mol Med, 2001. **7**(1): p. 21-5.

90. Sano, Y., K. Inamura, A. Miyake, S. Mochizuki, H. Yokoi, H. Matsushime, and K. Furuichi, *Immunocyte Ca2+ influx system mediated by LTRPC2.* Science, 2001. **293**(5533): p. 1327-30.

91. Perraud, A.L., A. Fleig, C.A. Dunn, L.A. Bagley, P. Launay, C. Schmitz, A.J. Stokes, Q. Zhu, M.J. Bessman, R. Penner, J.P. Kinet, and A.M. Scharenberg, *ADP-ribose gating of the calcium-permeable LTRPC2 channel revealed by Nudix motif homology.* Nature, 2001. **411**(6837): p. 595-9.

92. Lee, H.C., *Nicotinic acid adenine dinucleotide phosphate (NAADP)-mediated calcium signaling.* J Biol Chem, 2005. **280**(40): p. 33693-6.

93. Calcraft, P.J., M. Ruas, Z. Pan, X. Cheng, A. Arredouani, X. Hao, J. Tang, K. Rietdorf, L. Teboul, K.T. Chuang, P. Lin, R. Xiao, C. Wang, Y. Zhu, Y. Lin, C.N. Wyatt, J. Parrington, J. Ma, A.M. Evans, A. Galione, and M.X. Zhu, *NAADP mobilizes calcium from acidic organelles through two-pore channels.* Nature, 2009. **459**(7246): p. 596-600.

94. Berridge, G., G. Dickinson, J. Parrington, A. Galione, and S. Patel, *Solubilization of receptors for the novel Ca2+-mobilizing messenger, nicotinic acid adenine dinucleotide phosphate.* J Biol Chem, 2002. **277**(46): p. 43717-23.

95. Galione, A., A. McDougall, W.B. Busa, N. Willmott, I. Gillot, and M. Whitaker, *Redundant mechanisms of calcium-induced calcium release underlying calcium waves during fertilization of sea urchin eggs.* Science, 1993. **261**(5119): p. 348-52.

96. Lee, H.C., R. Aarhus, and T.F. Walseth, *Calcium mobilization by dual receptors during fertilization of sea urchin eggs.* Science, 1993. **261**(5119): p. 352-5.

97. Guse, A.H., C.P. da Silva, I. Berg, A.L. Skapenko, K. Weber, P. Heyer, M. Hohenegger, G.A. Ashamu, H. Schulze-Koops, B.V. Potter, and G.W. Mayr, *Regulation of calcium signalling in T lymphocytes by the second messenger cyclic ADP-ribose.* Nature, 1999. **398**(6722): p. 70-3.

98. Partida-Sanchez, S., D.A. Cockayne, S. Monard, E.L. Jacobson, N. Oppenheimer, B. Garvy, K. Kusser, S. Goodrich, M. Howard, A. Harmsen, T.D. Randall, and F.E. Lund, *Cyclic ADP-ribose production by CD38 regulates intracellular calcium release, extracellular calcium influx and chemotaxis in neutrophils and is required for bacterial clearance in vivo.* Nat Med, 2001. **7**(11): p. 1209-16.

99. Bruzzone, S., A. De Flora, C. Usai, R. Graeff, and H.C. Lee, *Cyclic ADP-ribose is a second messenger in the lipopolysaccharide-stimulated proliferation of human peripheral blood mononuclear cells.* Biochem J, 2003. **375**(Pt 2): p. 395-403.

100. Kato, I., Y. Yamamoto, M. Fujimura, N. Noguchi, S. Takasawa, and H. Okamoto, *CD38 disruption impairs glucose-induced increases in cyclic ADP-ribose, [Ca2+]i, and insulin secretion.* J Biol Chem, 1999. **274**(4): p. 1869-72.

101. Reyes-Harde, M., R. Empson, B.V. Potter, A. Galione, and P.K. Stanton, *Evidence of a role for cyclic ADP-ribose in long-term synaptic depression in hippocampus.* Proc Natl Acad Sci U S A, 1999. **96**(7): p. 4061-6.

102. De Flora, A., L. Guida, L. Franco, and E. Zocchi, *The CD38/cyclic ADP-ribose system: a topological paradox.* Int J Biochem Cell Biol, 1997. **29**(10): p. 1149-66.

103. Lee, H.C., E. Zocchi, L. Guida, L. Franco, U. Benatti, and A. De Flora, *Production and hydrolysis of cyclic ADP-ribose at the outer surface of human erythrocytes.* Biochem Biophys Res Commun, 1993. **191**(2): p. 639-45.

104. Lee, H.C., *Modulator and messenger functions of cyclic ADP-ribose in calcium signaling.* Recent Prog Horm Res, 1996. **51**: p. 355-88; discussion 389.

105. Berridge, M.J., *Cell signalling. A tale of two messengers.* Nature, 1993. **365**(6445): p. 388-9.

106. Chini, E.N., K.W. Beers, and T.P. Dousa, *Nicotinate adenine dinucleotide phosphate (NAADP) triggers a specific calcium release system in sea urchin eggs.* J Biol Chem, 1995. **270**(7): p. 3216-23.

107. Bruzzone, S., L. Guida, E. Zocchi, L. Franco, and A. De Flora, *Connexin 43 hemi channels mediate Ca2+-regulated transmembrane NAD+ fluxes in intact cells.* FASEB J, 2001. **15**(1): p. 10-12.

108. Kim, H., E.L. Jacobson, and M.K. Jacobson, *Synthesis and degradation of cyclic ADP-ribose by NAD glycohydrolases.* Science, 1993. **261**(5126): p. 1330-3.

109. Franco, L., L. Guida, S. Bruzzone, E. Zocchi, C. Usai, and A. De Flora, *The transmembrane glycoprotein CD38 is a catalytically active transporter responsible for generation and influx of the second messenger cyclic ADP-ribose across membranes.* FASEB J, 1998. **12**(14): p. 1507-20.

110. Guida, L., S. Bruzzone, L. Sturla, L. Franco, E. Zocchi, and A. De Flora, *Equilibrative and concentrative nucleoside transporters mediate influx of extracellular cyclic ADP-ribose into 3T3 murine fibroblasts.* J Biol Chem, 2002. **277**(49): p. 47097-105.

111. Lee, H.C., R. Aarhus, and R.M. Graeff, *Sensitization of calcium-induced calcium release by cyclic ADP-ribose and calmodulin.* J Biol Chem, 1995. **270**(16): p. 9060-6.

112. Galione, A., *Ca(2+)-induced Ca2+ release and its modulation by cyclic ADP-ribose.* Trends Pharmacol Sci, 1992. **13**(8): p. 304-6.

113. Wang, Y.X., Y.M. Zheng, Q.B. Mei, Q.S. Wang, M.L. Collier, S. Fleischer, H.B. Xin, and M.I. Kotlikoff, *FKBP12.6 and cADPR regulation of Ca2+ release in smooth muscle cells.* Am J Physiol Cell Physiol, 2004. **286**(3): p. C538-46.

114. Noguchi, N., S. Takasawa, K. Nata, A. Tohgo, I. Kato, F. Ikehata, H. Yonekura, and H. Okamoto, *Cyclic ADP-ribose binds to FK506-binding protein 12.6 to release Ca2+ from islet microsomes.* J Biol Chem, 1997. **272**(6): p. 3133-6.

115. Lee, H.C., R. Aarhus, R. Graeff, M.E. Gurnack, and T.F. Walseth, *Cyclic ADP ribose activation of the ryanodine receptor is mediated by calmodulin.* Nature, 1994. **370**(6487): p. 307-9.

116. Tanaka, Y. and A.H. Tashjian, Jr., *Calmodulin is a selective mediator of Ca(2+)-induced Ca2+ release via the ryanodine receptor-like Ca2+ channel triggered by cyclic ADP-ribose.* Proc Natl Acad Sci U S A, 1995. **92**(8): p. 3244-8.

117. Takasawa, S., A. Ishida, K. Nata, K. Nakagawa, N. Noguchi, A. Tohgo, I. Kato, H. Yonekura, H. Fujisawa, and H. Okamoto, *Requirement of calmodulin-dependent protein kinase II in cyclic ADP-ribose-mediated intracellular Ca2+ mobilization.* J Biol Chem, 1995. **270**(51): p. 30257-9.

118. Yamasaki-Mann, M., A. Demuro, and I. Parker, *cADPR stimulates SERCA activity in Xenopus oocytes.* Cell Calcium, 2009. **45**(3): p. 293-9.

119. Lukyanenko, V., I. Gyorke, T.F. Wiesner, and S. Gyorke, *Potentiation of Ca(2+) release by cADP-ribose in the heart is mediated by enhanced SR Ca(2+) uptake into the sarcoplasmic reticulum.* Circ Res, 2001. **89**(7): p. 614-22.

120. Macgregor, A.T., S. Rakovic, A. Galione, and D.A. Terrar, *Dual effects of cyclic ADP-ribose on sarcoplasmic reticulum Ca2+ release and storage in cardiac myocytes isolated from guinea-pig and rat ventricle.* Cell Calcium, 2007. **41**(6): p. 537-46.

121. Zong, X., M. Schieder, H. Cuny, S. Fenske, C. Gruner, K. Rotzer, O. Griesbeck, H. Harz, M. Biel, and C. Wahl-Schott, *The two-pore channel TPCN2 mediates NAADP-dependent Ca(2+)-release from lysosomal stores.* Pflugers Arch, 2009. **458**(5): p. 891-9.

122. Steen, M., T. Kirchberger, and A.H. Guse, *NAADP mobilizes calcium from the endoplasmic reticular Ca(2+) store in T-lymphocytes.* J Biol Chem, 2007. **282**(26): p. 18864-71.

123. Kolisek, M., A. Beck, A. Fleig, and R. Penner, *Cyclic ADP-ribose and hydrogen peroxide synergize with ADP-ribose in the activation of TRPM2 channels.* Mol Cell, 2005. **18**(1): p. 61-9.

124. Inageda, K., K. Takahashi, K. Tokita, H. Nishina, Y. Kanaho, I. Kukimoto, K. Kontani, S. Hoshino, and T. Katada, *Enzyme properties of Aplysia ADP-ribosyl cyclase: comparison with NAD glycohydrolase of CD38 antigen.* J Biochem, 1995. **117**(1): p. 125-31.

125. Kuhn, I., E. Kellenberger, D. Rognan, F.E. Lund, H. Muller-Steffner, and F. Schuber, *Redesign of Schistosoma mansoni NAD+ catabolizing enzyme: active site H103W mutation restores ADP-ribosyl cyclase activity.* Biochemistry, 2006. **45**(39): p. 11867-78.

126. Kukimoto, I., S. Hoshino, K. Kontani, K. Inageda, H. Nishina, K. Takahashi, and T. Katada, *Stimulation of ADP-ribosyl cyclase activity of the cell surface antigen CD38 by zinc ions resulting from inhibition of its NAD+ glycohydrolase activity.* Eur J Biochem, 1996. **239**(1): p. 177-82.

127. Ceni, C., N. Pochon, V. Brun, H. Muller-Steffner, A. Andrieux, D. Grunwald, F. Schuber, M. De Waard, F. Lund, M. Villaz, and M.J. Moutin, *CD38-dependent ADP-ribosyl cyclase activity in developing and adult mouse brain.* Biochem J, 2003. **370**(Pt 1): p. 175-83.

128. Takahashi, J., Y. Kagaya, I. Kato, J. Ohta, S. Isoyama, M. Miura, Y. Sugai, M. Hirose, Y. Wakayama, M. Ninomiya, J. Watanabe, S. Takasawa, H. Okamoto, and K. Shirato, *Deficit of CD38/cyclic ADP-ribose is differentially compensated in hearts by gender.* Biochem Biophys Res Commun, 2003. **312**(2): p. 434-40.

129. Meszaros, L.G., R.W. Wrenn, and G. Varadi, *Sarcoplasmic reticulum-associated and protein kinase C-regulated ADP-ribosyl cyclase in cardiac muscle.* Biochem Biophys Res Commun, 1997. **234**(1): p. 252-6.

130. Matsumura, N. and S. Tanuma, *Involvement of cytosolic NAD+ glycohydrolase in cyclic ADP-ribose metabolism.* Biochem Biophys Res Commun, 1998. **253**(2): p. 246-52.

131. Zhang, F., G. Zhang, A.Y. Zhang, M.J. Koeberl, E. Wallander, and P.L. Li, *Production of NAADP and its role in Ca2+ mobilization associated with lysosomes in coronary arterial myocytes.* Am J Physiol Heart Circ Physiol, 2006. **291**(1): p. H274-82.

132. Guse, A.H., *Regulation of calcium signaling by the second messenger cyclic adenosine diphosphoribose (cADPR).* Curr Mol Med, 2004. **4**(3): p. 239-48.

133. Ghosh, J., P.J. Anderson, S. Chandrasekaran, and M.G. Caparon, *Characterization of Streptococcus pyogenes {beta}-NAD+ glycohydrolase: Re-evaluation of enzymatic properties associated with pathogenesis.* J Biol Chem, 2009.

134. Davis, L.C., A.J. Morgan, M. Ruas, J.L. Wong, R.M. Graeff, A.J. Poustka, H.C. Lee, G.M. Wessel, J. Parrington, and A. Galione, *Ca(2+) signaling occurs via second messenger release from intraorganelle synthesis sites.* Curr Biol, 2008. **18**(20): p. 1612-8.

135. Polzonetti, V., S. Pucciarelli, A. Vita, S. Vincenzetti, and P. Natalini, *CD38 in bovine lung: A multicatalytic NADase.* J Membr Biol, 2009. **227**(3): p. 105-10.

136. Orciani, M., O. Trubiani, S. Guarnieri, E. Ferrero, and R. Di Primio, *CD38 is constitutively expressed in the nucleus of human hematopoietic cells.* J Cell Biochem, 2008. **105**(3): p. 905-12.

137. Yalcintepe, L., I. Albeniz, S. Adin-Cinar, D. Tiryaki, E. Bermek, R.M. Graeff, and H.C. Lee, *Nuclear CD38 in retinoic acid-induced HL-60 cells.* Exp Cell Res, 2005. **303**(1): p. 14-21.

138. Takasawa, S., T. Akiyama, K. Nata, M. Kuroki, A. Tohgo, N. Noguchi, S. Kobayashi, I. Kato, T. Katada, and H. Okamoto, *Cyclic ADP-ribose and inositol 1,4,5-trisphosphate as alternate second messengers for intracellular Ca2+ mobilization in normal and diabetic beta-cells.* J Biol Chem, 1998. **273**(5): p. 2497-500.

139. Fritz, N., N. Macrez, J. Mironneau, L.H. Jeyakumar, S. Fleischer, and J.L. Morel, *Ryanodine receptor subtype 2 encodes Ca2+ oscillations activated by acetylcholine via the M2 muscarinic receptor/cADP-ribose signalling pathway in duodenum myocytes.* J Cell Sci, 2005. **118**(Pt 10): p. 2261-70.

140. Kuemmerle, J.F. and G.M. Makhlouf, *Agonist-stimulated cyclic ADP ribose. Endogenous modulator of Ca(2+)-induced Ca2+ release in intestinal longitudinal muscle.* J Biol Chem, 1995. **270**(43): p. 25488-94.

141. Cancela, J.M., *Specific Ca2+ signaling evoked by cholecystokinin and acetylcholine: the roles of NAADP, cADPR, and IP3.* Annu Rev Physiol, 2001. **63**: p. 99-117.

142. Cancela, J.M., F. Van Coppenolle, A. Galione, A.V. Tepikin, and O.H. Petersen, *Transformation of local Ca2+ spikes to global Ca2+ transients: the combinatorial roles of multiple Ca2+ releasing messengers.* EMBO J, 2002. **21**(5): p. 909-19.

143. Prakash, Y.S., M.S. Kannan, T.F. Walseth, and G.C. Sieck, *Role of cyclic ADP-ribose in the regulation of [Ca2+]i in porcine tracheal smooth muscle.* Am J Physiol, 1998. **274**(6 Pt 1): p. C1653-60.

144. White, T.A., M.S. Kannan, and T.F. Walseth, *Intracellular calcium signaling through the cADPR pathway is agonist specific in porcine airway smooth muscle.* FASEB J, 2003. **17**(3): p. 482-4.

145. Deshpande, D.A., T.F. Walseth, R.A. Panettieri, and M.S. Kannan, *CD38/cyclic ADP-ribose-mediated Ca2+ signaling contributes to airway smooth muscle hyper-responsiveness.* FASEB J, 2003. **17**(3): p. 452-4.

146. Kang, B.N., J.A. Jude, R.A. Panettieri, Jr., T.F. Walseth, and M.S. Kannan, *Glucocorticoid regulation of CD38 expression in human airway smooth muscle cells: role of dual specificity phosphatase 1.* Am J Physiol Lung Cell Mol Physiol, 2008. **295**(1): p. L186-93.

147. Tirumurugaan, K.G., J.A. Jude, B.N. Kang, R.A. Panettieri, T.F. Walseth, and M.S. Kannan, *TNF-alpha induced CD38 expression in human airway smooth muscle cells: role of MAP kinases and transcription factors NF-kappaB and AP-1.* Am J Physiol Lung Cell Mol Physiol, 2007. **292**(6): p. L1385-95.

148. Kang, B.N., K.G. Tirumurugaan, D.A. Deshpande, Y. Amrani, R.A. Panettieri, T.F. Walseth, and M.S. Kannan, *Transcriptional regulation of CD38 expression by tumor necrosis factor-alpha in human airway smooth muscle cells: role of NF-kappaB and sensitivity to glucocorticoids.* FASEB J, 2006. **20**(7): p. 1000-2.

149. Barone, F., A.A. Genazzani, A. Conti, G.C. Churchill, F. Palombi, E. Ziparo, V. Sorrentino, A. Galione, and A. Filippini, *A pivotal role for cADPR-mediated*

Ca2+ signaling: regulation of endothelin-induced contraction in peritubular smooth muscle cells. FASEB J, 2002. **16**(7): p. 697-705.

150. Rakovic, S., Y. Cui, S. Iino, A. Galione, G.A. Ashamu, B.V. Potter, and D.A. Terrar, *An antagonist of cADP-ribose inhibits arrhythmogenic oscillations of intracellular Ca2+ in heart cells.* J Biol Chem, 1999. **274**(25): p. 17820-7.

151. Prakash, Y.S., M.S. Kannan, T.F. Walseth, and G.C. Sieck, *cADP ribose and [Ca(2+)](i) regulation in rat cardiac myocytes.* Am J Physiol Heart Circ Physiol, 2000. **279**(4): p. H1482-9.

152. Higashida, H., S. Yokoyama, N. Hoshi, M. Hashii, A. Egorova, Z.G. Zhong, M. Noda, M. Shahidullah, M. Taketo, R. Knijnik, Y. Kimura, H. Takahashi, X.L. Chen, Y. Shin, and J.S. Zhang, *Signal transduction from bradykinin, angiotensin, adrenergic and muscarinic receptors to effector enzymes, including ADP-ribosyl cyclase.* Biol Chem, 2001. **382**(1): p. 23-30.

153. Zhang, A.Y. and P.L. Li, *Vascular physiology of a Ca2+ mobilizing second messenger - cyclic ADP-ribose.* J Cell Mol Med, 2006. **10**(2): p. 407-22.

154. Ge, Z.D., D.X. Zhang, Y.F. Chen, F.X. Yi, A.P. Zou, W.B. Campbell, and P.L. Li, *Cyclic ADP-ribose contributes to contraction and Ca2+ release by M1 muscarinic receptor activation in coronary arterial smooth muscle.* J Vasc Res, 2003. **40**(1): p. 28-36.

155. Thai, T.L. and W.J. Arendshorst, *ADP-ribosyl cyclase and ryanodine receptors mediate endothelin ETA and ETB receptor-induced renal vasoconstriction in vivo.* Am J Physiol Renal Physiol, 2008. **295**(2): p. F360-8.

156. Zhang, F., S. Jin, F. Yi, M. Xia, W.L. Dewey, and P.L. Li, *Local production of O2- by NAD(P)H oxidase in the sarcoplasmic reticulum of coronary arterial myocytes: cADPR-mediated Ca2+ regulation.* Cell Signal, 2008. **20**(4): p. 637-44.

157. Yi, F., A.Y. Zhang, N. Li, F. Zhang, M. Xia, and P.L. Li, *Role of cyclic ADP-ribose-Ca2+ signaling in mediating renin production and release in As4.1 cells.* Cell Physiol Biochem, 2007. **19**(5-6): p. 293-302.

158. Fellner, S.K. and W.J. Arendshorst, *Angiotensin II Ca2+ signaling in rat afferent arterioles: stimulation of cyclic ADP ribose and IP3 pathways.* Am J Physiol Renal Physiol, 2005. **288**(4): p. F785-91.

159. Thai, T.L., S.K. Fellner, and W.J. Arendshorst, *ADP-ribosyl cyclase and ryanodine receptor activity contribute to basal renal vasomotor tone and agonist-induced renal vasoconstriction in vivo.* Am J Physiol Renal Physiol, 2007. **293**(4): p. F1107-14.

160. Higashida, H., J. Zhang, M. Hashii, M. Shintaku, C. Higashida, and Y. Takeda, *Angiotensin II stimulates cyclic ADP-ribose formation in neonatal rat cardiac myocytes.* Biochem J, 2000. **352 Pt 1**: p. 197-202.

161. Gul, R., J.H. Park, S.Y. Kim, K.Y. Jang, J.K. Chae, J.K. Ko, and U.H. Kim, *Inhibition of ADP-ribosyl cyclase attenuates angiotensin II-induced cardiac hypertrophy.* Cardiovasc Res, 2009. **81**(3): p. 582-91.

162. Dipp, M. and A.M. Evans, *Cyclic ADP-ribose is the primary trigger for hypoxic pulmonary vasoconstriction in the rat lung in situ.* Circ Res, 2001. **89**(1): p. 77-83.

163. Wilson, H.L., M. Dipp, J.M. Thomas, C. Lad, A. Galione, and A.M. Evans, *Adp-ribosyl cyclase and cyclic ADP-ribose hydrolase act as a redox sensor. a primary role for cyclic ADP-ribose in hypoxic pulmonary vasoconstriction.* J Biol Chem, 2001. **276**(14): p. 11180-8.

164. Galione, A., A. White, N. Willmott, M. Turner, B.V. Potter, and S.P. Watson, *cGMP mobilizes intracellular Ca2+ in sea urchin eggs by stimulating cyclic ADP-ribose synthesis.* Nature, 1993. **365**(6445): p. 456-9.

165. Clementi, E., M. Riccio, C. Sciorati, G. Nistico, and J. Meldolesi, *The type 2 ryanodine receptor of neurosecretory PC12 cells is activated by cyclic ADP-ribose. Role of the nitric oxide/cGMP pathway.* J Biol Chem, 1996. **271**(30): p. 17739-45.

166. Willmott, N., J.K. Sethi, T.F. Walseth, H.C. Lee, A.M. White, and A. Galione, *Nitric oxide-induced mobilization of intracellular calcium via the cyclic ADP-ribose signaling pathway.* J Biol Chem, 1996. **271**(7): p. 3699-705.

167. Edwards, T.M. and N.S. Rickard, *New perspectives on the mechanisms through which nitric oxide may affect learning and memory processes.* Neurosci Biobehav Rev, 2007. **31**(3): p. 413-25.

168. Welshhans, K. and V. Rehder, *Nitric oxide regulates growth cone filopodial dynamics via ryanodine receptor-mediated calcium release.* Eur J Neurosci, 2007. **26**(6): p. 1537-47.

169. Satriano, J., R. Cunard, O.W. Peterson, T. Dousa, F.B. Gabbai, and R.C. Blantz, *Effects on kidney filtration rate by agmatine requires activation of ryanodine channels for nitric oxide generation.* Am J Physiol Renal Physiol, 2008. **294**(4): p. F795-800.

170. Arendshorst, W.J. and T.L. Thai, *Regulation of the renal microcirculation by ryanodine receptors and calcium-induced calcium release.* Curr Opin Nephrol Hypertens, 2009. **18**(1): p. 40-9.

171. Noguchi, N., T. Yoshikawa, T. Ikeda, I. Takahashi, N.J. Shervani, A. Uruno, A. Yamauchi, K. Nata, S. Takasawa, H. Okamoto, and A. Sugawara, *FKBP12.6 disruption impairs glucose-induced insulin secretion.* Biochem Biophys Res Commun, 2008. **371**(4): p. 735-40.

172. Guse, A.H., *Back from the dormant stage: second messenger cyclic ADP-ribose essential for Toxoplasma gondii pathogenicity.* Sci Signal, 2008. **1**(17): p. pe18.

173. Bodrato, N., L. Franco, C. Fresia, L. Guida, C. Usai, A. Salis, I. Moreschi, C. Ferraris, C. Verderio, G. Basile, S. Bruzzone, S. Scarfi, A. De Flora, and E. Zocchi, *Abscisic acid activates the murine microglial cell line N9 through the second messenger cyclic ADP-ribose.* J Biol Chem, 2009. **284**(22): p. 14777-87.

174. Scarfi, S., C. Fresia, C. Ferraris, S. Bruzzone, F. Fruscione, C. Usai, F. Benvenuto, M. Magnone, M. Podesta, L. Sturla, L. Guida, E. Albanesi, G. Damonte, A. Salis, A. De Flora, and E. Zocchi, *The plant hormone abscisic acid stimulates the proliferation of human hemopoietic progenitors through the second messenger cyclic ADP-ribose.* Stem Cells, 2009. **27**(10): p. 2469-77.

175. Bruzzone, S., I. Moreschi, C. Usai, L. Guida, G. Damonte, A. Salis, S. Scarfi, E. Millo, A. De Flora, and E. Zocchi, *Abscisic acid is an endogenous cytokine in*

human granulocytes with cyclic ADP-ribose as second messenger. Proc Natl Acad Sci U S A, 2007. **104**(14): p. 5759-64.

176. Bruzzone, S., N. Bodrato, C. Usai, L. Guida, I. Moreschi, R. Nano, B. Antonioli, F. Fruscione, M. Magnone, S. Scarfi, A. De Flora, and E. Zocchi, *Abscisic acid is an endogenous stimulator of insulin release from human pancreatic islets with cyclic ADP ribose as second messenger.* J Biol Chem, 2008. **283**(47): p. 32188-97.

177. Nagamune, K., L.M. Hicks, B. Fux, F. Brossier, E.N. Chini, and L.D. Sibley, *Abscisic acid controls calcium-dependent egress and development in Toxoplasma gondii.* Nature, 2008. **451**(7175): p. 207-10.

178. Rah, S.Y., K.H. Park, T.S. Nam, S.J. Kim, H. Kim, M.J. Im, and U.H. Kim, *Association of CD38 with nonmuscle myosin heavy chain IIA and Lck is essential for the internalization and activation of CD38.* J Biol Chem, 2007. **282**(8): p. 5653-60.

179. Moreschi, I., S. Bruzzone, N. Bodrato, C. Usai, L. Guida, R.A. Nicholas, M.U. Kassack, E. Zocchi, and A. De Flora, *NAADP+ is an agonist of the human P2Y11 purinergic receptor.* Cell Calcium, 2008. **43**(4): p. 344-55.

180. Lee, H.C., *Multiple calcium stores: separate but interacting.* Sci STKE, 2000. **2000**(40): p. pe1.

181. Patel, S., G.C. Churchill, and A. Galione, *Coordination of Ca2+ signalling by NAADP.* Trends Biochem Sci, 2001. **26**(8): p. 482-9.

182. Berridge, M.J., P. Lipp, and M.D. Bootman, *The versatility and universality of calcium signalling.* Nat Rev Mol Cell Biol, 2000. **1**(1): p. 11-21.

183. Lukyanenko, V. and S. Gyorke, *Ca2+ sparks and Ca2+ waves in saponin-permeabilized rat ventricular myocytes.* J Physiol, 1999. **521 Pt 3**: p. 575-85.

184. Rakovic, S., A. Galione, G.A. Ashamu, B.V. Potter, and D.A. Terrar, *A specific cyclic ADP-ribose antagonist inhibits cardiac excitation-contraction coupling.* Curr Biol, 1996. **6**(8): p. 989-96.

185. Xie, G.H., S.Y. Rah, K.S. Yi, M.K. Han, S.W. Chae, M.J. Im, and U.H. Kim, *Increase of intracellular Ca(2+) during ischemia/reperfusion injury of heart is mediated by cyclic ADP-ribose.* Biochem Biophys Res Commun, 2003. **307**(3): p. 713-8.

186. Higashida, H., A.B. Salmina, R.Y. Olovyannikova, M. Hashii, S. Yokoyama, K. Koizumi, D. Jin, H.X. Liu, O. Lopatina, S. Amina, M.S. Islam, J.J. Huang, and M. Noda, *Cyclic ADP-ribose as a universal calcium signal molecule in the nervous system.* Neurochem Int, 2007. **51**(2-4): p. 192-9.

187. Barata, H., M. Thompson, W. Zielinska, Y.S. Han, C.B. Mantilla, Y.S. Prakash, S. Feitoza, G. Sieck, and E.N. Chini, *The role of cyclic-ADP-ribose-signaling pathway in oxytocin-induced Ca2+ transients in human myometrium cells.* Endocrinology, 2004. **145**(2): p. 881-9.

188. Lopatina, O., H.X. Liu, S. Amina, M. Hashii, and H. Higashida, *Oxytocin-induced elevation of ADP-ribosyl cyclase activity, cyclic ADP-ribose or Ca(2+) concentrations is involved in autoregulation of oxytocin secretion in the hypothalamus and posterior pituitary in male mice.* Neuropharmacology. **58**(1): p. 50-5.

189. Lam, C.M., P.K. Yeung, H.C. Lee, and J.T. Wong, *Cyclic ADP-ribose links metabolism to multiple fission in the dinoflagellate Crypthecodinium cohnii.* Cell Calcium, 2009. **45**(4): p. 346-57.

190. Bruzzone, S., G. Dodoni, N. Kaludercic, G. Basile, E. Millo, A. De Flora, F. Di Lisa, and E. Zocchi, *Mitochondrial dysfunction induced by a cytotoxic adenine dinucleotide produced by ADP-ribosyl cyclases from cADPR.* J Biol Chem, 2007. **282**(7): p. 5045-52.

191. Harrisingh, M.C. and M.N. Nitabach, *Circadian rhythms. Integrating circadian timekeeping with cellular physiology.* Science, 2008. **320**(5878): p. 879-80.

192. Dodd, A.N., M.J. Gardner, C.T. Hotta, K.E. Hubbard, N. Dalchau, J. Love, J.M. Assie, F.C. Robertson, M.K. Jakobsen, J. Goncalves, D. Sanders, and A.A. Webb, *The Arabidopsis circadian clock incorporates a cADPR-based feedback loop.* Science, 2007. **318**(5857): p. 1789-92.

193. Ohtsuji, M., K. Yagi, M. Shintaku-Kubota, Y. Kojima-Koba, N. Ito, M. Sugihara, N. Yamaaki, D. Chujo, A. Nohara, Y. Takeda, J. Kobayashi, M. Yamagishi, and H. Higashida, *Decreased ADP-ribosyl cyclase activity in peripheral blood mononuclear cells from diabetic patients with nephropathy.* Exp Diabetes Res, 2008. **2008**: p. 897508.

194. Behringer, E.J., L.D. Leite, N.E. Buchholz, M.G. Keeney, W.J. Pearce, C.K. Vanterpool, S.M. Wilson, and J.N. Buchholz, *Maturation and long-term hypoxia alters Ca2+-induced Ca2+ release in sheep cerebrovascular sympathetic neurons.* J Appl Physiol, 2009. **107**(4): p. 1223-34.

195. Salmina, A.B., O. Lopatina, M.V. Ekimova, S.V. Mikhutkina, and H. Higashida, *CD38/cADPR-SYSTEM: A NEW PLAYER FOR OXYTOCIN SECRETION AND REGULATION OF SOCIAL BEHAVIOUR.* J Neuroendocrinol.

196. Jin, D., H.X. Liu, H. Hirai, T. Torashima, T. Nagai, O. Lopatina, N.A. Shnayder, K. Yamada, M. Noda, T. Seike, K. Fujita, S. Takasawa, S. Yokoyama, K. Koizumi, Y. Shiraishi, S. Tanaka, M. Hashii, T. Yoshihara, K. Higashida, M.S. Islam, N. Yamada, K. Hayashi, N. Noguchi, I. Kato, H. Okamoto, A. Matsushima, A. Salmina, T. Munesue, N. Shimizu, S. Mochida, M. Asano, and H. Higashida, *CD38 is critical for social behaviour by regulating oxytocin secretion.* Nature, 2007. **446**(7131): p. 41-5.

197. Young, G.S. and J.B. Kirkland, *The role of dietary niacin intake and the adenosine-5'-diphosphate-ribosyl cyclase enzyme CD38 in spatial learning ability: is cyclic adenosine diphosphate ribose the link between diet and behaviour?* Nutr Res Rev, 2008. **21**(1): p. 42-55.

198. Young, G.S., E.L. Jacobson, and J.B. Kirkland, *Water maze performance in young male Long-Evans rats is inversely affected by dietary intakes of niacin and may be linked to levels of the NAD+ metabolite cADPR.* J Nutr, 2007. **137**(4): p. 1050-7.

199. Deaglio, S., R. Mallone, G. Baj, A. Arnulfo, N. Surico, U. Dianzani, K. Mehta, and F. Malavasi, *CD38/CD31, a receptor/ligand system ruling adhesion and signaling in human leukocytes.* Chem Immunol, 2000. **75**: p. 99-120.

200. Funaro, A., E. Ortolan, B. Ferranti, L. Gargiulo, R. Notaro, L. Luzzatto, and F. Malavasi, *CD157 is an important mediator of neutrophil adhesion and migration.* Blood, 2004. **104**(13): p. 4269-78.

201. Partida-Sanchez, S., L. Rivero-Nava, G. Shi, and F.E. Lund, *CD38: an ecto-enzyme at the crossroads of innate and adaptive immune responses.* Adv Exp Med Biol, 2007. **590**: p. 171-83.

202. Partida-Sanchez, S., A. Gasser, R. Fliegert, C.C. Siebrands, W. Dammermann, G. Shi, B.J. Mousseau, A. Sumoza-Toledo, H. Bhagat, T.F. Walseth, A.H. Guse, and F.E. Lund, *Chemotaxis of mouse bone marrow neutrophils and dendritic cells is controlled by adp-ribose, the major product generated by the CD38 enzyme reaction.* J Immunol, 2007. **179**(11): p. 7827-39.

203. Partida-Sanchez, S., S. Goodrich, K. Kusser, N. Oppenheimer, T.D. Randall, and F.E. Lund, *Regulation of dendritic cell trafficking by the ADP-ribosyl cyclase CD38: impact on the development of humoral immunity.* Immunity, 2004. **20**(3): p. 279-91.

204. Partida-Sanchez, S., P. Iribarren, M.E. Moreno-Garcia, J.L. Gao, P.M. Murphy, N. Oppenheimer, J.M. Wang, and F.E. Lund, *Chemotaxis and calcium responses of phagocytes to formyl peptide receptor ligands is differentially regulated by cyclic ADP ribose.* J Immunol, 2004. **172**(3): p. 1896-906.

205. Morita, K., M. Saida, N. Morioka, T. Kitayama, Y. Akagawa, and T. Dohi, *Cyclic ADP-ribose mediates formyl methionyl leucyl phenylalanine (fMLP)-induced intracellular Ca(2+) rise and migration of human neutrophils.* J Pharmacol Sci, 2008. **106**(3): p. 492-504.

206. Koch-Nolte, F., F. Haag, A.H. Guse, F. Lund, and M. Ziegler, *Emerging roles of NAD+ and its metabolites in cell signaling.* Sci Signal, 2009. **2**(57): p. mr1.

207. Cockayne, D.A., T. Muchamuel, J.C. Grimaldi, H. Muller-Steffner, T.D. Randall, F.E. Lund, R. Murray, F. Schuber, and M.C. Howard, *Mice deficient for the ecto-nicotinamide adenine dinucleotide glycohydrolase CD38 exhibit altered humoral immune responses.* Blood, 1998. **92**(4): p. 1324-33.

208. Barbosa, M.T., S.M. Soares, C.M. Novak, D. Sinclair, J.A. Levine, P. Aksoy, and E.N. Chini, *The enzyme CD38 (a NAD glycohydrolase, EC 3.2.2.5) is necessary for the development of diet-induced obesity.* FASEB J, 2007. **21**(13): p. 3629-39.

209. Lange, I., S. Yamamoto, S. Partida-Sanchez, Y. Mori, A. Fleig, and R. Penner, *TRPM2 functions as a lysosomal Ca2+-release channel in beta cells.* Sci Signal, 2009. **2**(71): p. ra23.

210. Thai, T.L. and W.J. Arendshorst, *Mice lacking the ADP ribosyl cyclase CD38 exhibit attenuated renal vasoconstriction to angiotensin II, endothelin-1, and norepinephrine.* Am J Physiol Renal Physiol, 2009. **297**(1): p. F169-76.

211. Iqbal, J. and M. Zaidi, *Extracellular NAD+ metabolism modulates osteoclastogenesis.* Biochem Biophys Res Commun, 2006. **349**(2): p. 533-9.

212. Ausiello, C.M., F. Urbani, R. Lande, A. la Sala, B. Di Carlo, G. Baj, N. Surico, J. Hilgers, S. Deaglio, A. Funaro, and F. Malavasi, *Functional topography of discrete domains of human CD38.* Tissue Antigens, 2000. **56**(6): p. 539-47.

213. Ausiello, C.M., A. la Sala, C. Ramoni, F. Urbani, A. Funaro, and F. Malavasi, *Secretion of IFN-gamma, IL-6, granulocyte-macrophage colony-stimulating factor and IL-10 cytokines after activation of human purified T lymphocytes upon CD38 ligation.* Cell Immunol, 1996. **173**(2): p. 192-7.

214. Zocchi, E., A. Daga, C. Usai, L. Franco, L. Guida, S. Bruzzone, A. Costa, C. Marchetti, and A. De Flora, *Expression of CD38 increases intracellular calcium concentration and reduces doubling time in HeLa and 3T3 cells.* J Biol Chem, 1998. **273**(14): p. 8017-24.

215. Kirkland, J.B., *Niacin status impacts chromatin structure.* J Nutr, 2009. **139**(12): p. 2397-401.

216. Kirkland, J.B., *Niacin status, NAD distribution and ADP-ribose metabolism.* Curr Pharm Des, 2009. **15**(1): p. 3-11.

217. Song, E.K., Y.R. Lee, H.N. Yu, U.H. Kim, S.Y. Rah, K.H. Park, I.K. Shim, S.J. Lee, Y.M. Park, W.G. Chung, J.S. Kim, and M.K. Han, *Extracellular NAD is a*

regulator for FcgammaR-mediated phagocytosis in murine macrophages. Biochem Biophys Res Commun, 2008. **367**(1): p. 156-61.

218. Mayo, L., J. Jacob-Hirsch, N. Amariglio, G. Rechavi, M.J. Moutin, F.E. Lund, and R. Stein, *Dual role of CD38 in microglial activation and activation-induced cell death.* J Immunol, 2008. **181**(1): p. 92-103.

219. Evans, A.M. and M. Dipp, *Hypoxic pulmonary vasoconstriction: cyclic adenosine diphosphate-ribose, smooth muscle Ca(2+) stores and the endothelium.* Respir Physiol Neurobiol, 2002. **132**(1): p. 3-15.

220. Henderson, K., S.L. Stella, S. Kobylewski, and C.D. Eckhert, *Receptor activated Ca(2+) release is inhibited by boric acid in prostate cancer cells.* PLoS One, 2009. **4**(6): p. e6009.

221. Barranco, W.T., D.H. Kim, S.L. Stella, Jr., and C.D. Eckhert, *Boric acid inhibits stored Ca2+ release in DU-145 prostate cancer cells.* Cell Biol Toxicol, 2009. **25**(4): p. 309-20.

222. Bennett, J.L., M.R. Blanchet, L. Zhao, L. Zbytnuik, F. Antignano, M. Gold, P. Kubes, and K.M. McNagny, *Bone marrow-derived mast cells accumulate in the central nervous system during inflammation but are dispensable for experimental autoimmune encephalomyelitis pathogenesis.* J Immunol, 2009. **182**(9): p. 5507-14.

223. Kou, W., S. Banerjee, J. Eudy, L.M. Smith, R. Persidsky, K. Borgmann, L. Wu, N. Sakhuja, M.S. Deshpande, T.F. Walseth, and A. Ghorpade, *CD38 regulation in activated astrocytes: implications for neuroinflammation and HIV-1 brain infection.* J Neurosci Res, 2009. **87**(10): p. 2326-39.

224. Khan, J.A., F. Forouhar, X. Tao, and L. Tong, *Nicotinamide adenine dinucleotide metabolism as an attractive target for drug discovery.* Expert Opin Ther Targets, 2007. **11**(5): p. 695-705.

225. Franco, L., N. Bodrato, I. Moreschi, C. Usai, S. Bruzzone, S. Scarf i, E. Zocchi, and A. De Flora, *Cyclic ADP-ribose is a second messenger in the lipopolysaccharide-stimulated activation of murine N9 microglial cell line.* J Neurochem, 2006. **99**(1): p. 165-76.

226. Feligioni, M., L. Raiteri, R. Pattarini, M. Grilli, S. Bruzzone, P. Cavazzani, M. Raiteri, and A. Pittaluga, *The human immunodeficiency virus-1 protein Tat and its discrete fragments evoke selective release of acetylcholine from human and rat cerebrocortical terminals through species-specific mechanisms.* J Neurosci, 2003. **23**(17): p. 6810-8.

227. Banerjee, S., T.F. Walseth, K. Borgmann, L. Wu, K.R. Bidasee, M.S. Kannan, and A. Ghorpade, *CD38/cyclic ADP-ribose regulates astrocyte calcium signaling: implications for neuroinflammation and HIV-1-associated dementia.* J Neuroimmune Pharmacol, 2008. **3**(3): p. 154-64.

228. Sieck, G.C., T.A. White, M.A. Thompson, C.M. Pabelick, M.E. Wylam, and Y.S. Prakash, *Regulation of store-operated Ca2+ entry by CD38 in human airway smooth muscle.* Am J Physiol Lung Cell Mol Physiol, 2008. **294**(2): p. L378-85.

229. da Silva, C.P., B.V. Potter, G.W. Mayr, and A.H. Guse, *Quantification of intracellular levels of cyclic ADP-ribose by high-performance liquid chromatography.* J Chromatogr B Biomed Sci Appl, 1998. **707**(1-2): p. 43-50.

230. Walseth, T.F., L. Wong, R.M. Graeff, and H.C. Lee, *Bioassay for determining endogenous levels of cyclic ADP-ribose.* Methods Enzymol, 1997. **280**: p. 287-94.

231. Takahashi, K., I. Kukimoto, K. Tokita, K. Inageda, S. Inoue, K. Kontani, S. Hoshino, H. Nishina, Y. Kanaho, and T. Katada, *Accumulation of cyclic ADP-ribose measured by a specific radioimmunoassay in differentiated human leukemic HL-60 cells with all-trans-retinoic acid.* FEBS Lett, 1995. **371**(2): p. 204-8.

232. Graeff, R.M., T.F. Walseth, and H.C. Lee, *Radioimmunoassay for measuring endogenous levels of cyclic ADP-ribose in tissues.* Methods Enzymol, 1997. **280**: p. 230-41.

233. Graeff, R.M., T.F. Walseth, K. Fryxell, W.D. Branton, and H.C. Lee, *Enzymatic synthesis and characterizations of cyclic GDP-ribose. A procedure for distinguishing enzymes with ADP-ribosyl cyclase activity.* J Biol Chem, 1994. **269**(48): p. 30260-7.

234. Graeff, R. and H.C. Lee, *A novel cycling assay for cellular cADP-ribose with nanomolar sensitivity.* Biochem J, 2002. **361**(Pt 2): p. 379-84.

235. Walseth, T.F., R. Aarhus, R.J. Zeleznikar, Jr., and H.C. Lee, *Determination of endogenous levels of cyclic ADP-ribose in rat tissues.* Biochim Biophys Acta, 1991. **1094**(1): p. 113-20.

236. Orciani, M., O. Trubiani, G. Cavaletti, S. Guarnieri, E. Salvolini, G. Tredici, and R. Di Primio, *Expression of CD38 in human neuroblastoma SH-SY5Y cells.* Int J Immunopathol Pharmacol, 2008. **21**(1): p. 97-105.

237. Graeff, R.M., K. Mehta, and H.C. Lee, *GDP-ribosyl cyclase activity as a measure of CD38 induction by retinoic acid in HL-60 cells.* Biochem Biophys Res Commun, 1994. **205**(1): p. 722-7.

238. Scarfi, S., C. Ferraris, F. Fruscione, C. Fresia, L. Guida, S. Bruzzone, C. Usai, A. Parodi, E. Millo, A. Salis, G. Burastero, A. De Flora, and E. Zocchi, *Cyclic ADP-ribose-mediated expansion and stimulation of human mesenchymal stem cells by the plant hormone abscisic acid.* Stem Cells, 2008. **26**(11): p. 2855-64.

239. Chidambaram, N. and C.F. Chang, *Functional role of glycosylation on the recombinant CD38/ADP-ribosyl cyclase in CHO cells.* Int J Biochem Cell Biol, 1998. **30**(9): p. 1011-8.

240. Wall, K.A., M. Klis, J. Kornet, D. Coyle, J.C. Ame, M.K. Jacobson, and J.T. Slama, *Inhibition of the intrinsic NAD+ glycohydrolase activity of CD38 by carbocyclic NAD analogues.* Biochem J, 1998. **335 (Pt 3)**: p. 631-6.

241. Hara-Yokoyama, M., I. Kukimoto, H. Nishina, K. Kontani, Y. Hirabayashi, F. Irie, H. Sugiya, S. Furuyama, and T. Katada, *Inhibition of NAD+ glycohydrolase and ADP-ribosyl cyclase activities of leukocyte cell surface antigen CD38 by gangliosides.* J Biol Chem, 1996. **271**(22): p. 12951-5.

242. Hara-Yokoyama, M., Y. Nagatsuka, O. Katsumata, F. Irie, K. Kontani, S. Hoshino, T. Katada, Y. Ono, J. Fujita-Yoshigaki, H. Sugiya, S. Furuyama, and Y. Hirabayashi, *Complex gangliosides as cell surface inhibitors for the ecto-NAD+ glycohydrolase of CD38.* Biochemistry, 2001. **40**(4): p. 888-95.

243. Smith, P.K., R.I. Krohn, G.T. Hermanson, A.K. Mallia, F.H. Gartner, M.D. Provenzano, E.K. Fujimoto, N.M. Goeke, B.J. Olson, and D.C. Klenk, *Measurement of protein using bicinchoninic acid.* Anal Biochem, 1985. **150**(1): p. 76-85.

244. Mandi, M. and J. Bak, *Nicotinic acid adenine dinucleotide phosphate (NAADP) and Ca2+ mobilization.* J Recept Signal Transduct Res, 2008. **28**(3): p. 163-84.

245. Altschul, S.F., W. Gish, W. Miller, E.W. Myers, and D.J. Lipman, *Basic local alignment search tool.* J Mol Biol, 1990. **215**(3): p. 403-10.

246. Pearson, W.R. and D.J. Lipman, *Improved tools for biological sequence comparison.* Proc Natl Acad Sci U S A, 1988. **85**(8): p. 2444-8.

247. Eddy, S.R., *Multiple alignment using hidden Markov models.* Proc Int Conf Intell Syst Mol Biol, 1995. **3**: p. 114-20.

248. Henikoff, J.G. and S. Henikoff, *Using substitution probabilities to improve position-specific scoring matrices.* Comput Appl Biosci, 1996. **12**(2): p. 135-43.

249. Taylor, W.R., *An investigation of conservation-biased gap-penalties for multiple protein sequence alignment.* Gene, 1995. **165**(1): p. GC27-35.

250. Krogh, A., M. Brown, I.S. Mian, K. Sjolander, and D. Haussler, *Hidden Markov models in computational biology. Applications to protein modeling.* J Mol Biol, 1994. **235**(5): p. 1501-31.

251. Bairoch, A., P. Bucher, and K. Hofmann, *The PROSITE database, its status in 1997.* Nucleic Acids Res, 1997. **25**(1): p. 217-21.

252. Landy, A., *Dynamic, structural, and regulatory aspects of lambda site-specific recombination.* Annu Rev Biochem, 1989. **58**: p. 913-49.

253. Graeff, R. and H.C. Lee, *A novel cycling assay for nicotinic acid-adenine dinucleotide phosphate with nanomolar sensitivity.* Biochem J, 2002. **367**(Pt 1): p. 163-8.

254. Zielinska, W., H. Barata, and E.N. Chini, *Metabolism of cyclic ADP-ribose: Zinc is an endogenous modulator of the cyclase/NAD glycohydrolase ratio of a CD38-like enzyme from human seminal fluid.* Life Sci, 2004. **74**(14): p. 1781-90.

255. Xie, G.H., S.Y. Rah, S.J. Kim, T.S. Nam, K.C. Ha, S.W. Chae, M.J. Im, and U.H. Kim, *ADP-ribosyl cyclase couples to cyclic AMP signaling in the cardiomyocytes.* Biochem Biophys Res Commun, 2005. **330**(4): p. 1290-8.

256. Trubiani, O., S. Guarnieri, E. Eleuterio, F. Di Giuseppe, M. Orciani, S. Angelucci, and R. Di Primio, *Insights into nuclear localization and dynamic association of CD38 in Raji and K562 cells.* J Cell Biochem, 2008. **103**(4): p. 1294-308.

257. Zhang, L., X. Xu, Z. Luo, D. Shen, and H. Wu, *Identification of an unusual AT(D)Pase-like activity in multifunctional NAD glycohydrolase from the venom of Agkistrodon acutus.* Biochimie, 2009. **91**(2): p. 240-51.